Republic of Iraq
Ministry of Higher Education & Scientific Research
University of Babylon
College of Education for Pure Sciences
Department of Physics

Determination of the Natural Radioactivity in Children's Food and the Effect of Radiotherapy on CBC

A Thesis
Submitted to the Council of the College of Education for Pure Sciences of University of Babylon in Partial Fulfillment of the Requirements for the Degree of Doctor of Philosophy in Education / Physics

By

Faten Ahmed Mahdi Hussein

B. Sc. in Physics
(University of Babylon, 2016)

M. Sc. in Physics
(University of Babylon, 2019)

Supervised by

Prof. Fouad A. Majeed
(Ph.D.)
University of Babylon
College of Education for Pure Sciences
Department of Physics

Prof. Nihad A. Salih
(Ph.D.)
University of Babylon
College of Sciences
Department of Physics

2023 A.D. **1445 A.H.**

بِسْمِ اللَّهِ الرَّحْمَٰنِ الرَّحِيمِ

وَيَسْأَلُونَكَ عَنِ الرُّوحِ ۖ قُلِ الرُّوحُ مِنْ أَمْرِ رَبِّي
وَمَا أُوتِيتُم مِّنَ الْعِلْمِ إِلَّا قَلِيلًا

صدق الله العلي العظيم

سورة الاسراء، الآية (٨٥)

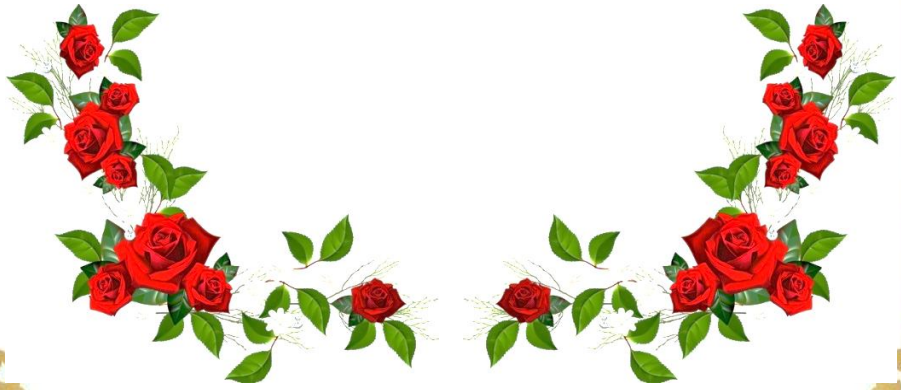

Dedication

To my beloved, late Mother and late uncle

Sayed Moayad,

Your passing during my PhD study caused profound pain. Your love and guidance are deeply missed and will be forever cherished in my heart. Your memory and support helped drive me to complete this work.

Faten

Acknowledgment

I would first like to thank my supervisors Prof. Fouad A. Majeed (Ph.D.) and Prof. Nihad A. Salih (Ph.D.), for their trust and support during my study.

I sincerely thank the administration and staff members of the Physics Department, College of Education for Pure Sciences, and the Physics Department, College of Science, for their help in their advanced nuclear laboratories.

I would like to offer my profound appreciation and gratitude to Dr. Ali Abd Abojassim for his constant support, guidance, and provision of resources throughout the research process. He played a crucial role in completing this work.

I am also grateful to Dr. Haider Hasan Shakir, the medical doctor, for his guidance and advice on the medical tests required for this study. Special thanks to Dr. Inaam Hani kadhim for her assistance in the nuclear laboratory. Finally, I thank my husband, Dr. Mohammad Ghanim Merdan, for his support and assistance throughout my research journey.

Faten

Supervisors' Certificate

We certify that this thesis entitled "**Determination of the Natural Radioactivity in Children's Food and the Effect of Radiotherapy on CBC**" was prepared by the student (**Faten Ahmed Mahdi Hussein**) under our supervision at the College of Education for Pure Sciences, University of Babylon as partial fulfillment of the requirement for the Degree Doctor of Philosophy in Education / Physics.

Signature:
Name: Dr. Fouad A. Majeed
Title: Professor
(Supervisor)
Date: / / 2023

Signature:
Name: Dr. Nihad A. Salih
Title: Professor
(Supervisor)
Date: / / 2023

Head of the Department Certificate

In view of the available recommendations, I forward this thesis for debate by the examining committee.

Signature:
Name: Dr. Khalid Haneen Abass
Title: Professor
(Head of Physics Department)
Date: / / 2023

Scientific Supervisor Certification

This is to certify that I have read this thesis, entitled "**Determination of the Natural Radioactivity in Children's Food and the Effect of Radiotherapy on CBC**" and I found that this thesis is qualified for debate.

Signature:

Name: Dr. Murtadha Shakir Aswood

Title: Professor

Address: University of Al-Qadisiyah, College of Education,
Department of Physics.

Date: / / 2023

Scientific Supervisor Certification

This is to certify that I have read this thesis, entitled "**Determination of the Natural Radioactivity in Children's Food and the Effect of Radiotherapy on CBC**" and I found that this thesis is qualified for debate.

Signature:

Name: Dr. Fadhil I. Sharrad

Title: Professor

Address: University of Alkafee, College of Health and Medical Technology.

Date: / / 2023

Linguistic Supervisors Certification

This is to certify that I have read this thesis, entitled "**Determination of the Natural Radioactivity in Children's Food and the Effect of Radiotherapy on CBC**" and I found that this thesis is qualified for debate.

Signature:

Name: Dr. Ahmed Rawdhan Salman

Title: Asst Prof

Address: University of Al-Mustaqbal

Date: / / 2023

Committee Certificate

We certify that we have read the thesis entitled "**Determination of the Natural Radioactivity in Children's Food and the Effect of Radiotherapy on CBC**" for the student (**Faten Ahmed Mahdi Hussein**) as a committee examining the student in its contents and according to our opinion, it is accepted as a thesis for Degree of Doctor of Philosophy in Education / Physics.

Signature:
Name: Dr. Ali Khalaf Hasan
Title: Professor
(Chairman)
Date: / / 2023

Signature:
Name: Dr. Khalid S. Jassim
Title: Professor
(Member)
Date: / / 2023

Signature:
Name: Dr. Salar H. Ibrahem
Title: Assistant Professor
(Member)
Date: / / 2023

Signature:
Name: Dr. Inaam H. Kadhim
Title: Assistant Professor
(Member)
Date: / / 2023

Signature:
Name: Dr. Fatima M. Hussain
Title: Assistant Professor
(Member)
Date: / / 2023

Signature:
Name: Dr. Fouad A. Majeed
Title: Professor
(Member / Supervisor)
Date: / / 2023

Signature:
Name: Dr. Nihad A. Salih
Title: Professor
(Member / Supervisor)
Date: / / 2023

Approved by the Council of the College of Education for Pure Sciences.

Signature:
Name: Dr. Bahaa H. Rabee
Title: Professor
(Dean)
Date: / / 2023

Abstract

The natural radioactivity levels were investigated in various types of food samples commonly consumed by children in Iraq and estimated the radiation hazard indices and annual effective doses due to the intake of natural radionuclides. A total of 59 food samples of powdered milk, biscuit, indomie, chips, cerelac, and corn flakes were collected and analyzed using gamma spectroscopy with NaI(Tl) detector.

The measured specific activity, annual effective dose (AED), excess lifetime cancer risk factor (ELCR), radium equivalent activity (Ra_{eq}), and internal hazard index (H_{in}) were calculated and assessed. All the results for the natural radionuclides in the food samples were compared within the worldwide median ranges declared in the United Nations Scientific Committee on the Effects of Atomic Radia (UNSCEAR) report.

The results for the specific activity showed that $^{40}K > {}^{238}U > {}^{232}Th$ for milk and cerelac, whereas for biscuit, indomie, chips, and corn flakes, the values have to be $^{40}K > {}^{232}Th > {}^{238}U$. The lowest and highest values of the average specific activity for ^{40}K were 190.459 $\pm$ 2.8 Bq/kg for chips and 283.316 $\pm$4.793 Bq/kg for cerelac, respectively. These results indicate significant differences between those for ^{40}K compared with the highest measured values for ^{232}Th and ^{238}U of 16.314 $\pm$0.797 Bq/kg and 18.2 $\pm$ 1.16 Bq/kg for biscuit and milk, respectively. The high measured value of total AED is 1.470 mSv/y for biscuit (children case), while the lowest value was observed in chips (0.147 mSv/y).

The influence of these results leads to the highest and lowest ELCR values of 5.145×10^{-3} and 0.514×10^{-3} for biscuit and chips, respectively. The evaluation results for other food samples lie within these ranges, and for all these types of foods, excluding biscuits, the AED results were below the worldwide limit of 1 mSv/y. For Ra_{eq}, the highest calculated value of 52.151 Bq/kg was found for powdered milk, while the lowest value of 44.731 Bq/kg for chips.

However, all values were below the worldwide average limit of 370 Bq/kg. Powdered milk samples had the highest internal H_{in} value of 0.190, while chips samples had the lowest value of 0.149, and all values were below the allowable limit of 1. Overall, the results indicated that the natural radioactivity levels in the analyzed samples of Iraqi childrens food pose a minimal radiation risk.

Furthermore, the thesis investigated the effects of high radiation doses from radiotherapy on hematological parameters for children treated for cancer at a specialized hospital. The statistical analysis showed a significant decrease for the last month as the following: hemoglobin 9.916 $\pm$ 0.16 g/dl compared with the control of 12.23 $\pm$ 0.46 g/dl; white blood cells 6.523 $\pm$ 0.81 $\times$ $10^3/\mu$L compared with the control of 12.15 $\pm$ 0.60 $\times$ $10^3/\mu$L; and platelets 268.0 $\pm$ 17.61 $\times$ $10^3/\mu$L compared with the control 347.5 $\pm$ 34.25 $\times$ $10^3/\mu$L. A correlation analysis between the annual effective doses of different food types and hemoglobin levels for the patients showed varying degrees of correlation. For cerelac samples, we found a good positive correlation between AED and Hb g/dl with a correlation coefficient is $R^2 = 0.68$. However, while the natural radioactivity levels in the analyzed food samples were found to pose a minimal risk to children in Iraq, the high radiation doses received during cancer treatment can have adverse effects on blood parameters.

Contents

List of Abbreviations & Symbols

Abb. Symbol	Abb. Definition
AED	Annual Effective Dose
Sv	Sievert
y	year
Bq/kg	Becquerel per kilogram
CBC	Complete Blood Count
DL	Detection Limit
ELCR	Excess Lifetime Cancer Risk
HIC	Hazard Index of Carcinogenicity
$t_{1/2}$	Half-Life
IAEA	International Atomic Energy Agency
H_{in}	Internal Hazard Index
IR	Ionizing Radiation
kg	Kilogram
MeV	Mega-electron Volt
NaI(Tl)	Sodium Iodide (Thallium-doped)
NCRP	National Council on Radiation Protection and Measurements
Ra_{eq}	Radium Equivalent Activity
UNSCEAR	United Nations Scientific Committee on the Effects of Atomic Radia
Hb	Hemoglobin level
WBC	White Blood Cells level
PLT	Platelets Level
μ L	Micro Litter= 10^{-6} Litter
SD	Standard Deviation
g/dl	grams (g) per deciliter (dl)=10 (grams/Litter)

List of Tables

List of Figures

Chapter 1

General Introduction

1.1 Introduction

A radionuclide is a nuclide that has an imbalanced and unstable nucleus. It is also known as a radioactive nuclide. An atom that has both a specified atomic number and a definite neutron number is referred to as a nuclide. The term atom originates from the Greek word atomos, which means indivisible.The prefix a- means not, and the word tomos means a cut. The smallest component of a chemical element is called an atom, and it may be found as a tiny structure in all of the common stuff that surrounds us [1, 2]. A radionuclide is a nuclide whose nucleus is asymmetrical and unstable. A nuclide is an atom that has both an atomic number and a neutron number that may be specified. Natural radioactivity is pervasive in the earth's environment and exists in a variety of geological formations in soil, minerals, vegetation, water, and air. Numerous things around us, including food, oxygen, and buildings, are radioactive and contain various radionuclides. Even though they are radioactive, they can be viewed as a background level, within which humans and all other living organisms can survive unless there is an effect on the environment that causes this level to rise due to human activities. These radionuclides are of natural origin, and concern about them began in 1904 when radium scales were discovered in oil and gas industries' pipes, pumps, and other equipment. This natural radionuclide has a term called NORM, but this term is now associated with the presence of natural origin radionuclides [3–5].

International Atomic Energy Agency (IAEA) defines NORM (Natural

Occurring Radioactive Material) as Radioactive material comprising no significant quantities of radionuclides other than naturally occurring radionuclides. NORM has multiple origins, including the formation of the earth, cosmic radiation, and human activities. Cosmic rays, primordial radionuclides, and secondary radionuclides are the three principal categories [6].

1.2 Natural Decay Series

Radioactive decay involves the release of energy in the form of ionizing radiation, which can encompass alpha particles, beta particles, and gamma rays. This process takes place within unstable atoms referred to as radionuclides. Essential sources of NORM, primordial radionuclides in the earth's crust, have a lengthy half-life and were present at the earth's formation. ^{238}U, ^{235}U, and ^{232}Th are the most critical natural radionuclides of primary origin, and they incessantly produce secondary radionuclides that are radioactive and decompose into their other products, constituting a radioactive decay chain. The first member of each series has a very long half-life and is a gas; the last member of each series is a stable lead isotope [7, 8].

All heavy elements with an atomic number greater than $z > 83$ are radioactive. They decay and generate daughters, forming a series of radionuclides that terminate with stable lead. There are three main series, and all radionuclides found in nature belong to one of them. The Uranium series as presented in Fig. (1.1) begins with $^{238}_{91}$U and ends with $^{206}_{82}$Pb and has a half-life of $t_{1/2} = 4.468 \times 10^9$ years, with ^{230}Th, ^{226}Ra, and ^{222}Rn being the most prominent subseries. ^{226}Ra decomposes into ^{222}Rn, a noble gas with a half-life of $t_{1/2} = 3.82$ days. A significant concern regarding ^{222}Rn is that its short-lived alpha emitter offspring ^{218}Po and ^{214}P pose health risks. The house in which we reside, our place of employment, and building materials

may contain ^{222}Rn that has been transferred from the soils and rocks to the atmosphere and then to the buildings with low airflow, where it may reach high concentrations and cause a large fraction of the annual dose to the general public. In 1990, the Health Protection Agency (HPA) took action to control and limit the risk, recommending that the average level of radon is 200 Bq/m^3, and if it exceeds this level, the homeowner must take action. People exposed to high radon levels may develop lung cancer, the other reason for lung cancer after smoking [8]. The shortest series begins with $^{232}_{90}$Th (see Fig. (1.2)), ends with $^{208}_{82}$Pb, and has a half-life of $t_{1/2} = 1.39 \times 10^{10}$ years. Uranium actinium has a half-life of $t_{1/2} = 7.038 \times 10^8$ years, beginning with $^{235}_{92}$U and ending with stable $^{207}_{82}$Pb as shown in Fig. (1.3) [9, 10].

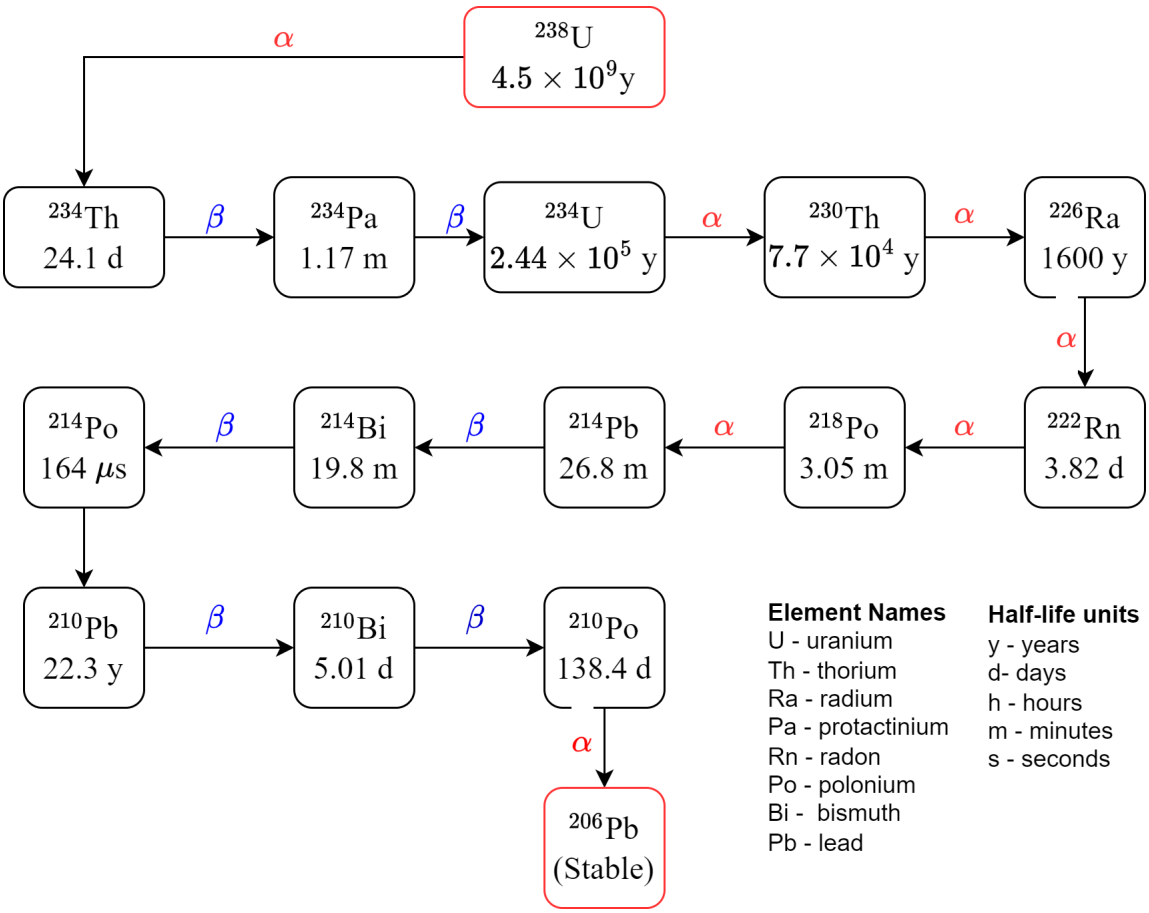

Figure 1.1: The ^{238}U radioactive decay series.

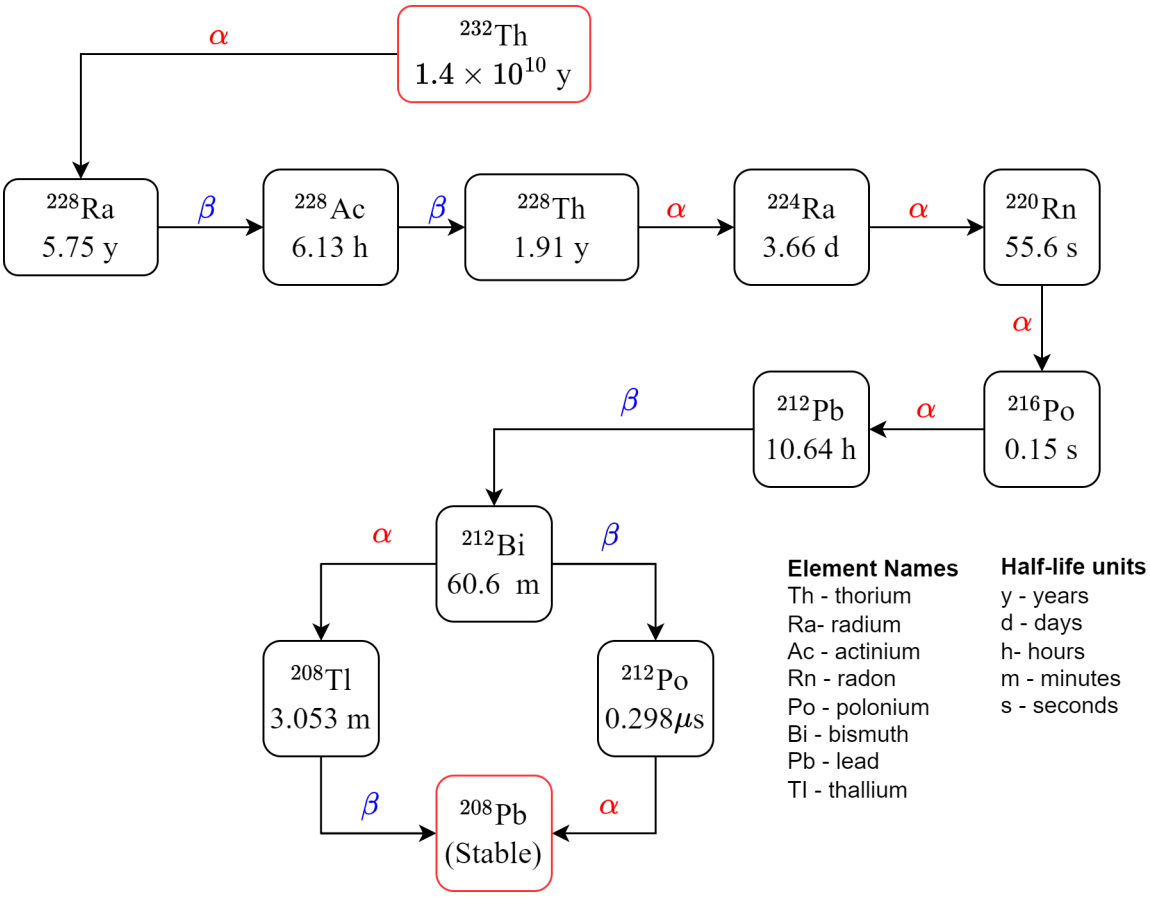

Figure 1.2: The ^{232}Th radioactive decay series.

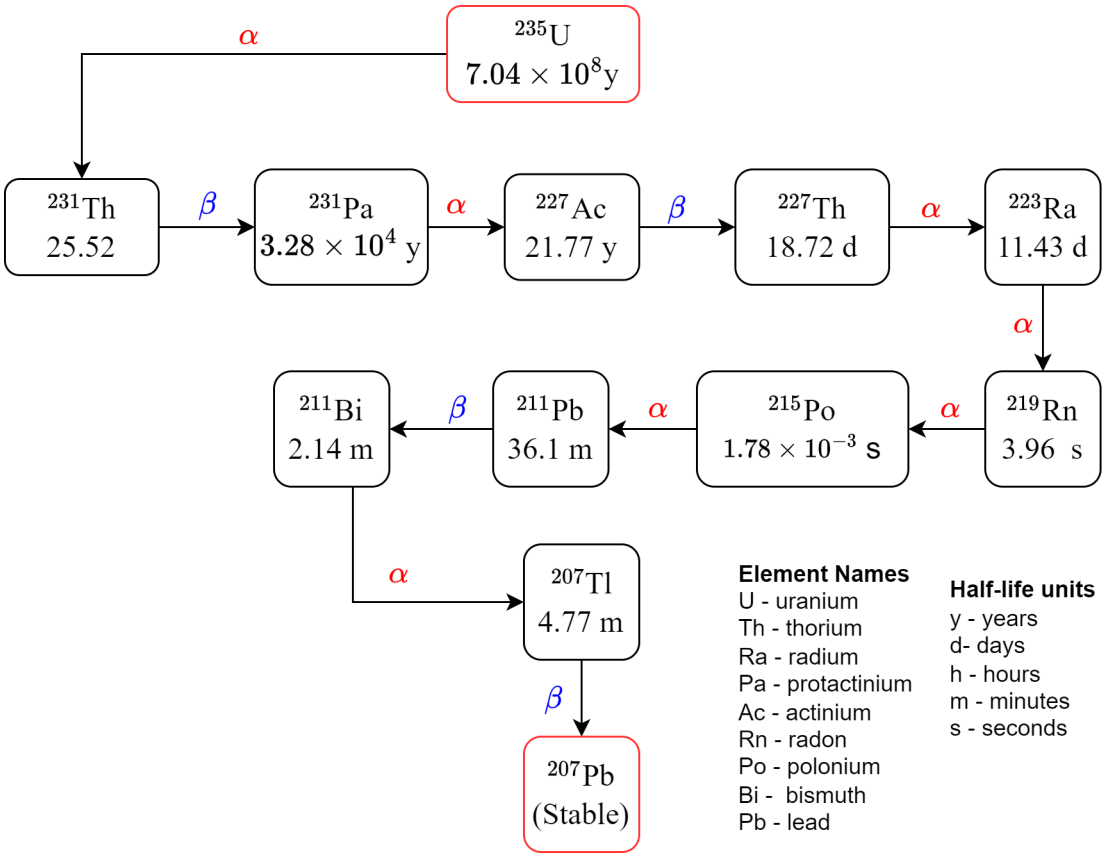

Figure 1.3: The ^{235}U radioactive decay series.

1.3 Sources of Nuclear Radiation

The release of energy in the form of high-speed charged particles or electromagnetic waves is referred to as nuclear radiation, also known as ionising radiation. Radiation may originate from a wide variety of sources, including natural and man-made ones. Rocks, sunshine, and cosmic rays are the primary sources of background radiation that all living things are subjected to on a continuous basis. Radiation coming from a variety of sources hits us constantly and incessantly. Every living thing that has ever lived on Earth has done so in an environment in which it has been subjected to radiation coming from the planet's natural background. Humans and other species have only very lately been exposed to artificial sources that have been produced over the course of the previous century or so. Over eighty percent of our radiation exposure comes from natural sources, while the remaining twenty percent comes from radiation produced by artificial sources, most of which are radiation applications used in medical settings [8, 11].

We can classify different types of radiation exposure according to their origins, with an emphasis on what the general population is exposed to. Radiation exposure is taken into account for a variety of different groups for the objectives of regulatory agencies (such as radiation protection). Because of this, extra information on patients, who are exposed owing to the medical use of radiation, as well as those who are exposed at workplaces, is supplied here. Irradiation is yet another classification system that may be used for radiation exposure [12, 13].

Our bodies may be irradiated from the outside or externally by radioactive chemicals and radiation that are present in the environment. If we breathe in the chemicals while they are in the air, ingest them when they are in our food and drink, or absorb them through our skin and open wounds, then they will

irradiate us from the inside out. When compared on a global scale, the dosages received from internal and exterior exposure are about equivalent [14–18].

1.4 Natural sources

Since the beginning of time, the environment of the Earth has been subjected to radiation from a variety of sources, including cosmic rays as well as radioactive elements present in the planet's crust and core. There is no way to escape being exposed to radiation from these natural sources, which, in reality, are the primary contributors to the radiation exposure experienced by the majority of the people of the globe. The effective yearly dosage received by a person varies from 1 to more than 10 mSv depending on where they reside in the world, with the worldwide average being approximately 2.4 mSv. There is a radioactive gas known as radon that may get trapped inside buildings, or the building materials themselves may contain radionuclides that result in increased radiation exposure. Even though the sources are found in nature, the amount of exposure we get may be altered by the decisions we make about how and where we live, as well as the foods and beverages we consume [14, 19, 20]. The sources of radiation are summarized in Fig. 1.4, and we can discuss them in detail in the following sections.

1.4.1 Cosmic sources

A significant portion of one's natural radiation exposure comes from the sun's cosmic rays. Although the vast majority of these rays come from far out in interstellar space, the sun also emits some of them when it experiences solar flares. They not only irradiate the Earth itself, but they also interact with the atmosphere, which results in the production of a variety of forms of radiation and radioactive material. They constitute the most significant source of radiation

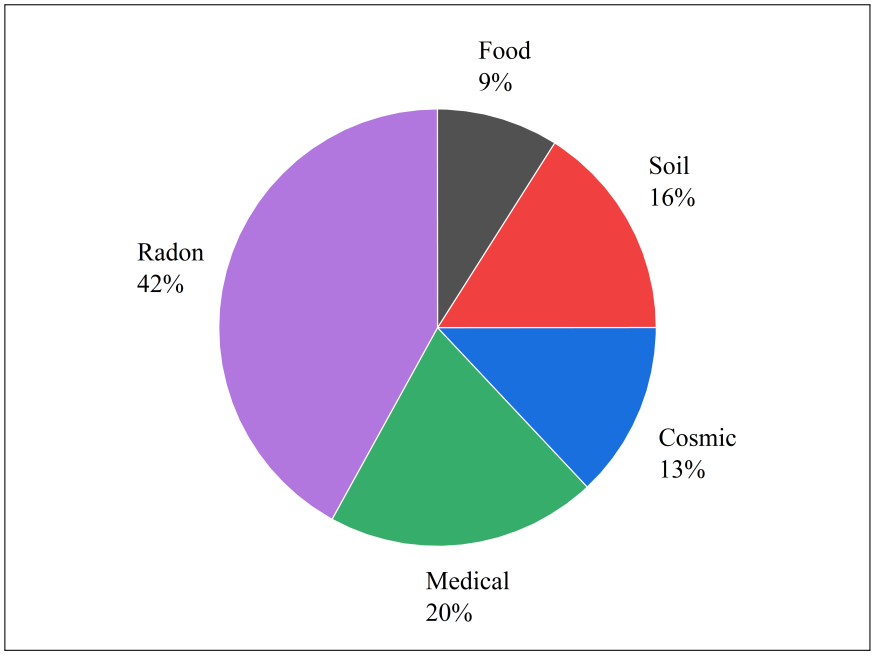

Figure 1.4: Distribution of radiation exposure all across the world [14].

in the cosmos. Even while the atmosphere and magnetic field of the Earth significantly decrease the amount of cosmic radiation that reaches the surface, there are still regions on the planet that are more susceptible to the effects of the radiation than others. The North Pole and the South Pole get a greater amount of cosmic radiation than the equatorial areas because the magnetic field deflects it to those places [21, 22].

Additionally, the amount of exposure rises with altitude since there is less air above to function as a barrier. This makes the level of exposure higher. Therefore, individuals who live at sea level get, on average, an effective dosage of around 0.3 mSv yearly from cosmic sources of radiation. This accounts for roughly 10-15 percent of the overall dose that they receive from natural sources. People who live at an altitude of more than 2,000 meters get several times this amount. As the radiation exposure from cosmic sources relies not only on altitude but also during the duration of flights, it is possible that passengers on aeroplanes will be subjected to even larger doses. This is because the height is just one factor in the calculation. For instance, at cruising altitudes, the average effective dosage for a 10-hour trip is between 0.03 and 0.08 mSv [14, 23].

1.4.2 Terrestrial sources

Terrestrial radiation is the term given to the radiation released by radioactive materials found in the rocks, soils, and minerals of the Earth. Elements such as radon (Rn), radon progeny, which are the relatively short-lived decay products of ^{226}Ra, ^{40}K, isotopes of thorium, and isotopes of uranium are responsible for the majority of the radiation that is emitted from the Earth's surface. The degree of exposure to the elements is very variable from one region to the next [24, 25].

According to studies conducted in countries such as France, Germany, Italy, Japan, and the United States, for instance, over 95% of the populace reside in places where the average yearly dosage of radiation received from the outdoors ranges from 0.3 to 0.6 mSv. However, it is possible for humans to get doses that are greater than one mSv on a yearly basis in some parts of these nations. There are other locations on our planet that have an even greater background level of radiation exposure from terrestrial sources. For instance, on the southwestern coast of Kerala in India, there is a 55-kilometre-long strip of land that is heavily inhabited and includes thorium-rich sands. In this area, individuals absorb an average of 3.8 mSv of radiation each year. There are also reported to be areas in Brazil, China, the Islamic Republic of Iran, Madagascar, and Nigeria that contain significant quantities of naturally occurring terrestrial sources of radiation [14, 26].

1.4.3 Sources in Food and Drink

Primordial and perhaps other radionuclides may be found in food and drink, the majority of which come from natural sources. Rocks and minerals that are present in the water and soil may be a source of radionuclides, which can subsequently be passed on to plants and eventually to animals. Because of this, the dosages are different based on the amounts of radionuclides in the food and

water as well as the eating habits of the local population. For instance, fish and shellfish contain relatively high levels of ^{210}Pb and ^{210}Po, and as a result, persons who consume significant quantities of seafood may get considerably larger doses of these radioactive elements than the general population does [7].

People who live in northern locations and consume substantial quantities of reindeer meat are exposed to dosages that are comparably greater than the average person. Because reindeer in the Arctic feed on lichen, their bodies have collected unusually large quantities of the radioactive isotope ^{210}Po. According to estimations provided by UNSCEAR, the average effective dose received from natural sources in food and drink is 0.3 mSv. This is mostly attributable to ^{40}K as well as radionuclides belonging to the ^{238}U and ^{232}Th families. In addition to radionuclides originating from natural sources, radionuclides originating from man-made sources may also be found in foodstuffs. On the other hand, the contribution that these radionuclides' allowed emissions to the environment make in terms of dosage is often not very significant at all [16, 27].

1.5 Artificial Sources

Since the beginning of the 20th century, scientists have learned to harness the power of the atom for a broad range of applications, including those in the fields of medicine (such as the treatment of cancer), the generation of electricity (such as smoke detectors), and the military. As a result, the number of radiation applications has expanded substantially over the course of the last few decades. Both individuals and the community as a whole get an additional radiation dosage as a result of these and other artificial sources, which adds to the radiation dose received from natural sources. The individual dosages of radiation received from man-made sources of radiation are very variable. The majority of individuals get a dosage that is far lower than the average from these

kinds of sources, while a few people get doses that are very higher. Radiation protection techniques are typically effective in controlling the level of radiation emitted by artificial sources [7, 14].

1.6 Medical Applications of Radiation

Since the application of radiation in medicine for the purposes of diagnosing and treating certain diseases plays such an essential role, it is currently, by far, the most important artificial source of exposure in the world. After natural sources, it is the second largest contributor to population exposure globally, accounting for around 20 percent of the total. On average, it is responsible for 98 percent of the radiation exposure that is caused by all manmade sources combined. In developed countries, where there are greater resources for medical care available and, as a result, much more extensive use of radiology equipment, the vast majority of people are subjected to this type of radiation. This has even resulted in some nations having a yearly average effective dose from medical usage that is comparable to the one from natural sources. This is the case in several countries [14, 28, 29].

There are several important distinctions to be made between medical exposure and the majority of the other types of exposure. In contrast to other types of exposure, medical exposure often only affects a limited region of the body. Other types of exposure, on the other hand, frequently affect the entirety of the body. In most cases, the age range of patients spans a longer span of years than does the age range of people in the general population. In addition, considering that patients gain an indirect benefit from their exposure, it is imperative that the doses that result from medical exposure be compared with those that arise from other sources with extreme caution [14, 30–34].

The field of **diagnostic radiology** focuses on interpreting images produced

via X-rays in procedures such as plain radiography (such as chest or dental X-rays), fluoroscopy (such as with barium meal or enema), and computer tomography. The UNSCEAR does not discuss imaging techniques that use non-ionizing radiation, such as ultrasound or magnetic resonance tomography [35].

In order to detect and treat disorders, **interventional radiology** makes use of image-guided methods that are only minimally intrusive (for example, to guide a catheter inside of a blood artery). The worldwide average effective dose from diagnostic radiological procedures increased from 0.35 mSv in 1988 to 0.62 mSv in 2007, almost doubling from its previous value of 0.35 mSv. This increase may be attributed to the increased usage of CT, which has a large dosage per examination. The most recent study that was conducted by UNSCEAR found that CT scanning is currently responsible for 43 per cent of the total collective dose that is caused by radiology. These figures might be different depending on where you live. Approximately 25 per cent of the global population that lives in developed nations receives around two-thirds of all radiological operations. Even with relatively straightforward dental X-ray exams, the yearly frequency of treatments that are performed on the remaining 75% of the world's population has remained rather stable [36].

Nuclear medicine is the practice of administering radioactive chemicals into the body in an unsealed form (that is, in a form that is soluble and is not encapsulated). This is done mostly to produce pictures that offer information on either the structure or the function of an organ and less often to treat specific conditions, including hyperthyroidism and thyroid cancer. In most cases, a radionuclide will be altered in order to produce a radiopharmaceutical, which will then typically be given either intravenously or orally. After that, it travels throughout the body in a pattern determined by its physical or chemical properties, which enables a scan to be performed. Therefore, the radiation that

is released from the radionuclide inside the body is analyzed so that diagnostic pictures may be produced from it or it is utilized to cure ailments. From about 24 million in 1988 to approximately 33 million in 2007, the number of diagnostic procedures using nuclear medicine saw significant growth globally. This led to a substantial rise in the yearly collective effective dosage, which went from 74,000 to 202,400 man Sv as a consequence. The use of nuclear medicine for therapeutic purposes is expanding as well, now reaching over 0.9 million people annually throughout the globe. Again, there is a significant geographical divide in the use of nuclear medicine, with industrialized nations accounting for 90 per cent of all exams [28, 29].

Radiation therapy, which is also known as radiotherapy, is a kind of treatment that makes use of radiation to treat a variety of ailments, most often cancer but also benign tumors. External radiotherapy, often known as teletherapy, is a method of treating patients that involves the use of a radiation source that is located outside of the patient's body. In this method, either a device that contains a highly radioactive source (often cobalt-60) or a high-voltage device that emits radiation (such as a linear accelerator) is used. The placement of radioactive sources into a patient, either temporarily or permanently, for the purpose of treatment is referred to as brachytherapy. This therapy may be conducted either momentarily or permanently [37, 38].

During the years 1997-2007, an estimated 5.1 million patients were treated yearly with radiation all across the world. This number is increased significantly from the estimated 4.3 million patients treated in 1988. Approximately 4.7 million patients were treated with teletherapy, whereas 0.4 million were treated using brachytherapy. Seventy percent of all radiation treatments given throughout the globe and forty percent of all brachytherapy operations are administered to the population that makes up the 25 percent that lives in developed nations [39, 40].

Patients are subjected to high amounts of radiation as part of the treatment process for some types of medical conditions, such as radiotherapy, interventional radiology, and nuclear medicine. When used improperly, they have the potential to cause severe injury or even result in death. Patients, as well as doctors and other staff members who were in the area at the time, are among the individuals who are in danger. Errors made by humans have been the primary contributor to most of these mishaps. Some examples include administering the incorrect dosage as a result of mistakes in treatment planning, failing to utilize equipment in the appropriate manner, and exposing the incorrect organ or, on rare occasions, the incorrect patient. Even though major radiation mishaps are uncommon, over one hundred of them have been recorded. Fig. 1.5 presents the findings of the worldwide study, which are given in terms of percentages of the number of times exams or procedures were performed, as well as the total doses received from all of these modalities combined [39].

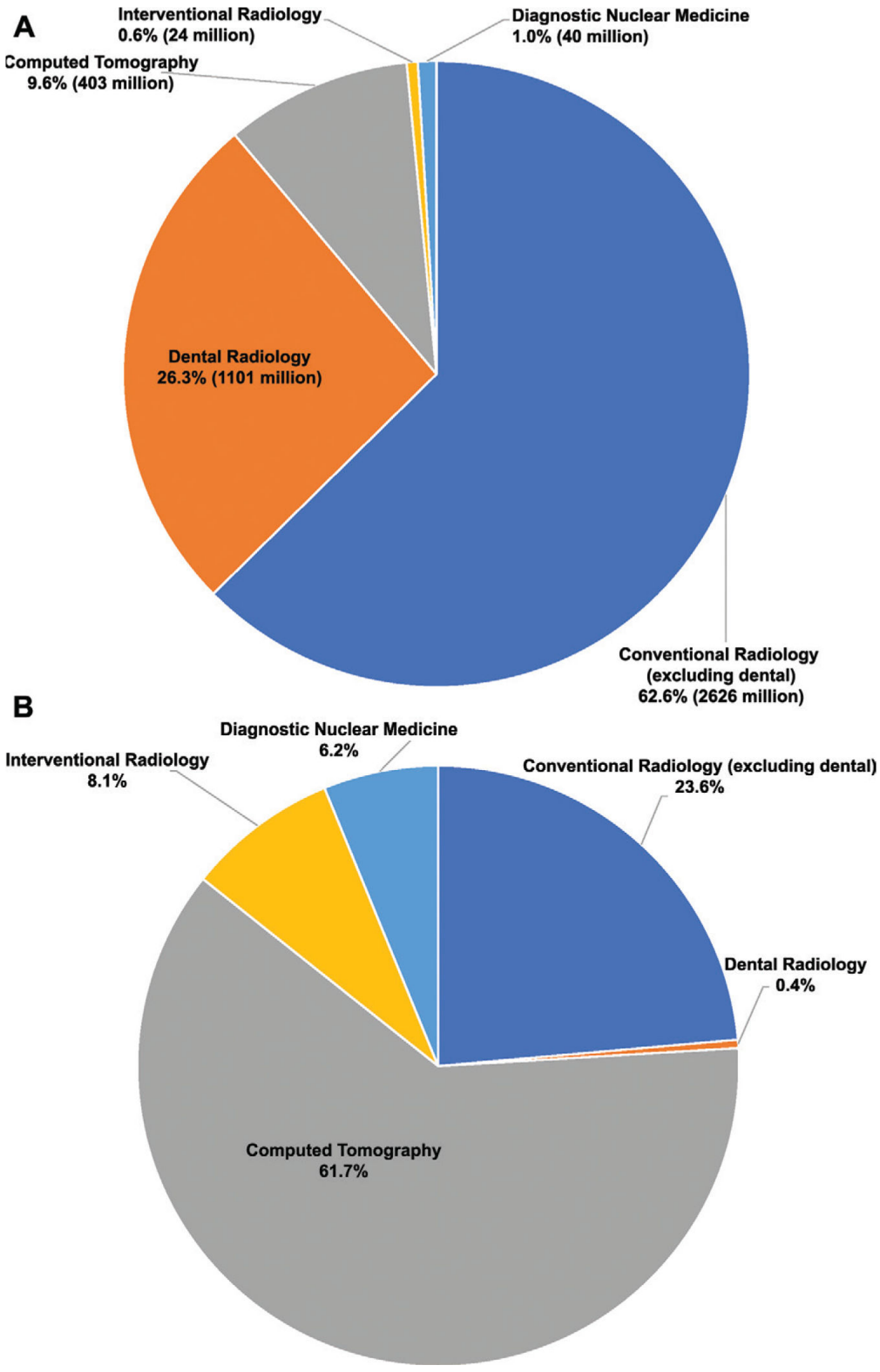

Figure 1.5: Relative contributions, per modality category, to (A) estimated global yearly number of examinations and/or procedures (2009-2018) and (B) estimated annual collective effective dose (based on tissue weighting parameters established by the International Commission for Radiological Protection) [39].

1.7 Cancer and Effects on Children

Cancer is a group of diseases characterized by abnormal cell growth that can invade or spread to other regions of the body. Cancer is the second most prevalent cause of death overall, after cardiovascular disease, in developed countries, yet it is responsible for around twenty percent of all deaths. Even in cases when the individual has never been exposed to radiation, there is still a risk that they may acquire cancer some time during their lifetime. This risk is estimated to be about forty percent of the general population. In recent years, the types of cancer diagnosed most frequently in males have been lung, prostate, colorectum, stomach, and liver cancer. In contrast, the types of cancer diagnosed most frequently in women have been breast, colorectum, lung, cervix, and stomach cancer [41, 42].

The progression of cancer is a complicated process that takes place over the course of several phases. The process is started by a phenomenon known as an initiating phenomenon, which most likely affects a single cell. However, a sequence of additional occurrences is necessary before the cell can turn malignant and the tumor can form. Human health effects are contingent on a variety of physical factors. As a result of anatomical and physiological differences, the effects of radiation exposure on children and adults vary. In addition, because children have smaller bodies and less protection from overlying tissues, the dose to their internal organs will be greater for a given external exposure than for adults. Additionally, because children are shorter than adults, they may be exposed to higher quantities of radionuclides deposited on the ground [14, 43].

Regarding internal exposure, because children are smaller and their organs are therefore closer together, radionuclides concentrated in one organ are more likely to irradiate other organs than in adults. Children are more likely than

adults to develop cancer after exposure to radiation, but it may not manifest until they reach the age at which cancer typically manifests. Regarding the induction of cancer, radiosensitivity refers to the incidence of tumors caused by irradiation. According to studies comparing the radiosensitivity of adults and children, children are more susceptible to developing thyroid, brain, skin, and breast cancer, as well as leukemia. Children's early health effects following exposure to high concentrations of radiation (such as those received in radiotherapy) are complex and can be explained by the interaction of various tissues and biological mechanisms. Some effects are more evident in childhood than in maturity (e.g., brain defects, cataracts, and thyroid nodules), and children's tissues are more resistant to certain effects (e.g., lungs and ovaries) [14].

1.8 Radiation Therapy and Complete Blood Count (CBC)

A complete blood count (CBC), often referred to as a full blood count (FBC), is a series of tests performed in a medical laboratory that gives information about the cells that are present in a person's blood. These tests can also go by the name "complete blood count". The complete blood count (CBC) provides information on the number of white blood cells, red blood cells, and platelets in addition to the concentration of hemoglobin and the hematocrit, which represents the volume percentage of red blood cells. A white blood cell differential, which counts the various types of white blood cells, and the red blood cell indices, which reflect the average size and hemoglobin content of red blood cells, are both provided. Additionally, a white blood cell differential may be included in the report [44].

The quantity of white blood cells, commonly known as leukocytes, in the blood, is measured by the white blood cell count (WBC count). White blood

cells, which aid the body in its battle against illness. A white blood cell count that is abnormal may be an indicator of an infection, inflammation, or other form of stress in the body. An illustration of this would be how a bacterial infection can induce a significant rise or reduction in the white blood cell count. The human body has five distinct subsets of white blood cells (WBC). Inflammation or infection can be found everywhere in the body if the white blood cell count is high. On the other hand, if the WBC count is low, it may indicate that the individual is more susceptible to certain diseases, such as blood marrow disorders or auto-immune disorders. The high number may mean Infection, inflammation, leukemia, intense exercise, stress, corticosteroids. The normal range for WBC is between 4,000 and 10,000 cells/μL [45, 46].

Red blood cells (RBC) contain a specific kind of protein called hemoglobin (HGB). Red blood cells transport oxygen throughout the body. Because it is primarily responsible for transporting oxygen throughout the body, hemoglobin is an extremely vital component of the human body. It is also possible to use it to check how effectively therapy for anemia is working.The Normal Range for hemoglobin men 13-17 gm/dl, women 12-15 gm/dl [47, 48].

The platelet count (also known as PLT) is an essential component in the process of blood clotting and the control of bleeding. Platelets will cluster together and seal an injured blood vessel until the blood clots. This happens when a blood vessel is damaged. When the number of platelets in the blood is too low, a person's risk of bleeding in any region of the body increases significantly. Platelet counts that are abnormally low (known medically as thrombocytopenia) or abnormally high (known medically as thrombocytosis) are typically an indication of an underlying medical issue; however, they can also constitute a negative reaction to medicine. The normal range for platelets is between 150,000 to 410,000 per μL of blood [49].

The high-energy radiation dosage can affect a complete blood count (CBC) test, mainly if the patient receives a high radiation dose. As we mentioned, the CBC test measures the levels of various blood components, including red blood cells, white blood cells, and platelets. Radiation therapy can harm the bone marrow, where blood cells are produced, leading to changes in blood cell numbers and function. The extent to which CBC test results are affected by radiation therapy depends on various factors, such as the dose of radiation, the duration of the treatment, and the location of the radiation field [27, 50].

1.9 Literatures Reviews

F. E. Yang et al., in 1995, conducted a study to analyze the behavior of peripheral blood levels during partial body radiation therapy. The findings indicated a significant decline in leukocytes during the first week of treatment, followed by a 3.3% decrease per week until week 7. The total mean leukocyte decrease over seven weeks was 30%. Platelets declined by 9% on average during the first week and then by 1.4% per week. Hemoglobin levels did not show a statistically significant decrease. The study concluded that localized breast and prostate cancer patients are unlikely to require routine CBCs if initial levels are normal. The authors suggested that avoiding weekly CBC blood levels in these patients alone could potentially result in savings of up to $40 million a year nationally [51].

F. L. Melquiades and C. R. Appoloni, in 2004, measured the radioactivity levels of powdered milk samples and discussed radionuclide transference from the environment to humans. They quantified ^{40}K, ^{137}Cs, and ^{208}Tl radionuclides using high-resolution gamma-ray spectrometry and an HPGe detector. The average activity of ^{40}K was 482 ± 37Bq/kg, while the lower level of detection for ^{137}Cs and ^{208}Tl was 3.7 ± 1.1 and 0.5 ± 0.2(Bq/kg), respectively. The levels of natural radioactivity were found safe for human consumption without any restrictions [52].

Zaid Q. Ababneh et al., in 2009, measured the activity concentrations of ^{40}K, ^{226}Ra, ^{228}Ra and ^{137}Cs in 14 brands of powdered milk consumed in Jordan. The milk samples were imported from countries including New Zealand, Argentina, and Europe. The average ^{40}K concentration was 348 ± 26 Bq kg^{-1}. ^{226}Ra and ^{228}Ra were only detected in 5 brands, with concentrations

of 0.50-2.14 and 0.78-1.28 Bq kg^{-1} respectively. ^{137}Cs showed geographical variations, being undetected in milk from Argentina, uniformly distributed in European milk at 0.43 ± 0.05 Bq kg^{-1}, and varying from undetected to 1.55 Bq kg^{-1} in New Zealand milk. The estimated annual effective dose from ingestion was highest for infants at 332 mSv, followed by children at 138 mSv, and adults at 43 mSv. The results indicate that the radioactivity levels in powdered milk consumed in Jordan do not pose a significant radiation dose to the public. [53].

N. Sarayegord Afshari et al., in 2009, measured the concentration of natural radionuclide ^{40} K in milk and milk powder samples consumed in Tehran, Iran. Using gamma spectrometry, they found the average activity concentrations for ^{40}K in milk and milk powder to be 31.0 ± 6.1 and 17.1 ± 3.3 Bq/kg, respectively. The effective dose was calculated to be 14 μSv/y for adults and in the range of 6.4-15.9 μSv/day for children. The authors concluded that the obtained data from liquid milk samples showed an almost uniform distribution of ^{40}K and the calculated effective doses were too low to induce important health hazards [54].

T. Alrefae et al., in 2012, investigated the radioactivity of long-lived gamma emitters in breakfast cereal consumed in Kuwait and estimated the annual effective doses to various age groups. Samples of 27 different brands of breakfast cereal originating from 9 different countries were collected from the local market and analyzed for ^{238}U, ^{232}Th, and ^{40}K. While ^{40}K was detected in all samples, ^{238}U and ^{232}Th were detected in most samples. The activity concentration of each targeted radionuclide varied from one sample to another. The estimated annual effective doses were 129, 185, and 351 μSv/y for the adult, child, and infant age groups, respectively. The obtained activity concentrations were found to agree with those reported in the literature, and the estimated

annual effective doses were found to be safe [55].

J. H. Al-Zahrani, in 2012, studied the concentration of natural radioactivity and heavy metals in powdered infant's milk consumed in Saudi Arabia. They found that the main radioactivity detected was ^{40}K, with an average activity of 234.18 ± 1.9 Bq/kg, while the average activities of ^{238}U and ^{232}Th were 0.46 Bq/kg and 0.35 Bq/kg, respectively. The heavy metals detected were Fe, Zn, Mn, Cu, and Pb, with daily intake levels below the limit proposed by US-IPA. The total average effective dose due to annual intake of ^{238}U, ^{232}Th, and ^{40}K from the ingestion of the powdered milk for infants was estimated to be lower than the allowed value of 1mSv. This study provides baseline data for radiation and heavy metals exposure to infant's milk and their impact on infant's health [56].

Ali. Abid Abojassim et al., in 2014, measured the specific activity of uranium (^{238}U), thorium (^{232}Th), and potassium (^{40}K) in 12 different types of wheat flour samples from Iraqi markets. They used gamma spectrometry method with NaI(Tl) detector to calculate radiation hazard indices and ingestion effective dose. Results showed that specific activity in wheat flour samples varied from (1.086 $\pm$ 0.0866) Bq/kg to (12.532 $\pm$ 2.026) Bq/kg for ^{238}U, (0.126 $\pm$ 0.066) Bq/kg to (4.298 $\pm$ 0.388) Bq/kg for ^{232}Th, and (41.842 $\pm$ 5.875) Bq/kg to (264.729 $\pm$ 3.843) Bq/kg for ^{40}K. They found that the natural radioactivity, radiation hazard indices, and ingestion effective dose were lower than the safe limits [57].

S. Shahid et al., in 2014, assessed the hematological parameters of medical workers exposed to chronic ionizing radiation in hospitals. The study found that most of the hematological parameters of radiation-exposed workers were below the normal range, with the most affected parameter being mean

corpuscular hemoglobin. There was a decline in platelet count, hematocrit, and lymphocytes, and an increase in neutrophils associated with annual average effective dose. The study suggests that even low doses of chronic ionizing radiation exposure can impact health and alter immune response or cause anemia. Specifically, the study observed a decrease in white blood cell count, lymphocytes, and platelets in radiation-exposed workers compared to the control group [58].

Ali. Abid Abojassim, in 2015 investigated the natural radioactivity of 13 instant noodle samples available in Iraqi supermarkets using gamma-ray spectroscopy. The study found that all specific activities of ^{226}Ra, ^{232}Th, and ^{40}K investigated in the noodle samples were within the threshold limit of UNSECR (2000) standard. Radium equivalent activity and internal hazard indices were also lower than the worldwide average. The study concluded that all the samples of fast noodles (Indomie) available in the Iraqi market are safe for consumption but cautioned against the accumulation of natural radioactivity over time, especially in samples near the threshold limit. The study highlights the importance of monitoring the release of radioactivity into the environment and the need to establish radioisotope concentrations to provide meaningful information on population exposure and setting up base data [59].

Ali. Abid Abojassim et al., in 2015, conducted a study to investigate the natural radioactivity in children's biscuits in Iraq. The study aimed to determine radiation hazard indices and annual effective doses from biscuit consumption among different age groups. The investigation analyzed ten different biscuit samples from three countries collected from the Iraqi market using gamma spectroscopy. The researchers found that the specific activities of ^{238}U, ^{232}Th, and ^{40}K were within safe levels, as were the average radium equivalent activity

and internal hazard index. The estimated total average annual effective dose from consumption by adults, children, and infants was below the worldwide median values for all groups, indicating that the values found for specific activity, radiation hazard indices, and annual effective dose in all samples were lower than worldwide median values for all groups and considered safe [60].

S. Shahid et al. in (2015) conducted a study on the impact of low-dose terrestrial ionizing radiation exposure on the hematopoietic indices of Pakistani inhabitants. The study found that long-term exposure to low-dose ionizing radiation resulted in anemia and immune modulation in radiation-exposed residents. The mean values of several complete blood count (CBC) parameters were examined, and seven CBC parameters, including hemoglobin (HB), white blood cells (WBC), platelets (PLT), hematocrit (HCT), neutrophils (NEUT), mean corpuscular hemoglobin (MCH), and mean corpuscular hemoglobin concentration (MCHC), showed a decrease trend in radiation-exposed residents. The odds of developing low MCH and MCHC were significantly higher for radiation-exposed individuals. However, two CBC parameters, including red blood cells (RBC) and lymphocyte count (LYM), showed an increased trend [61].

Daher. M. Daher, in 2017, conducted a study on the natural radioactivity of chips samples in local Iraqi markets. The study aimed to determine the contents of ^{238}U, ^{232}Th, and ^{40}K in 14 samples of chips using a scintillation detector (NaI(Tl)). The results showed that the average specific activity for^{238}U, ^{232}Th, and ^{40}K were within the allowed world limit, and there was no health effect for humans according to radiation contents. The study concluded that the natural radioactivity in chips samples from local Iraqi markets was comparable to the world limit and did not pose a health risk to humans [62].

Taghreed A. Hafiz et al., in 2018, conducted a study on the efficiency of granulocytes and monocytes in Saudi females with breast cancer following radiotherapy. The study found that patients had a significant reduction in total white blood cell counts, platelets, and lymphocytes count, and a significant increase in red blood cell counts and hemoglobin level at the end of radiotherapy. However, after six weeks, changes in CBC and phagocytic activities of granulocytes and monocytes were non-significant. The study suggests that breast cancer patients in Saudi Arabia may be at hematological and immunological risk following radiotherapy, and their follow-up needs to include the assessment of phagocytic activities besides CBC [63].

Ali Abid. Abojassim et al., in 2019 conducted a study to measure the concentration of natural and anthropogenic radioisotopes in canned milk samples available in Iraq's markets. They found that the specific activities of ^{238}U, ^{232}Th, and ^{40}K in powdered milk samples ranged from 0.115$\pm$0.062 to 25.000$\pm$1.067 (Bq/kg), from 0.562$\pm$0.065 to 2.930$\pm$0.807 (Bq/kg), and from 104.171$\pm$2.984 to 461.351$\pm$8.450 (Bq/kg), respectively. The Radon activity concentrations in liquid milk samples were found to be lower than the reference limits indicated by the World Health Organization and the regulatory bodies of the European Union. The study also estimated the Total Effective Dose associated with exposure due to annual intake of ^{238}U, ^{232}Th, and ^{40}K from ingestion of powdered milk, finding them to be below the recommended reference limits [64].

Anwar. Q. Ahmed et al., in 2019, conducted a study to determine the levels of natural radioactivity in cerelac baby food samples commonly used in Iraq. The study aimed to calculate the specific activity of ^{238}U, ^{232}Th, and ^{40}K, as well as the annual effective dose due to the ingestion of cerelac baby

food available in the Iraqi markets. The samples were collected from the local market in Najaf from different countries of origin. The specific activities for ^{238}U, ^{232}Th, and ^{40}K were found to be within safe limits, with an average value of 8.49±2.18, 4.50±0.80, and 223.85±29.22 Bq/kg, respectively. The study also estimated that the total average annual effective dose caused by ^{238}U, ^{232}Th, and ^{40}K for children is 0.571±0.05 mSv/y, which is lower than the worldwide median values for children, indicating that the cerelac baby food samples tested are safe for consumption [65].

H.N.E. Surniyantoro et al., in (2019), conducted a study to assess the effects of ionizing radiation on the hematological parameters of 74 radiation-exposed workers and 83 controls in several Indonesian governmental hospitals. The results showed that the red blood cell and monocyte counts were significantly higher in radiation-exposed workers compared to controls, while white blood cells, hematocrit, mean corpuscular volume, and lymphocytes values were significantly lower in radiation-exposed workers. Linear regression analysis revealed a significant correlation between equivalent dose and red blood cells, with a decline in RBC level of $0.541\times10^{6}/\mu L$ per 1 mSv increase of radiation dose. The study suggests that further investigations should use a larger sample size and include various independent variables to study the long-term effects of low-dose radiation exposure on radiation-exposed workers [66].

Van-Hao Duong et al., in 2021, analyzed eight popular brands of Vietnamese fresh milk for concentrations of ^{232}Th, ^{238}U, ^{137}Cs, and ^{40}K using gamma-spectrometry. The study found that the concentrations of these radionuclides in all brands ranged from 0.60 ± 0.19 to 2.45 ± 0.24 Bq/kg for ^{232}Th, 1.45 ± 0.18 to 2.45 ± 0.24 Bq/kg for ^{226}Ra, below detection limit to 0.13 ± 0.06 Bq/kg for ^{137}Cs, and 341 ± 6 to 387 ± 7 Bq/kg (dry w.t) for

^{40}K. The calculated annual effective dose for all age groups was similar for all brands and ranged from 0.12 to 0.18 mSv/year, which is far below the World Health Organization's guidance levels of 1 mSv/year for the general public and 0.1 mSv/year for infants. Therefore, the study concluded that all brands of Vietnamese fresh milk investigated are safe for consumption [67].

Ning. Liu et al., in 2021 conducted a prospective cohort study to investigate the correlation between low-dose ionizing radiation and changing hematological parameters among medical workers. The study found that exposure to low-dose ionizing radiation resulted in an increase and then a decrease in platelet counts among the medical workers. The Poisson regression and restricted cubic spline models showed a dose-response relationship between cumulative radiation dose and changing platelets, with a change of β^a $0.008 \times 10^9/L$ during biennially after adjusting for gender, age at baseline, service at baseline, occupation, medical level, and smoking habits. The study highlights the need for monitoring the health effects of low-dose ionizing radiation on medical workers [68].

Jia-Jia Guo et al., in 2022, conducted a prospective cohort study on 705 industrial irradiation workers to assess the dose-response effects of low-dose ionizing radiation on blood parameters. Results showed a nonlinear dose-response relationship between cumulative radiation dose and red blood cell, platelet, and hemoglobin counts. Red blood cell counts decreased then increased, before decreasing again with increasing ionizing radiation. The total platelet count, on the other hand, had a curve that increased after irradiation. A radiation dose of 2.904 mSv was identified as the turning point for the nonlinear curve of hemoglobin count changes. These findings suggest that long-term, low-dose ionizing radiation affects blood cell levels in industrial irradiation workers and should alert radiation workers to seek preventive medical treatment before the occurrence of any serious hematopoietic disease [69].

1.10 The Objective of Study

The aim of this study is to conclude whether the natural radioactivity levels in the analyzed food samples pose a minimal risk to children in Iraq, and to investigate if high radiation doses during cancer treatment can significantly affect blood parameters. This objective can be achieved by the following steps:

1. Measure the gamma-ray spectroscopy of natural radioactivity in various types of food samples commonly consumed by children in Iraq. The food samples include powdered milk, biscuits, indomie noodles, chips, cerelac and corn flakes. This aim can be achieved by the following steps:

2. Calculate the specific activity, annual effective dose, excess lifetime cancer risk factor, radium equivalent activity, and internal hazard index of the radioisotopes ^{238}U, ^{232}Th, and ^{40}K in the food samples.

3. Compare the results to worldwide average limits to assess the radiation hazard of the food samples.

4. Analyze the hematological parameters for 30 pediatric cancer patients aged 1-13 years undergoing radiation therapy over three months. Investigate the effect of radiation on hemoglobin, white blood cells and platelets.

5. Perform a correlation analysis between the annual effective doses of the different food types and hemoglobin levels for the patients.

Chapter 2

Theory

2.1 Fundamentals of Radioactivity

The inherently unstable nuclei of radionuclides are responsible for the characteristic known as radioactivity. After Becquerel's discovery of natural radioactivity in 1896, Frederic Soddy and Ernest Rutherford defined radioactivity in 1902 as the spontaneous breakdown of a radioactive element by the emission of particles, with the end consequence being the formation of new elements [70].

Today, the process of spontaneous nuclear transformation of radionuclides is thought to be the phenomenon known as radioactive decay. This process is accompanied by the emission of particles $(\alpha, \beta, \beta^{+})$, electron capture, proton emission, or the emission of fragments (i.e., the most common decay modes), as well as the emission of radiation. The term radioactivity may also refer to the process of radioactive transformation. Both natural processes and those induced by humans are capable of producing radioactivity. It was determined via experimentation that the nuclei of atoms are stable, meaning that they do not undergo radioactive decay, with the exception of certain conditions involving the neutron to proton ratio (N:Z). This ratio is either exactly one in stable light nuclei, or it is just slightly more than one in such nuclei (the nuclei of and are exceptions) [30, 30].

In the most massive nuclide $^{209}_{83}$Bi that is stable, it rises to 1.52 atomic units.If the composition of the nucleus deviates from the ideal range of the N:Z ratio that is, if the nucleus has either too few or too many neutrons in

relation to the amount of protons it contains then the nucleus will be unstable (for example, in oxygen, the isotopes ^{14}O, ^{15}O, ^{19}O, and ^{20}O), then the nucleus becomes radioactive, which means that It undergoes spontaneous decay, most often to another nucleus. This causes the nucleus to lose its stability and become unstable. The following is a symbolically accurate description of the process:

$$^{\mathrm{A}}_{\mathrm{Z}}\mathrm{X} \rightarrow (\mathrm{A}_1, \mathrm{Z}_1)\,\mathrm{Y} + (\mathrm{A}_2, \mathrm{Z}_2)\ \text{particle},$$

where X is the parent nuclide and Y is the daughter nuclide. It is possible for more than one light particle to be released during the decay process, and this release is often accompanied by the release of gamma radiation. During the process of radioactive decay, energy is lost in an exoergic reaction, and the products of this reaction always have some amount of kinetic energy. This is only conceivable if the primary nucleus has a higher rest energy (mass) than the total rest energy (mass) of the products of the decay, which are as follows:

$$\mathrm{M}(\mathrm{X}) > \mathrm{M}(\mathrm{Y}) + \mathrm{M}(\text{ particle }).$$

This imbalance is the essential need for radioactivity to exist. The energy released as a result of radioactive decay is equal to the mass difference between the two products. This release of energy takes place in radioactive decay by the emission (to a large degree) of one or more of the following three forms of radiation: alpha particles, beta particles and gamma rays (α, β, γ) [15–17, 23].

2.2 Decay Rates and units for Radioactivity

The ability of some nuclides to spontaneously produce particles or gamma radiation gives them the attribute of radioactivity. The process by which radioactive nuclides decay is unpredictable, and it is not possible to pinpoint the specific moment at which a single nucleus will become unstable and decay. The equation that describes the link between activity, the number of atoms, and the decay constant is as follows [2, 31]:

$$A = \lambda N, \tag{2.1}$$

where:

$$\begin{aligned} A &= \text{ Activity of the nuclide (disintegrations / second),} \\ \lambda &= \text{ decay constant of the nuclide } \left(\text{second}^{-1} \right), \\ N &= \text{ Number of atoms of the nuclide in the sample.} \end{aligned}$$

Because λ is unchanging, the activity level and the total number of atoms will always be proportionate to one another. The Curie (Ci) and the Becquerel (Bq) (1 curie $= 3.7 \times 10^{10}$ becquerels) are two of the most popular units used to quantify a chemical's activity. One disintegration every 3.7 x 10^{10} disintegrations seconds is equivalent to one curie, which is the unit of measure for the rate of radioactive decay. This is comparable to the number of disintegrations that will take place in one second for one gram of ^{226}Ra. A more basic unit of measurement for radioactive decay is called a becquerel, and it is equivalent to one disintegration for every second. At the moment, the curie is the unit of measurement that is used most often in the United States; however, it is reasonable to anticipate that the becquerel will begin to be utilized more frequently as the metric system gradually gains more popularity [4].

According to Eq. (2.1), the rate at which a particular radionuclide sample decays is equal to the product of the number of atoms and the decay constant.

This is a statement that may be verified experimentally. Calculus may be used to generate an equation from this fundamental connection, and then that expression can be used to determine how the number of atoms that are present will vary over the course of time. The explanation of how the Equation was derived is outside the scope of this thesis, but the answer given in the following equation:

$$N = N_{\circ} e^{-\lambda t}, \tag{2.2}$$

where:

$$\begin{aligned} N &= \text{number of atoms present at time } t, \\ N_{\circ} &= \text{number of atoms initially present,} \\ \lambda &= \text{decay constant } \left(\text{ time }^{-1}\right), \\ t &= \text{time.} \end{aligned}$$

Since activity and atomic number are always proportional, they can be used interchangeably to characterize any radionuclide population. Consequently, the following holds true [16, 30],

$$A = A_{\circ} e^{-\lambda t}. \tag{2.3}$$

2.3 Radioactive Half-Life

The radioactive half-life is one of the most helpful concepts to have when attempting to estimate how rapidly a nuclide would decay. The period of time needed for the activity to drop to one-half of its original value is what is meant by the term radioactive half-life. It is possible to determine the half-life by solving Eq. (2.3) for the period, t, at which the present activity, A, is equivalent to one-half of the beginning activity A_o [15, 33, 71],

$$\frac{A}{A_o} = e^{-\lambda t}, \tag{2.4}$$

or

$$t = \frac{-\ln\left(\frac{A}{A_{\circ}}\right)}{\lambda}. \tag{2.5}$$

If A is equivalent to half of $A_\circ$, then $A/A_\circ$ is also equal to half. This produces an expression for $t_{1/2}$ when substituted into the above equation,

$$\mathrm{t}_{1/2} = \frac{-\ln\left(\frac{1}{2}\right)}{\lambda},$$

$$t_{1/2} = \frac{\ln 2}{\lambda} = \frac{0.693}{\lambda}. \tag{2.6}$$

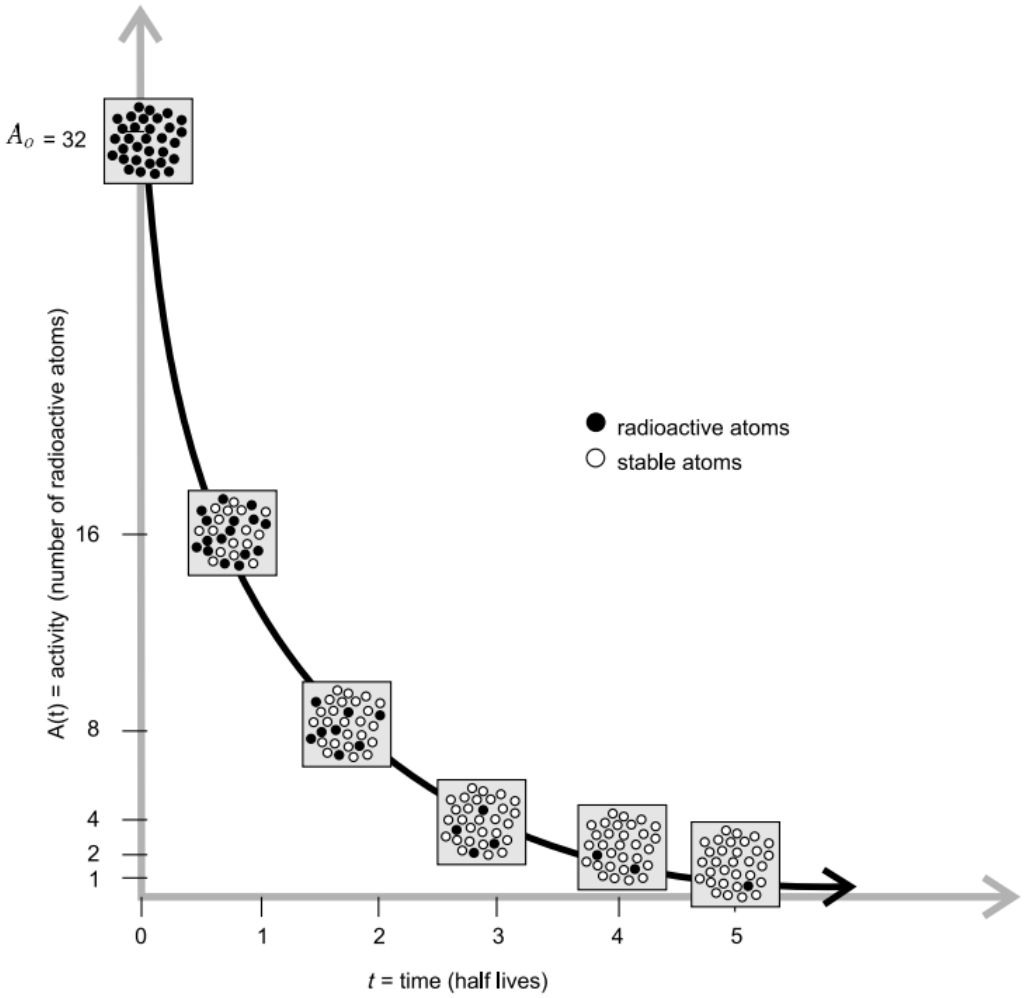

Figure 2.1: Decay curve, Note the progressive replacement of radioactive atoms with stable atoms, as depicted in each box's schematic [15].

It is not remarkable that $t_{1/2}$ is also the time required for half of the remaining atoms to decay. This process will continue until the number of nuclide atoms is so close to zero that it can be considered complete. Fig. 2.1 depicts a plot of the activity remaining, denoted by A. This curve, and consequently the average behaviour of the radioactive sample, can be

characterized by the decay equation [71],

$$A(t) = A_{\circ} e^{-0.693 t/t_{1/2}}. \tag{2.7}$$

2.4 Specific Activity

One way to describe a radioactive substance is in terms of its specific activity, or S, which is the substance's activity expressed as a percentage of its total mass. A radioactive species specific activity is measured in becquerels per gram [8],

$$S = \lambda N = \frac{\ln 2}{t_{1/2}} \frac{N_A}{M}, \tag{2.8}$$

where N is the number of nuclei in one gram, M is the atomic mass of the radionuclide expressed in (atomic mass units u), $t_{1/2}$ is the half-life of the radionuclide expressed in seconds, and N_A is Avogadro's number. Table. 2.1 provides detailed information on the actions of a selection of radionuclides [72]. It is clear from the definition of the term and from the data shown in Table. 2.1 that high specific activity is linked to a relatively short half-life. Therefore, the specific activity of ^{238}Pu is 275 times higher than that of ^{239}Pu, which corresponds to a half-life that is approximately 275 times shorter than that of ^{239}Pu. Because they have the shortest half-lives, the radionuclides ^{90}Sr and ^{137}Cs have the highest specific activity, as indicated in Table. 2.1. Radionuclides that have considerably shorter half-lives still have a greater specific activity, but they typically pose less of a threat since they dissipate more quickly. One illustration of this is how they contribute less to the danger posed by nuclear waste. In the event that one is contemplating an element that contains more than one major isotope, which is typically the situation when talking about natural radioactivity, then Eq. (2.8) needs to be changed so that it takes into account the contributions made by all of the isotopes. Regarding the component, the

particular action is equal to the aggregate of the individual contributions S_i,

$$S_i = \frac{\ln 2}{t_i} \frac{f_i N_A}{M_E}, \tag{2.9}$$

here, M_E refers to the atomic mass of the element, f_i refers to the fractional isotopic abundance of isotope i (measured in terms of the number of atoms), and t_i refers to the half-life of the isotope [8, 32].

Table 2.1: Specific activities S of selected radionuclides [72].

Nuclide	Isotopic Abund.(%)	Atomic Mass (u)	Half-life, T (years)	S (Bq/g)	S (μCi/g)
^{239}Pu	-	239.05	2.411×10^4	2.30×10^9	6.20×10^4
^{238}Pu	-	238.05	87.7	6.34×10^{11}	1.71×10^7
^{237}Np	-	237.05	2.14×10^6	2.60×10^7	7.03×10^2
^{238}U	99.27	238.05	4.468×10^9	1.24×10^4	0.336
^{235}U	0.72	235.04	0.704×10^9	8.00×10^4	2.16
^{232}Th	100.00	232.04	14.05×10^9	4.06×10^3	0.110
^{226}Ra	-	226.03	1600	3.66×10^{10}	9.89×10^5
^{137}Cs	-	136.91	30.07	3.21×10^{12}	8.68×10^7
^{90}Sr	-	89.91	28.79	5.11×10^{12}	1.38×10^8
^{87}Rb	27.83	86.91	47.5×10^9	3.20×10^3	0.087
^{40}K	0.0117	39.96	1.277×10^9	2.59×10^5	7.01

The specific activity of natural uranium, for instance, is 2.53×10^4 Bq/g, which is more than twice as high as that of pure ^{238}U. Other contributors include ^{235}U, which has a low isotopic abundance and a relatively long half-life, and ^{234}U, which has a $t_{1/2}$ value of 2.455×10^5 years and is in secular equilibrium (see next Sections) with ^{238}U and has the same ratio f_i/t_i as ^{238}U. Both of these contributors contribute very little to the total.

2.5 Radioactive Equilibrium

A radioactive nuclide is said to be in a state of radioactive equilibrium when its rate of decay is equal to the rate at which it is being created. The number of atoms that are present stays the same over the course of time since the production rate and the decay rate are both equal [3, 73].

2.5.1 Secular Equilibrium

Suppose the half-life of the daughter radionuclide B in a radioactive decay chain is significantly less than the half-life of the parent radionuclide A. In that case, the radioactive decay chain will have reached a state of secular equilibrium. Because the half-life of A is so much longer than the time scales that are being studied, the decay rate of A and, as a consequence, the production rate of B will be nearly the same in this case. The quantity of radionuclide B increases until the rate at which B atoms decay per unit of time is equal to the rate at which new B atoms are created. After this, the quantity of radionuclide B reaches a value that is stable and in balance. Assuming that the original concentration of radionuclide B was zero, it typically takes several half-lives of radionuclide B for full equilibrium to be established [74].

The amount of radionuclide B that is present when the state of secular equilibrium has been attained is dependent on the amount of its parent radionuclide A as well as the half-lives of the two radionuclides. This is evident from the rate of change in the amount of radionuclide B over a period of time, which is as follows [17, 28],

$$\frac{dN_B}{dt} = \lambda_A N_A - \lambda_B N_B, \tag{2.10}$$

where λ_A and λ_B are the decay constants of radionuclide A and B, respectively, and are linked to their half-lives $t_{1/2}$ by $\lambda = \ln(2)/t_{1/2}$, and where N_A and N_B

are the number of atoms of A and B at a given time. Secular equilibrium occurs when $dN_B/dt = 0$, or,

$$N_B = \frac{\lambda_A}{\lambda_B} N_A. \tag{2.11}$$

There is only an approximation of a secular equilibrium after sufficiently long periods of time, which is comparable to the half-life of radionuclide A. N_A decreases over time according to,

$$N_A(t) = N_A(0)e^{-\lambda_A t}. \tag{2.12}$$

In turn, the "equilibrium" amount of radioactivity B drops. For times that are short compared to the half-life of A, the exponential can be approximated as 1. The secular equilibrium is shown in Fig. 2.2

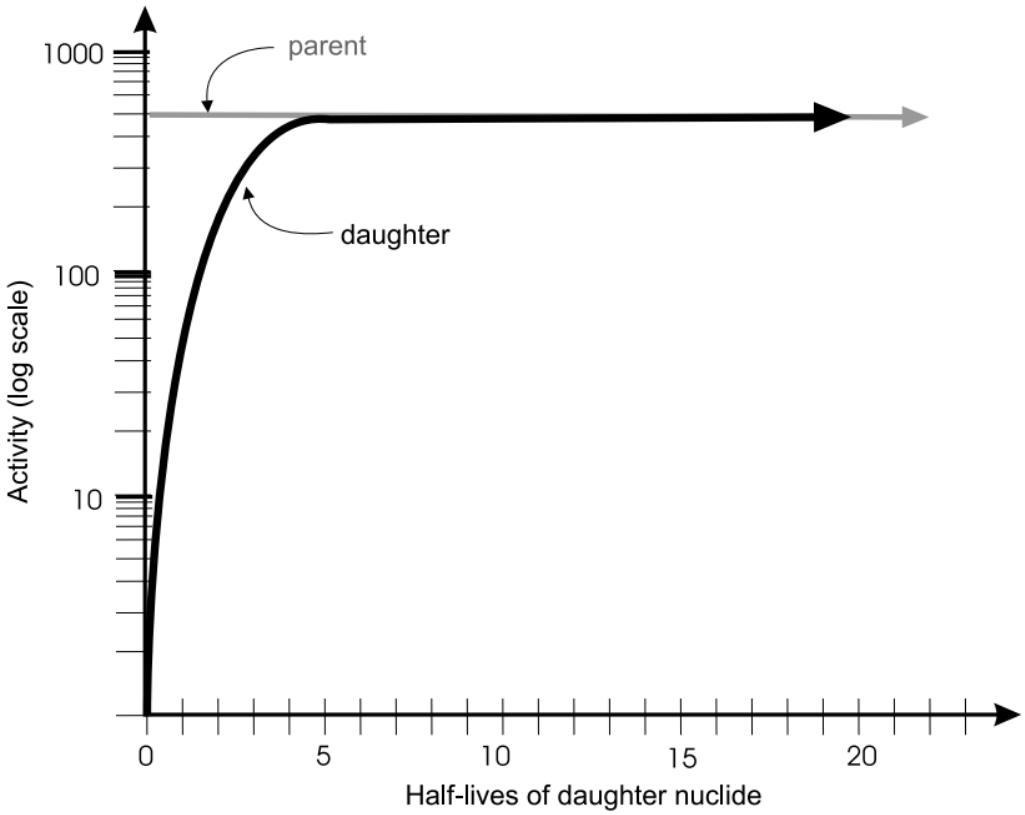

Figure 2.2: Secular equilibrium [15].

2.5.2 Transient Equilibrium

Suppose the half-life of the daughter radionuclide B in a radioactive decay chain is significantly less than the half-life of the parent radionuclide A. In that case, the radioactive decay chain will have reached a state of secular equilibrium. Because the half-life of A is so much longer than the time scales that are being studied, the decay rate of A and, as a consequence, the production rate of B will be nearly the same A situation known as transitory equilibrium occurs when a pair of radioactive isotopes, a parent and a daughter, achieve a state of equilibrium. In this case, the half-life of the daughter is shorter than that of the parent; hence the daughter outlives her parent. In contradiction to the concept of secular equilibrium, the half-life of the daughter is not insignificant in comparison to that of the father [17, 73]. This type is shown in Fig. 2.3;

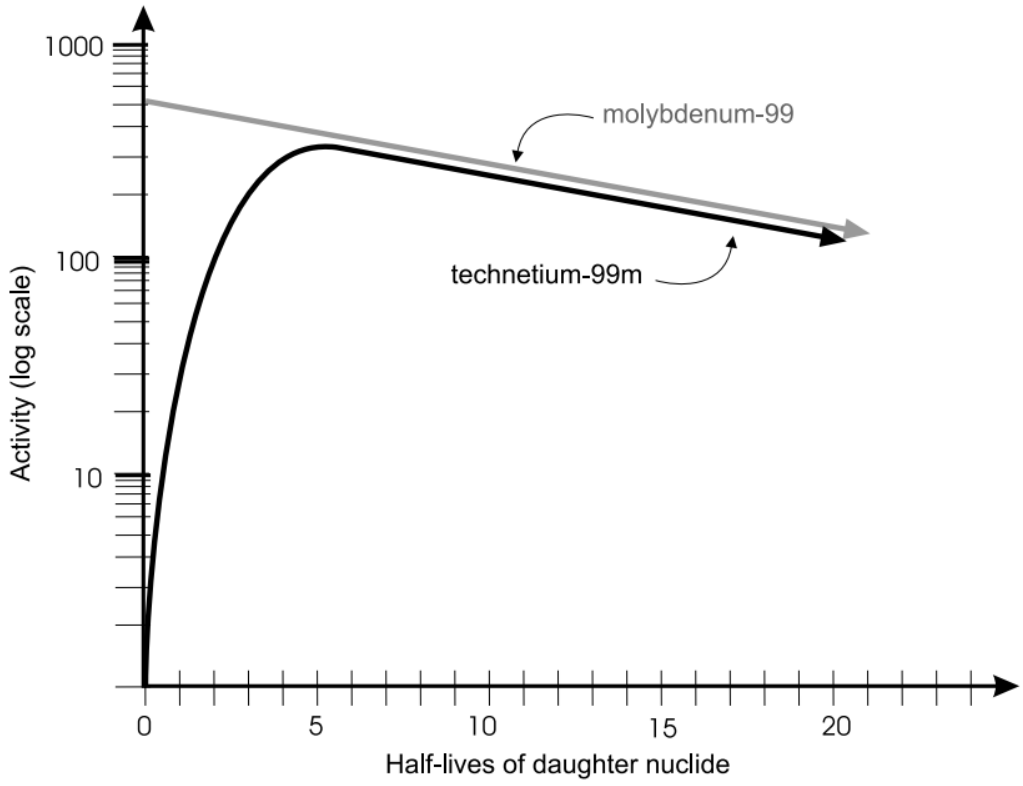

Figure 2.3: Transient equilibrium [15].

a molybdenum-99 generator, which produces technetium-99 for use in nuclear medicine diagnostic procedures, is one example of this type of device. Because the daughter product, which in this case is technetium-99, is milked at regular intervals, this type of generator is frequently referred to as a cow. On average, transient equilibrium is reached following the completion of four half-lives [75].

2.5.3 No Equilibrium

In instances where equilibrium is absent, it can be observed that the half-life of the parent is comparatively shorter than that of the daughter. In instances where the half-life of the parent is shorter than that of the daughter, the daughter's activity experiences a period of growth until it reaches a maximum level, after which it undergoes decay in accordance with its unique half-life [22]. Fig. 2.4 show the activities as a function of time when $t_2 > t_1$

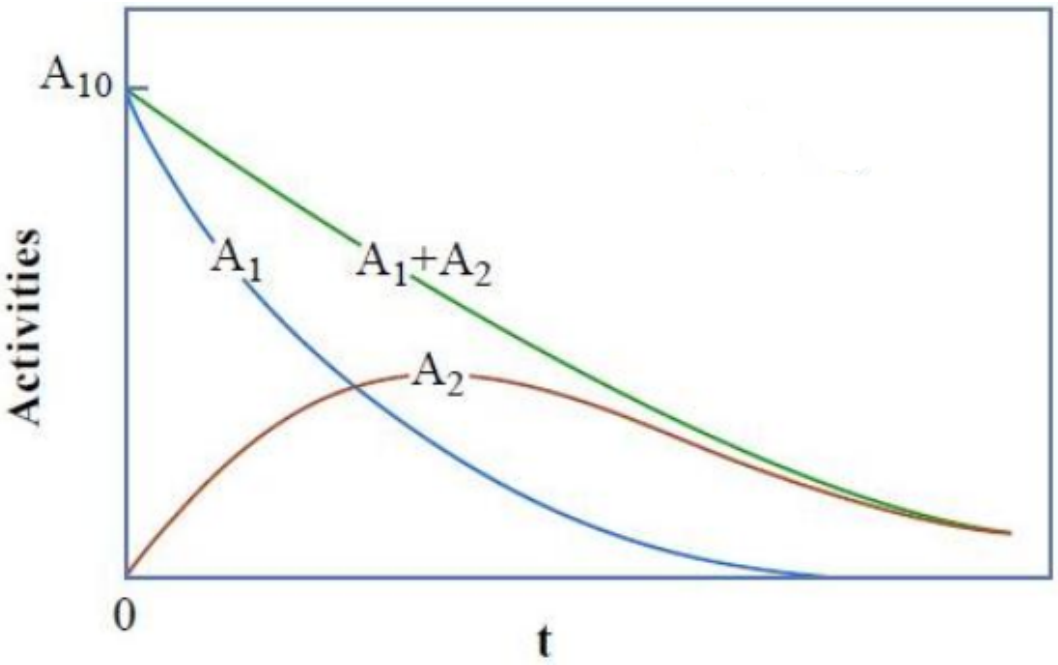

Figure 2.4: Activities according to time when $t_2 > t_1$ [5].

2.6 Energetics of Radioactive Decay

In this section, the energies that are involved in the various types of radioactive decay will be discussed. The energy of the particles that are emitted as a result of the decaying process is of particular importance [17].

2.6.1 Gamma Decay

Numerous nuclear reactions produce a nuclide whose nucleus is left in an excited state after the process. These excited nuclei often return to their ground state very quickly, typically within 10^{-9} seconds, by expelling the excitation energy in the form of a photon that is known as a gamma ray. However, certain excited nuclei are able to maintain their excited state for far longer periods of time before undergoing gamma emission, which causes them to decay. *Isomers* and *metastable* nuclei are two names for the same type of long-lived excited nucleus. This type of excited nuclide is said to have undergone an isomeric transition when it underwent decay due to gamma emission . ${}^{97m}_{43}\mathrm{Tc}$'s first excited state is a metastable one with a half-life of 90.5 days, making it a metastable state. It does so by emitting a gamma photon with a 96.5 keV energy level when it decays to the ground state. It is possible to write out the gamma-decay reaction of an excited isotope of element P as [15, 17, 18],

$$\gamma\,\text{decay:} \quad {}^{A}_{Z}\mathrm{P}^{*} \rightarrow {}^{A}_{Z}\mathrm{P} + \gamma. \tag{2.13}$$

2.6.2 Alpha- Particle Decay

Our prior discussion of nuclear structure taught us that nucleons tend to form subunits of ${}^{4}_{2}\mathrm{He}$ nuclei, commonly referred to as alpha particles. Alpha-particle emission is therefore not surprising as a plausible mode of decay to a more stable state for proton-rich heavy nuclei. The nucleus of the progenitor atom ${}^{A}_{Z}\mathrm{P}$

emits an alpha particle during alpha decay. The nucleus for the daughter atom ${}^{A-4}_{Z-2}\mathrm{D}$ has two fewer neutrons and two fewer protons. Initially, the daughter has two extra Z electrons, making her a doubly negative ion $[{}^{A-4}_{Z-2}\mathrm{D}]^{2-}$. However, these extra electrons rapidly escape the atom, leaving the atom in a neutral state. The fast-moving, doubly charged alpha particle dissipates its kinetic energy by ionizing and exciting atoms along its path of travel, acquiring two orbital electrons to become a neutral He atom. Since the daughter's atomic number differs from that of the parent, the daughter is a distinct chemical element. Therefore, the alpha decay reaction is represented by [15, 17, 18],

$$\alpha \text{ decay:} \quad {}^{A}_{Z}\mathrm{P} \longrightarrow \left[{}^{A-4}_{Z-2}\mathrm{D}\right]^{2-} + {}^{4}_{2}\alpha \longrightarrow {}^{A-4}_{Z-2}\mathrm{D} + {}^{4}_{2}\mathrm{He}. \tag{2.14}$$

2.6.3 Beta-Particle Decay

During the decay process of many neutron-rich radioactive nuclides, one of the neutrons in the parent (P) nucleus is converted into a proton, and an energetic electron is released. This process of decay is known by a wide variety of names, including electron decay, beta minus decay, negation decay, negative electron decay, negative beta decay, and plain old beta decay. The electron that was expelled is known as a beta particle, and its symbol is β^-. The daughter atom, which has one more proton in its nucleus, does not originally have one electron in its orbit, and as a result, it is a single charged positive ion, represented by the symbol $[{}^{A}_{Z-1}\mathrm{D}]^{+}$. On the other hand, the daughter immediately picks up an additional orbital electron from the medium that is around it. The β^- decay is given by [18],

$$\beta^- \text{decay:} \quad {}^{A}_{Z}\mathrm{P} \longrightarrow \left[{}^{A}_{Z+1}\mathrm{D}\right]^{+} + {}^{0}_{-1}\mathrm{e} + \bar{\nu}. \tag{2.15}$$

In this context, $\bar{\nu}$ denotes a (anti) neutrino, which is an elementary particle that has no net charge and extremely little or no rest mass. The measured energy and momentum of the β^- particle that is released provide strong evidence that

the β^- decay process involves the involvement of a third product particle. If the sole products of the decay were the daughter nucleus and the β^- particle, then the laws of conservation of energy and linear momentum would dictate that the decay energy must be distributed between these two entities in very specific proportions for the process to be consistent with a decay [15, 30, 33].

2.7 Interaction of radiation with matter

When radiation collides with matter, the results are contingent not only on the characteristics of the radiation but also on the makeup of the matter. Radiation energy is first transferred to the atoms and molecules of the material, which either heats the substance or modifies its structure, depending on the outcome of the process. If the energy of a bombardment particle or photon is completely transferred to the irradiated matter, it will look as though the radiation has been stopped within the irradiated substance [31].

On the other hand, if the energy is not totally deposited in the matter, the residual energy will emerge as though the matter were transparent or at least translucent. This occurs when the energy is not completely placed. Some of the physical processes can be discussed that are involved when radiation interacts with matter. In particular, we will explore, independently at first, how photons (gamma rays and x-rays) and charged particles (alpha and beta particles) interact with matter. Photons have the ability to influence the atomic structure of matter as they go through it. The atomic number (Z) of the components that make up the matter, as well as the energy of the photons, determine the sort of interaction that occurs between them [17, 23].

When electrons with an energy of 550 keV are utilized, the form of interaction that predominates in materials with lower atomic numbers, such as human tissue (Z = 7.5), is called Compton scattering. In materials with

greater atomic numbers, such as lead (Z = 82), the photoelectric effect is the predominant form of contact that occurs between the particles. Pair creation is a third sort of interaction that can take place between photons and matter, but it is only seen at very high photon energy (more than 1020 keV), and as a result, it is not significant in clinical nuclear medicine. The primary form of interaction is depicted in Fig. 2.5 for a variety of different combinations of the atomic numbers of the absorber and the photons that are incident [17].

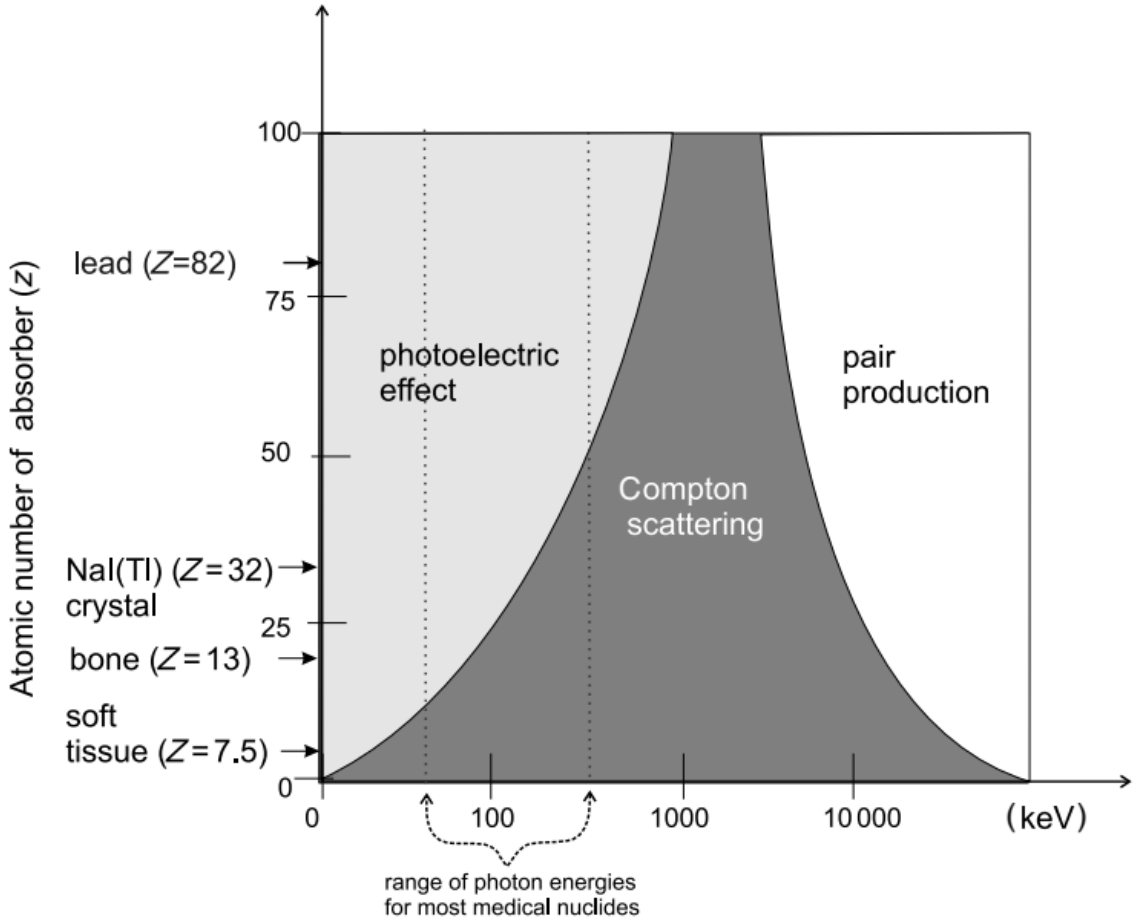

Figure 2.5: Interaction type that predominates for a variety of different combinations of photons in the incident beam and atomic numbers in the absorber [15].

2.7.1 Compton Scattering

During the process of Compton scattering, the incident photon transmits some of its energy to an outer shell or (basically) ”free” electron, which then causes the electron to be ejected from the atom. This electron becomes known as a Compton electron once it has been ejected. The amount of energy passed from the photon to the electron determines the angle at which the photon is scattered when it interacts with the electron (see Fig. 2.6 a). The scattering angle can go almost anywhere between 0 and 180 degrees. The scattering angles of 135 and 45 degrees are depicted in Fig. 2.6 b [17, 23, 73].

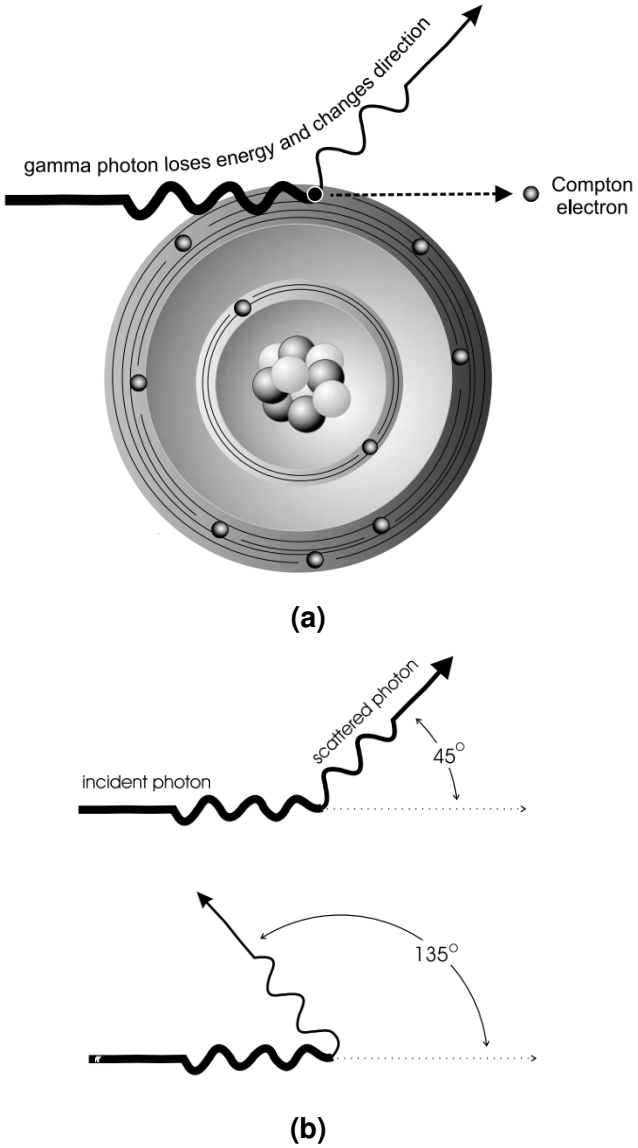

Figure 2.6: Compton scattering (a) and the angle of photon scattering (b) [15].

2.7.2 Photoelectric Effect

It is possible for a gamma ray with low energy or one that has lost most of its energy through Compton interactions to transfer what little energy it has left to an orbital electron, which is often an electron in an inner shell. This phenomenon is known as the photoelectric effect, and the electron that is liberated in the process is referred to as a photoelectron Fig. 2.7. This electron escapes the atom with an energy that is equivalent to the energy of the gamma ray that hit it, minus the electron's binding energy.The vacancy in the inner shell is subsequently filled by an electron from the outer shell, and the surplus energy is released as an x-ray [2, 17],

$$E_{photoelectron} = E_{photon} - E_{binding}. \tag{2.16}$$

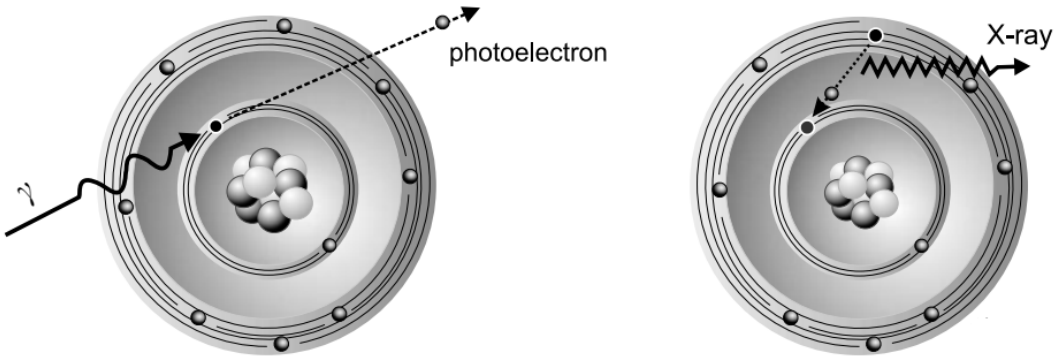

Figure 2.7: Photoelectric Effect [15].

2.7.3 Pair Production

The interaction of γ rays invariably takes place in close proximity to an atomic nucleus, which undergoes a recoil effect. The gamma-ray transfers its energy to initiate the formation of a pair of particles consisting of an electron and a positron. The interaction of γ rays invariably takes place in close proximity to an atomic nucleus, which subsequently undergoes a recoil. The gamma-ray

transfers its energy to initiate the formation of a pair of particles consisting of an electron and a positron. The minimum energy required for two photons to produce an electron-positron pair is 1.02 MeV, which corresponds to the energy equivalent of two electrons. The aforementioned phenomenon primarily occurs in the case of high-energy gamma rays. Apart from fundamental interactions, there exist additional interactions between individual radioactive decay products and not only the atomic electrons of matter but also the nuclei. The impact of ionizing radiation on both abiotic and living matter is determined by the interplay between emitted particles or other byproducts of radioactive decay and matter. This interplay also serves as the fundamental basis for measuring radiation [7, 17, 23].

2.8 Health Risk of Gamma-Ray and Alpha-Particle

The presence of radium and thorium atoms in humans is attributed to the isotopes ^{238}U and ^{232}Th. These isotopes are acquired through the consumption of food, which in turn obtains them from the soil in which it was grown or grazed upon. Potassium belongs to this category and ^{40}K, a naturally occurring radioactive isotope, is of particular interest in the present study. Radionuclide ^{40}K is the most prevalent radioactive constituent found in human tissues and in the majority of food sources [76–78].

It holds significant importance in terms of the dose associated with naturally occurring radionuclides.The increasing global interest in natural radiation exposure has resulted in comprehensive surveys conducted in numerous countries. Estimation of external gamma dose resulting from terrestrial sources is a crucial aspect to consider, not only due to its significant contribution of 0.46 mSv/y to the collective dose but also due to the variations in individual doses associated with this pathway. The dosage levels vary based on the concentration

of natural radionuclides, namely ^{238}U, ^{232}Th, and their daughter products, as well as ^{40}K, present in food items. These concentrations are influenced by the geological characteristics of specific global regions [60, 78, 79].

The potential health risk posed by potassium-40 is linked to the ionizing radiation generated by its radioactive decay, which can lead to cellular damage and ultimately increase the risk of cancer development. The assessment of radioactivity levels in potassium-enriched food items holds significant importance in terms of radiation protection. The current study presents findings on the radioactivity levels detected in potassium-enriched vegetation. The onset of ionizing radiation's biological effects occurs when the molecules within a living cell interact with radiant energy, either through precipitation or exposure. The direct effect of ionizing radiation on a molecule occurs when the energy deposited and absorbed by the molecule leads to excitation. This effect primarily affects DNA molecules through direct ionization in the target tissues of atoms, as well as through Compton reactions and the photoelectric effect, which results in energy absorption. The energy present in the system is deemed adequate to eject electrons from the molecule. Consequently, the bonds that hold the DNA strands together may be disrupted, leading to the breakage of one or both of the strands. Upon absorption of ionizing radiation by water molecules in the human body, indirect effects ensue, leading to the formation of transient chemical reaction products that interact with other molecules at distinct sites within the organism [80, 81].

2.9 Gamma-Ray Spectroscopy

The mechanism for detecting gamma rays is contingent upon the interaction between gamma-ray photons and the material of the detector. The detector volume has the potential to facilitate all primary types of gamma-ray

interactions. However, the photoelectric effect and Compton scattering are the most noteworthy types that hold crucial significance in the detection of photons. In these instances, the principal gamma-ray photons and/or the resultant scattered secondary photons engage with the atoms of the detector, thereby producing expeditious electrons within the detector's confines that possess energy commensurate with that of the primary photon [82, 83].

The high-velocity electrons have the capability to produce additional electrons as they traverse the detector's spatial domain. The collection of secondary electrons has the potential to generate electrical pulses. The conversion of charges can be achieved by means of a preamplifier, resulting in the generation of a voltage signal that is directly proportional to the magnitude of the gamma-ray energy that was initially deposited within the detector. Scintillation devices are comprised of a crystal and a photomultiplier tube (PMT) that facilitates the conversion of light into an electrical signal [84].

2.10 The Specific Activity (Activity Concentration)

For primordial radionuclides (^{238}U, ^{232}Th and ^{40}K), the specific activity (activity concentration) of the gamma-emitting radionuclides in the sample can be calculated from the following equation,

$$A = \frac{N}{I_\gamma \, \varepsilon \, M \, t} \mp \frac{\sqrt{N}}{I_\gamma \, \varepsilon \, M \, t} \qquad \left(\frac{\text{Bq}}{\text{kg}}\right), \tag{2.17}$$

where A is the specific activity of the radionuclide in the sample, N is the net area under photopeak, I_γ is the probability of gamma decay, ε is the efficiency of the gamma-ray detector, M is the weight of the measured sample in kg, and t is the life time for collecting the spectrum in seconds. The term with sign plus and minus in the above equation indicates the uncertainty in measuring the specific activity [85, 86].

2.11 Radium Equivalent Activity (Ra_{eq})

In order to assess the gamma radiation dose to human beings due to internal or external exposure to them, it is necessary to evaluate how to consider the specific radioactivity properly. To this purpose a suitable and practical index, the so-called Radium Equivalent Activity index Raeq has been introduced by E. I. Hamilton from the UK National Radiological Protection Board (NRPB) [87]. Based on the assumption that 10 Bq/Kg of ^{238}U, 7 Bq/kg of ^{232}Th, and 130 Bq/kg of ^{40}K produced the same -ray dose rates, the radium equivalent activity (Ra_{eq}) is the sum of the activities of ^{238}U, ^{232}Th, and ^{40}K. The calculated value for the equivalent radioactivity can be found as [88],

$$\mathrm{Ra_{eq}(Bg/kg)} = A_{\mathrm{U}} + 1.43\, A_{\mathrm{Th}} + 0.077\, A_{\mathrm{K}}, \tag{2.18}$$

where A_{Ra}, A_{Th}, and A_K are the activity concentration of ^{238}U (^{214}Bi), ^{232}Th, and ^{40}K in Bq/Kg,respectively.

2.12 Radiation Internal Hazard Indices

The radiation hazard indices are defined to calculate the radiation hazard. The internal exposure to (^{222}Rn) and its radioactive progeny is controlled by the (internal hazard index). It can be calculated according to the following equation [57, 59],

$$\mathrm{H_{in}} = \frac{A_{\mathrm{U}}}{185} + \frac{A_{\mathrm{Th}}}{259} + \frac{A_{\mathrm{K}}}{4810}. \tag{2.19}$$

In this study, we will focus on this hazard index because we deal with consumed food by children.

2.13 Annual Effective Dose Equivalent (AEDE)

The annual effective dose is calculating from consumption the samples of foods. Due to the proportionate link between its importance and other factors, this amount was thought to be among the most crucial. Both value and the induced health effects can be calculated from radiation intake equation which is given by [60, 64],

$$\text{AED} = A \times I \times E, \tag{2.20}$$

where AED stands for the annual effective dose (Sv/y) to an individual due to ingesting radionuclides, A is the activity concentration of radionuclides in the ingested sample (Bq/kg), I represents the annual intake of the food sample (kg/y), and E for the ingested dose conversion factor for radionuclides. According to the International Commission on Radiological Protection (ICRP) of 1996, the annual intake of powdered milk (kg/y) depends on a given age (Sv/Bq). [89].

2.14 Excess Lifetime Cancer Risk

This variable quantifies the probability of developing cancer over the course of one's lifetime as a result of a particular degree of exposure. The standard life expectancy for an individual is deemed to be 70 years in this context. This particular risk factor can be given as,

$$\text{ELCR} = \text{AED} \times DL \times RF, \tag{2.21}$$

where AED is the outdoor annual effective dose, the term DL is the normal Duration of Life (70 years), and RF is the Risk Factor (1/Sv). For the stochastic impact, generally, ICRP utilizes RF as 0.05 [86, 90].

Chapter 3

Experimental Part

3.1 Introduction

In this chapter, the important practical steps that were followed to achieve the main objective of this thesis will be discussed. Six different samples were collected from the central Euphrates governorates in Iraq to measure the radioactivity in these samples. The Sodium Iodide detector doped with the Thallium (NaI) (Tl) was used to measure the gamma-ray spectroscopy, and biological examinations for children with cancer were also measured before exposure to radiation treatment.

3.2 Foods Samples Collections

Six various samples of foods that children commonly eat were collected from different markets in the center of Iraq. These markets are placed in Najaf, Karbala, and Hilla governorates. These samples are: children's milk, biscuits, Indomie, chips, Cornflex, and Cerelac, with ten different types from each sample except nine different types from powdered milk. We collected 59 samples in total to scan and calculate the levels of natural radioactivity.

All of the samples were dried in an oven to produce a constant weight, and then they were crushed using an electric mill and a mesh sieve (0.8 mm pore size sieve) to guarantee that the results were consistent. The samples were packaged in plastic (polyethylene), and the symbols used to identify the samples' countries of origin were printed on the plastic. The samples were placed in plastic (Marinelli containers) of a fixed volume (the containers, prior

Table 3.1: Types and origins of the powdered milk samples.

Code of samples	Name of samples	Country of origin
M1	Novalac	Germany
M2	Bebelac	France
M3	Menalac	U.S.A
M4	Primalac	Holland
M5	Similac Gold	Ireland
M6	S 26Gold	Singapore
M7	Sunny Baby	France
M8	Guigoz Expert	Holland
M9	Pediasure Complete	Singapore

to use, were washed with distilled water and labeled to distinguish between samples), and their corresponding net weights were measured and recorded using a highly sensitive digital weighting with an accuracy of 0.05 percent. After this, the Marinelli beakers were hermetically sealed for at least four weeks to achieve a state of radioactive equilibrium between the parent and daughter radionuclides.

The food samples are tabled according to their name, country of origin, and production date. As we mentioned earlier, various types for each sample were selected, and a unique code was chosen for each sample, as shown in Tables. 3.1 to 3.6,

Table 3.2: Samples of biscuit, their types, and places of origin.

Code of Samples	Name of samples	Country of origin
B1	Original Cream Crackers	Malaysia
B2	Digestive	Iran
B3	Digestive Original	Turkiye
B4	Petit Beurre	Iran
B5	Classic Biscuit	Iraq
B6	Petit Beurre Biscuit	Turkiye
B7	Petit Beurre Tea Biscuit with Milk	Turkiye
B8	Finger Biscuit	Turkiye
B9	Digestive Oats Orange	Spain
B10	Lotus Biscoff	Belgium

Table 3.3: Samples of corn flex, their types, and places of origin.

Code of Samples	Name of samples	Country of origin
Co1	Ozmo	Turkiye
Co2	Flower Powder	Egypt
Co3	Bakalland Grain Flakes	Poland
Co4	Temmys	Egypt
Co5	Poppins Frosted Flakes	Lebanon
Co6	Happy Flakes Corn Flakes	Ukraine
Co7	Poppins Toasted Corn Flakes	Lebanon
Co8	Oatibiz Oat Flakes	U.S.A
Co9	Cocoa Flakes Happy Flakes	Ukraine
Co10	Nawras Corn Choco	Turkiye

Table 3.4: Samples of indomie, their types, and places of origin.

Code of Samples	Name of samples	Country of origin
I1	Sam Yang	South Korea
I2	Beijing Jjang Ramen	South Korea
I3	SuTah Ramen	South Korea
I4	Seafood Party	South Korea
I5	Chost Pepper Spicy Chicken	South Korea
I6	Reeva	Ukraine
I7	Indomi Chicken Flavored	Saudi Arabia
I8	Supermi Vegetable Flavored	Saudi Arabia
I9	Nawras Chicken Flavored	Indonesia
I10	Popmie	United Arab Emirates

Table 3.5: Samples of cerelac, their types, and places of origin.

Code of Samples	Name of samples	Country of Origin
Ce1	Cerelac (wheat and honey)	Spain
Ce2	Cerelac (wheat and dates)	Spain
Ce3	Cerelac (wheat and fruits)	Spain
Ce4	Cerelac (Rice)	Spain
Ce5	Hero Baby Semolint and	Switzerland
Ce6	Hero Baby Rice and Banana	Switzerland
Ce7	HeroBaby 8 Cereals and	Switzerland
Ce8	fruits with Milk	Switzerland
Ce9	Klodi (Wheat)	Oman
Ce10	Klodi (Rice)	Oman

Table 3.6: Samples of chips, their types, and places of origin.

Code of Samples	Name of samples	Country of origin
Ch1	Chips al Fawaz	Iraq
Ch2	Chips al Shani Mixed	Iraq
Ch3	MunCheese	Iraq
Ch4	MazMaz	Iran
Ch5	Tarboosh ketchup flavoured	Iraq
Ch6	Doritos	Egypt
Ch7	Shababeek	Iraq
Ch8	NiNi	Iraq
Ch9	Danadana RIN6	Iraq
Ch10	Hendreen	Iraq

3.3 Crystal Scintillation Detector

A transparent solid material, commonly referred to as a crystal, has the ability to convert gamma rays into visible light. Sodium iodide (NaI) crystals are extensively utilized and are known for their fragility, rendering them susceptible to cracking. Sodium iodide crystals necessitate an air-tight aluminium container due to their propensity to absorb moisture from the surrounding atmosphere. Small quantities of stable Thallium (Tl) are introduced into sodium iodide crystals through a process known as doping. The dispersion of thallium atoms within the crystal has been observed to enhance its sensitivity towards gamma ray photons, as depicted in Fig. 3.1. The conversion of gamma rays into light is a multifaceted process, albeit succinctly explicable as the assimilation of gamma ray energy by a crystal, resulting in the excitation of its electrons. The gamma photon undergoes one or multiple Compton or photoelectric interactions within the crystal, resulting in the transfer of its energy. The gamma ray interactions

result in the production of energetic electrons, which subsequently transfer their energy to electrons in the crystal, inducing an excited state in the latter. Upon reverting to their initial state, a portion of the energy of these entities is emitted as photons of light (refer to Fig. 3.2). It has been observed that the absorption of gamma ray energy by the crystal at a rate of one kiloelectronvolt (keV) results in the emission of approximately forty light photons. Photomultiplier tubes are capable of detecting light photons [91, 92].

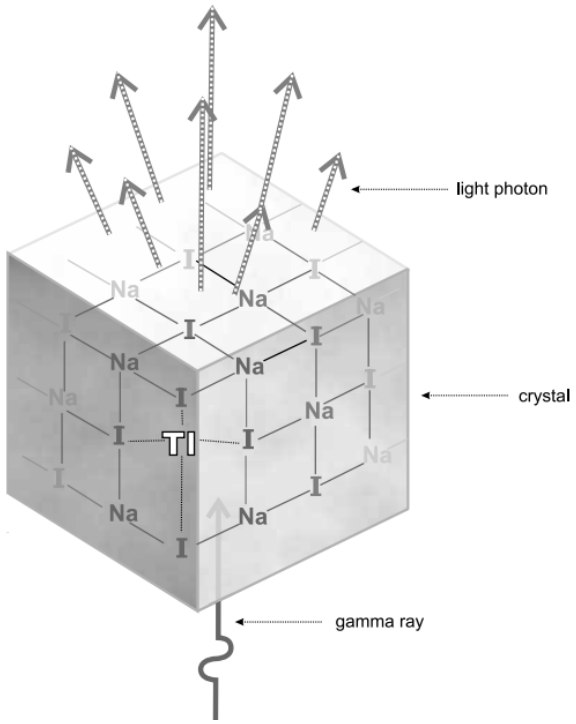

Figure 3.1: Scintillation crystal. The thallium-doped sodium iodide crystal converts gamma rays into light photons [15].

The efficacy of the crystal is affected by its design. Crystals of sodium iodide range in thickness from less than one centimeter to several centimeters. By absorbing more of the original and scattered gamma rays, thicker crystals have a comparatively high sensitivity in which nearly all of the gamma ray energy reaching the crystal is absorbed Fig. 3.3. Thinner crystals are less sensitive because more photons are able to escape [15].

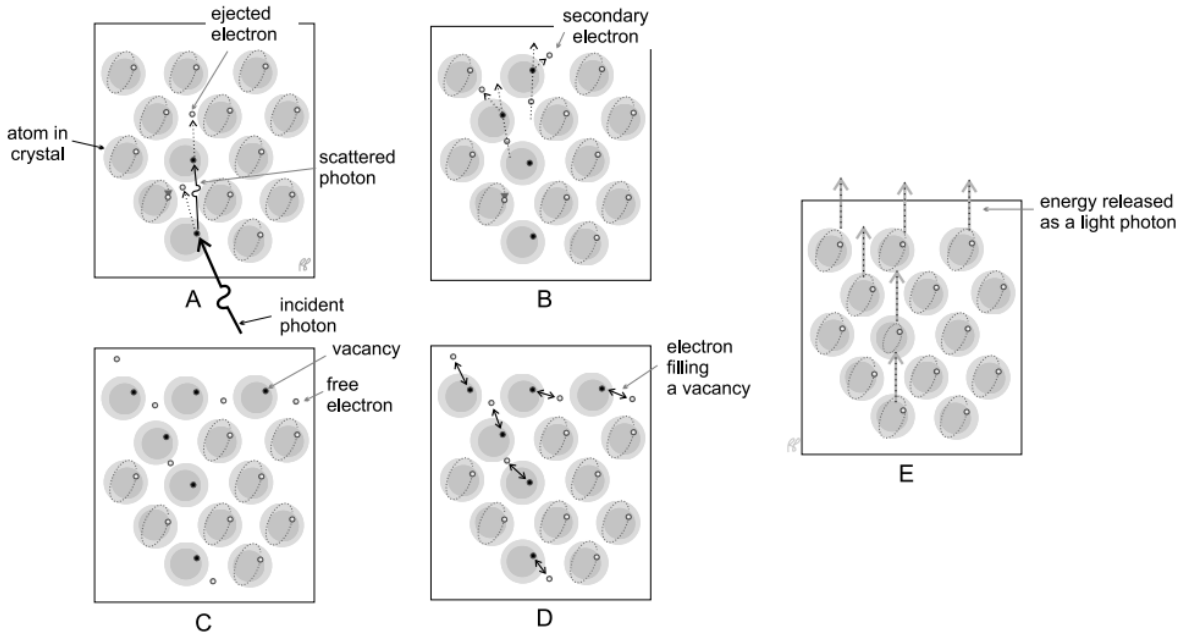

Figure 3.2: Light photons. (A) Gamma rays eject electrons from the crystal through Compton scattering and the photoelectric effect. (B, C) The ejected electrons in turn produce a large number of secondary electrons. (D, E) During de-excitation (oversimplified in this drawing) energy is released in visible light [15].

Figure 3.3: Thick crystals stop a larger fraction of the photons [15].

3.4 Photomultiplier Tubes

The photomultiplier tube is a vacuum tube that features a photocathode located at one end, which is positioned in close proximity to the crystal. A photocathode refers to a transparent glass surface that exhibits photosensitivity. The aforementioned procedure involves the application of a light-conductive transparent gel onto the crystal's surface, as depicted in Fig. 3.4. The gel that is transparent in nature exhibits an identical refractive index to that of the crystal

and the window of the photomultiplier tube (PMT). The emission of electrons, commonly known as photoelectrons, is triggered by the impact of light on the photocathode. Typically, the photocathode receives a range of four to six light photons per photoelectron generated. The amplification of electron production at the photocathode is significantly enhanced by the multiplying effect occurring within the tube, as depicted in Fig. 3.5. Upon their production, the electrons undergo a cascade effect along the multiplier segment of the tube, sequentially colliding with each of the dynodes within the tube. The aforementioned are metallic electrodes, with each being maintained at a gradually increasing positive potential in comparison to its predecessor. When an electron collides with a dynode, it induces the emission of two to four additional electrons. These newly generated electrons subsequently combine with the existing stream of electrons, which gradually amplifies in size, and ultimately travels toward the anode located at the terminal end of the tube. Stated differently, when a single electron enters a sequence of only three dynodes, the resulting cascade produces an output of approximately 23 to 43 electrons. If the cascade were to occur across ten dynodes, the output would increase to approximately 210 to 410 electrons [7, 16, 84].

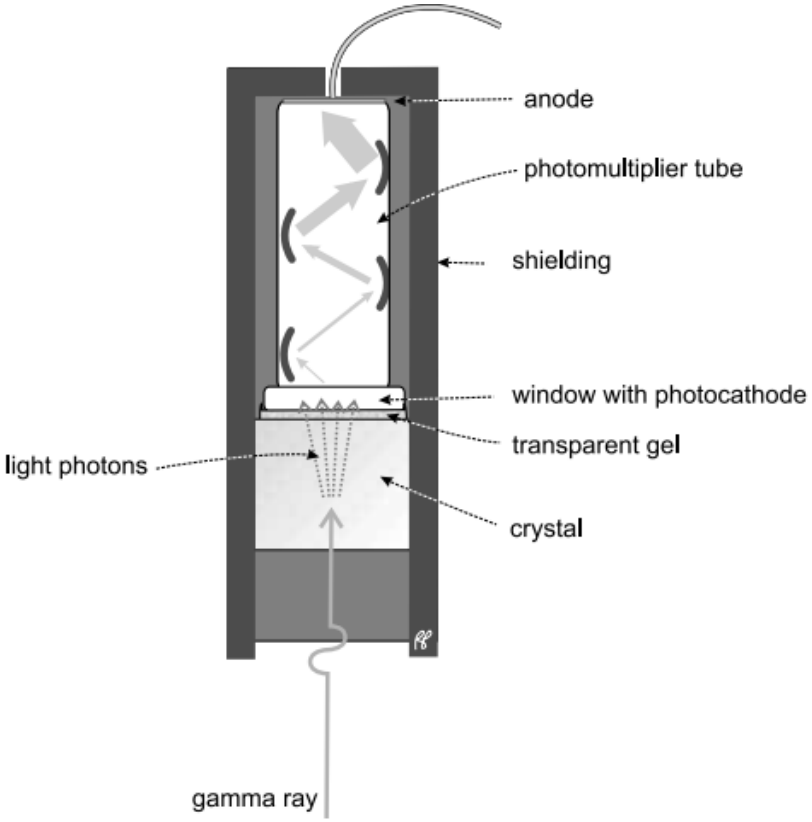

Figure 3.4: Sodium iodide crystalscintillation detector [15].

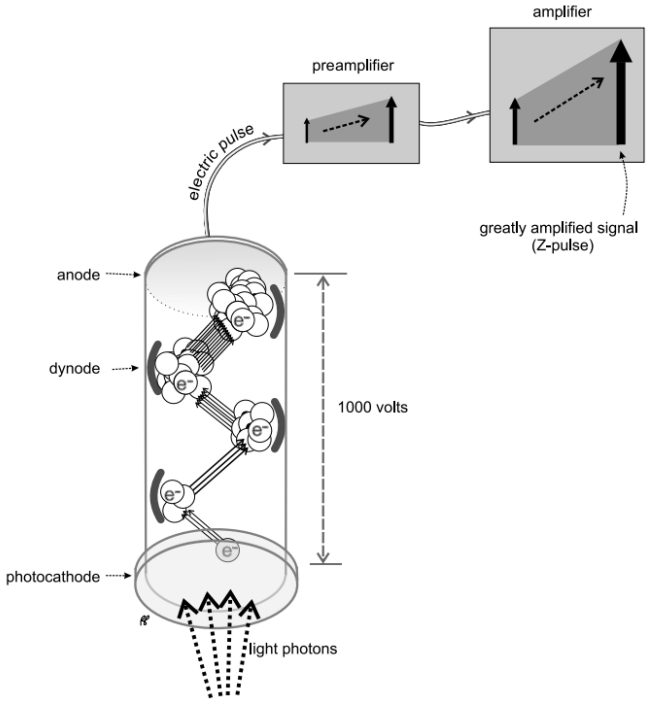

Figure 3.5: Photomultiplier tube and its preamplifier and amplifier [15].

3.5 Preparing and calibrating the measurement system

3.5.1 NaI(Tl) Detector System

The NaI(Tl) detector was utilized, which consists of a scintillation detector with crystal dimensions of (3×3). The crystal is enclosed in an aluminum case. With a range of 4096 channels and an ADC (analog to digital converter) unit, ORTEC Components, Inc. designed this particular detector equipped with an ADC (analog to digital converter) unit. A multi-channel Analyzer (MCA) is affixed to the back of the detector, and a single USB cable connects the MCA to a personal computer. The detector is designed with a built-in amplifier and utilizes the laboratory's (Maestro-32) software to achieve high voltage settings [60, 93].

3.5.2 High Voltage Power Supply

The NaI(Tl) detector requires high voltage for the job, and the range of reagent (0-1300) Volts and the voltage employed in the study is 800 volts. This voltage is within the range of stability of the working voltage of the detector, and it was provided with voltages of the classy type [94, 95].

3.6 Energy Calibration

The relationship between the number of channels and the energy the detector absorbs constitutes energy calibration [96]. The energy calibration of the NaI(Tl) spectroscopy system is determined by measuring the position of selected full-energy gamma-ray peaks with large peak-height to background ratios and precisely determined energies [97]. As shown in Table. 3.7, this detector's energy is calibrated using a set of standard γ-ray sources (^{137}Cs, ^{60}Co and ^{22}Na) from USNRC and State License Expert Quantities, "Gamma

Table 3.7: Properties of Radioactive sources used in the present study [98, 99].

Isotopes	Activity (μCi)	Energy (keV)	Serial number	Production date	$\mathbf{I}_\gamma\%$
^{137}Cs	1	661.66	IRS-126	1/1/2009	85.21
^{60}Co	1	1173.24	IRS-141	1/1/2009	99.9
		1332.5			99.88
		2505.74			20
^{22}Na	1	511	IRS-139	1/2/2009	181
		1274			99.95

Source Set," Model RSS8. Fig. 3.6 represents the energy calibration curve. The linear relationship between channel number (C_N) and energy is derived from the energy calibration figure and is represented by the following equation [98]:

$$E = 7.5005\, C_N - 47.595. \tag{3.1}$$

The energy resolution is the ability of a detector to distinguish between two peaks with a small energy difference. The following equation can be used to calculate resolution [99]:

$$\text{Energy Resolution} = \frac{FWHM}{C_N} \times (100\ \%), \tag{3.2}$$

where "FWHM" is the full width at half maximum for photo peak of the spectrum of gamma rays source and C is channel number at the centroid the gamma peak.

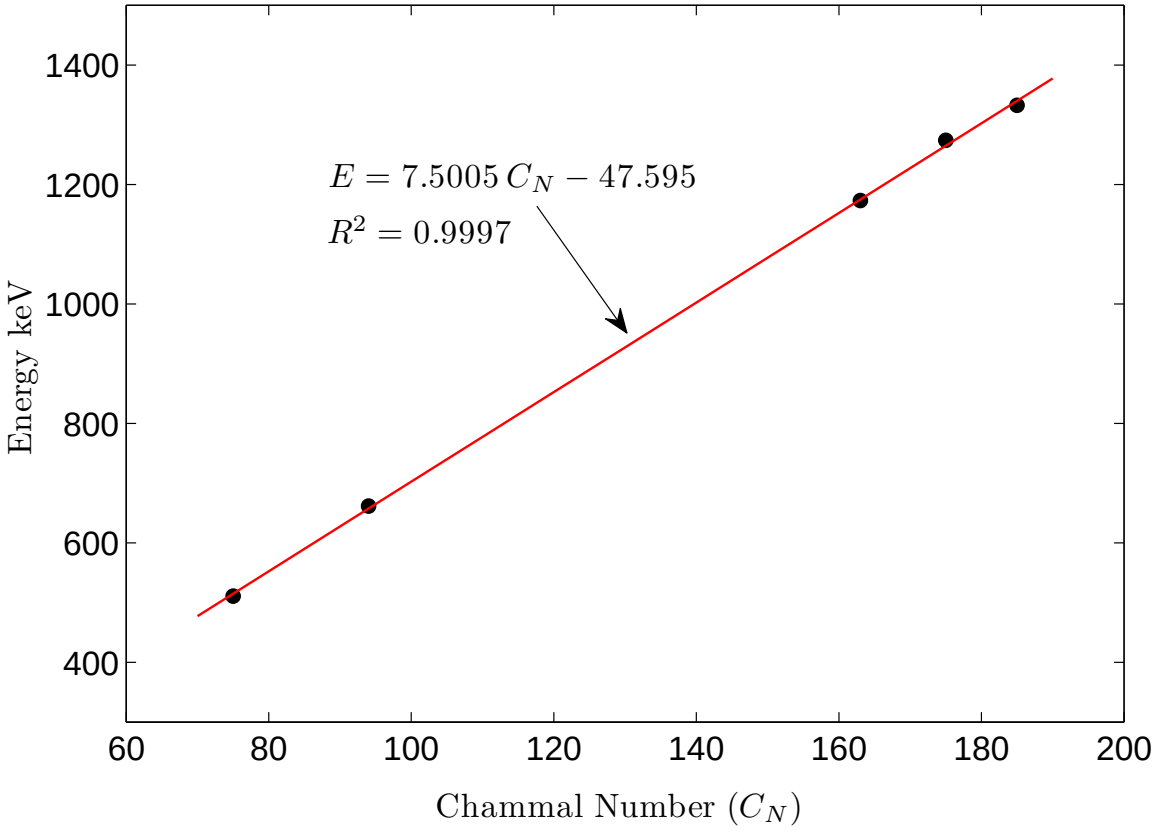

Figure 3.6: The Energy calibration curve of NaI (Tl) $3'' \times 3''$.

3.7 Efficiency Calibration

The ratio of the number of particles or photons recorded by the detector to the number of particles emitted by the source is the definition of detection efficiency [100]. The efficiency of the detector measuring system for a specific energy is calculated using the following equation [98, 99],

$$\varepsilon = \frac{C_p}{I_\gamma\, t\, A} \times (100\%), \tag{3.3}$$

where C_p is the count area under the specified energy peak after subtracting the background, t is the time (in second for the spectrum collected, I is the transition probability of the emitted gamma-ray, and A is the activity sources during the experiment. Calculating the activity of the standard source is as follows:

$$A = A_o e^{-\lambda \Delta t}, \tag{3.4}$$

where A_0 is the initial activity (Bq) of each source at a time t_o, A is the activity (Bq) of the source at time t, is the decay constant, and ($\Delta t = t - t_o$). The variation in the absolute photo-peak detector efficiency with gamma-ray energy was calibrated using four sources; ^{137}Cs, ^{60}Co, and ^{22}Na, as shown in Fig. 3.7. From the this figure, the fitting curve for efficiency as a function of energy (E)

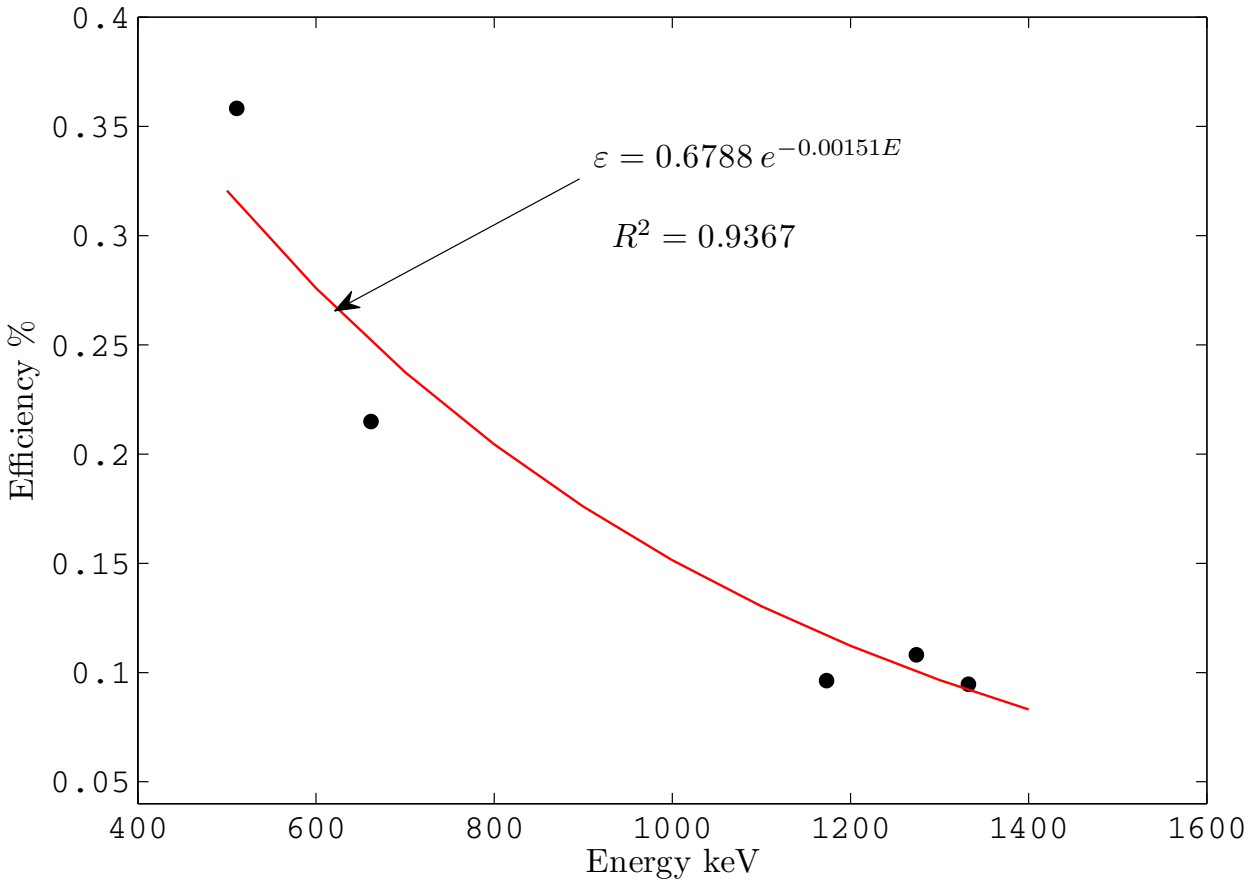

Figure 3.7: The Efficiency calibration curve of NaI (Tl) $3'' \times 3''$.

has the square correlation coefficient of 0.9367 with the exponential equation given by,

$$\varepsilon = 0.6788 e^{-0.00151E}, \tag{3.5}$$

where ε is the efficiency and E is the energy in keV. From this equation we can estimate the efficiency values for the isotopes ^{238}U (^{214}Bi), ^{232}Th (^{208}Ti) and ^{40}K as shown in Table. 3.8.

Table 3.8: The efficiency values for isotopes ^{238}U (^{214}Bi), ^{232}Th (^{208}Tl) and ^{40}K.

Isotopes and Daughter	Energy (keV)	ε
^{40}K	1460	0.037
^{238}U (^{214}Bi)	1764.5	0.020
^{232}Th (^{208}Ti)	2614	0.004

3.8 Gamma Radiation Measurement

After the end of storage, a secular equilibrium is achieved between radioactive isotopes of food samples in plastic Marinelli containers with a capacity of one liter (see Fig. 3.9). The Marinelli was placed on a NaI(Tl) detector (around the detector) at five hours to obtain the gamma-ray spectrum. Using the Maestro-32 information examination bundle, the net zone under the comparing photograph peaks is determined in the energy range by subtracting the check due to background sources from the net zone of a specific peak. All measurement record background radiation from natural radioactivity in earth materials, cosmic rays, structural materials within the system, and surrounding building materials. This background varies from location to location based on the detector's quality and size and the sort of shield employed. The radiation background will increase due to its interaction with the system's shield. The range of the background is estimated using a capacity of empty (1L) polyethylene plastic Marinelli. Due to the inadequate resolution of the NaI(Tl) detector at low gamma energies, which do not have well-isolated photo-peaks,

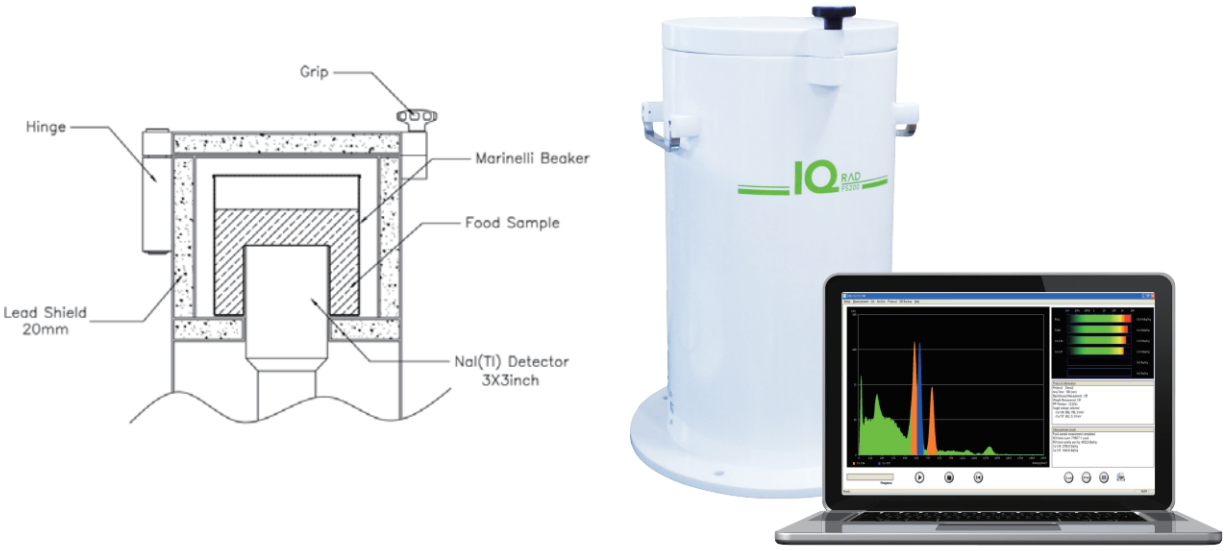

Figure 3.8: Marinelli beaker and the design of its geometry and computer software [101].

containers on the indicator and checking in the meantime for sample estimations are required. Thus, the specific activity (Bq/kg) activity concentrations can be measured at well-separated photo-peaks with high energies, such as those acquired in our results from the gamma beams produced by the descendants of (^{232}Th) and (^{238}U), which are in common harmony with them, whereas (^{40}K) was evaluated specifically by its 1460 keV gamma-line (^{40}Ar). Consequently, the specific activity of (^{238}U) was determined using the 1765 keV (^{214}Bi) gamma lines. Results have been calculated for (^{232}Th) using the gamma-ray lines at 2614 keV (^{208}Tl). Fig. 3.9 shows the background spectrum in the advanced nuclear physics laboratory, department College of Science, the University of Babylon, using a measurement time of 18000 second.

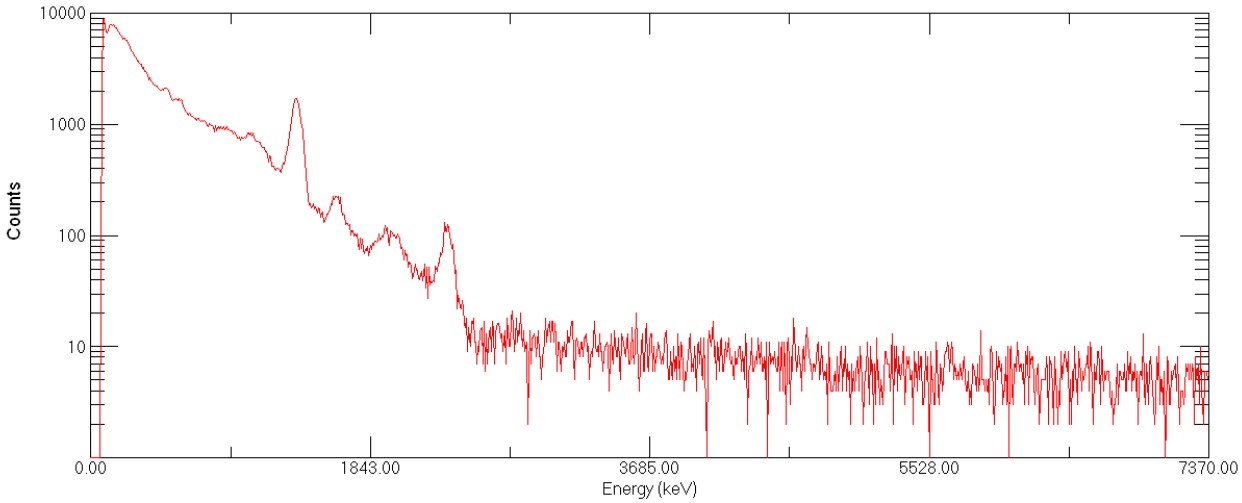

Figure 3.9: Background specterum inside the labrotary.

3.9 Blood Samples Collection

Blood samples were collected from healthy and cancer-stricken children of varying ages at the Warith International Cancer Institute in the holy city of Karbala. These samples were collected under the supervision of the medical staff specialized in this institution. Many analyses and medical examinations were conducted for children with cancer within this institution, where we obtained copies of these analyses and examinations before and after exposure to radiation doses resulting from radiation therapy sessions.

3.10 Truebeam Linear Accelerator

Varian Medical Systems' TrueBeam radiotherapy system is a medical linear accelerator. It provides high-precision image-guided stereotactic radiosurgery and radiotherapy to treat tumors and lesions in various body regions, such as the lungs, breasts, head, and neck. In April 2011, the device received marketing approval in China and in June 2011 in Japan. In August 2011, the Food and Drug Administration (FDA) of the United States approved the device for clinical use. The device is also CE-marked. The primary components of the TrueBeam radiotherapy device are a beam-producing system for producing

photon, electron, and diagnostic X-ray radiation and a control console. The beam-producing system is installed in a vault to shield radiation, while the control panel operating the device software is outside the treatment chamber. The device with LaserGuard II requires between 2.5MV and 25MV of energy to operate. Additionally, it incorporates the previously FDA-approved Trilogy radiotherapy system and associated accessories.

The kV radiation source has mouthguards and a capacitive collision detection system (kV CCDS) for added safety. This allows for proximity detection in addition to kV detectors and positioning devices.

The system includes six rotational recliners, a motion management interface (MMI), and a visual coaching device. In addition, it includes a comprehensive suite of Cone-Beam (CB) CT (CBCT) imaging capabilities, including 4D CBCT, gated CBCT imaging, brief ARC CBCT, extended-length CBCT, and multi-scan CBCT acquisition. Compared to 20 to 40 sessions of conventional radiation therapy, the TrueBeam radiotherapy system enables patients to recover in as few as one to five sessions [102–105].

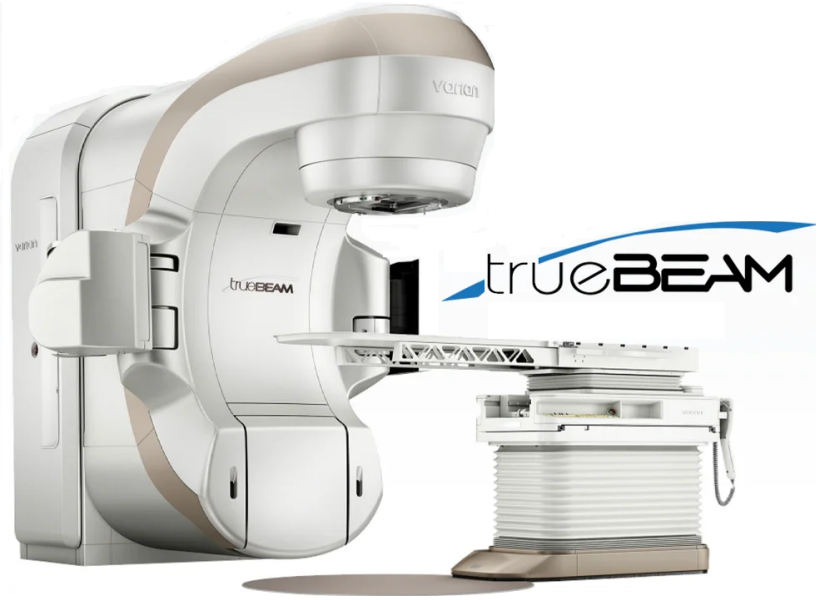

Figure 3.10: Truebeam 2.7 radiotherapy system [106].

Al-Warith Center, located in the Holy Karbala city for treating cancer and tumor, has a TrueBeam radiotherapy system. In this center, many children with cancer in different parts of their bodies have been treated. We have collected analyses and medical examinations for many children with cancer, especially a complete blood count (CBC). These analyses were used to conduct a statistical study of a correlation between a complete blood count and the radiation doses that may be present in the food eaten by infected children.

Chapter 4

Results, Discussion and Conclusions

4.1 Introduction

This chapter's summary gives the outcomes of the experiments carried out for this study. The natural radioactivity for natural gamma-ray due to long-lived gamma emitters in 59 samples of children's foods regularly consumed by children in the middle Euphrates governorates/Iraq was analyzed. The gamma spectroscopy system with NaI(Tl) has been utilized to estimate the activity concentration of radionuclides of ^{238}U, ^{232}Th, and ^{40}K in these food samples. We discuss the specific activity, annual effective dose, Radium equivalent activity, and the excess lifetime cancer risk factor for the samples with one kind of food. The average specific activities of the natural radioactive isotopes in the food samples were compared within the world median ranges in the UNSCEAR report.

We have also performed a statistical study for the many children infected with different types of cancer in their bodies. This study has been achieved at the Warith International Foundation for Oncology in Karbala city of Iraq. We chose children who consumed a lot of milk, biscuits, chips, cerelac, indomie, and corn flakes. These kinds of foods contain natural gamma-ray radioactivity from the radionuclide isotopes ^{238}U, ^{232}Th and ^{40}K that may be the cause of cancer in these children. At the Warith Cancer and tumor center, we work under the supervision of the staff to take into consideration about 30 blood samples from a large number that satisfies the condition of our study. These children were treated using the Truebeam radiotherapy system at this center for three months

and with four medical treatment sessions per month. The complete blood count (CBC) was taken after and before each session for the patient. However, we performed a statistical study based on a T-test using Graph-pad Prism version 10 software for the CBC test, especially for Hemoglobin (Hb), white blood cells (WBC), and Platelets (PLT). The statistical analysis for the Hb measurements with the annual effective dose (AED) was performed due to our first part study's consumption of the food types. Hence, in this statistical study, we investigated whether a correlation may occur between the Hb test with AED results. As discussed in this chapter, we conclude that some parameters correlate and others do not.

4.2 The Specific Activity

In this section, we will discuss the specific activity (activity concentration) calculated by Eq. (2.10) for canned powdered milk, biscuits, indomie, chips, cerelac, and corn flakes, with results presented in Tables. 4.1 to 4.7. As we mentioned before, the number of samples for powdered milk is nine; for other food types, we take ten samples each; hence the total is 59 samples under investigation.

It can be seen from Table. 4.1 the activity concentration varies from 15.11 ± 1.06 (M4 sample) to 20.72 ± 1.24 (M9 sample) for ^{226}Ra. For ^{232}Th, the minimum and maximum values are 4.26 ± 0.34 (M7 sample) and 12.58 ± 0.59 (M2 sample) respectively. For ^{40}K, the minimum and maximum values are 158.28 ± 3.59 (M2 sample) and 333.51 ± 5.21 (M7 sample), respectively.

We also notice from the table that the average value for ^{40}K records the highest numbers compared with others. These results agree with those reported in previous works in Iraq [64] and Saudi Arabia [56] as presented in Table. 4.2. The value for ^{238}U is approximately twice that for ^{232}Th. We also have an

Table 4.1: Specific Activity (Bq/kg) in powdered milk samples

Sample Code	Specific Activity (Bq/kg)		
	^{238}U	^{232}Th	^{40}K
M1	18.03 ± 1.16	8.82 ± 0.49	231.03 ± 4.34
M2	19.45 ± 1.21	12.58 ± 0.59	158.28 ± 3.59
M3	19.15 ± 1.2	10.26 ± 0.53	213.76 ± 4.17
M4	15.11 ± 1.06	10.76 ± 0.55	332.54 ± 5.2
M5	15.63 ± 108	11.25 ± 0.56	333.51 ± 5.21
M6	17.73 ± 1.15	10.01 ± 0.53	265.25 ± 4.65
M7	18.7 ± 1.18	4.26 ± 0.34	266.88 ± 4.66
M8	19.3 ± 1.2	9.62 ± 0.52	289.03 ± 4.85
M9	20.72 ± 1.24	7.19 ± 0.45	303.78 ± 4.97
Average	18.2 ± 1.16	9.417 ± 0.507	266.007 ± 4.627

acceptable agreement for these two isotopes compared with other works. There is a high inconsistency in values between our results and those from different countries; except for ^{40}K, the values are reported high.

Table 4.2: Comparison of the average specific activities (Bq/kg) of ^{226}Ra, ^{232}Th and ^{40}K in powdered milk with data published in other countries (where the average values is missing the range of values is indicated).

Region	^{238}U	^{232}Th	^{40}K	Reference
Iraq	18.2 ± 1.16	9.42 ± 0.51	266.01 ± 4.63	Present Work
Iraq	15.27 ± 8.24	1.62 ± 0.643	297.52 ± 125.78	[64]
Saudi Arabia	9.64	6.77	74.51	[89]
Saudi Arabia	0.46	0.35	234 ± 1.9	[56]
Jordan	$0.5 - 2.14$	$0.78 - 1.28$	$349 - 392$	[53]
Indian	2.5	1.02	34.35	[107]
Syria	$\cdots$	$\cdots$	$129 - 435$	[108]
Venezuela	$\cdots$	$\cdots$	401.7 ± 32.1	[109]
Egypt	0.44 ± 0.23	$\cdots$	$47.\ 25 \pm 123.6$	[110]
New Zealand	$0.149 - 0.186$	$0.147 - 0.166$	$549 - 605$	[109]
Germany	0.064 ± 0.018	0.094 ± 0.027	610.0 ± 18.3	[109]
Iran	$\cdots$	$\cdots$	17.3 ± 3.3	[54]
France	0.05 ± 0.011	0.142 ± 0.026	434.1 ± 13.0	[109]

For biscuit samples, as shown in Table. 4.3, the highest numbers of the specific activity are also for ^{40}K with the range between the minimum value of 141.25 ± 2.38 (B4 sample) and the maximum value of 235.43 ± 3.07 (B9 sample). It can be noticed that the values vary from 25.16 ± 1 (B4 sample) to 20.56 ± 0.9 (B8 sample) for ^{232}Th whereas for ^{238}U the variation is between 4.62 ± 0.48 (B9 sample) and 18.84 ± 0.97 (B4 sample). However, the average value for ^{40}K is also higher than others, but the low average value is for ^{238}U. The average values of our results are in good agreement with those reported in Ref [60].

Table 4.3: Specific Activity (Bq/kg) in Biscuit samples

Sample Code	Specific Activity (Bq/kg)		
	^{238}U	^{232}Th	^{40}K
B1	16.93 ± 0.92	10.95 ± 0.66	200.31 ± 2.83
B2	5.98 ± 0.55	19.8 ± 0.89	227.41 ± 3.02
B3	8.04 ± 0.64	13.57 ± 0.73	244.29 ± 3.13
B4	18.84 ± 0.97	25.16 ± 1	141.25 ± 2.38
B5	11.1 ± 0.75	12.46 ± 0.7	204.04 ± 2.86
B6	18.28 ± 0.96	10.24 ± 0.64	215.86 ± 2.94
B7	11.11 ± 0.75	18.06 ± 0.85	180.78 ± 2.69
B8	13.56 ± 0.83	20.56 ± 0.9	232.62 ± 3.05
B9	4.62 ± 0.48	13.41 ± 0.73	235.43 ± 3.07
B10	3.01 ± 0.39	18.93 ± 0.87	183.71 ± 2.71
Average	11.147 ± 0.724	16.314 ± 0.797	206.57 ± 2.868

For the indomie food type, ^{40}K still has the highest specific activity values with a maximum value of 229.58 ± 3.03 (I6 sample) and a minimum value of 128 (I10 sample). The ^{232}Th has the maximum and minimum values of 22.38 ± 0.94 (I7 sample) and 7.5 ± 0.55 (I8 sample), respectively, after that comes ^{238}U in order with lower values than other radioactive isotopes. The highest and lowest values are 18.38 ± 0.96 (I5 sample) and 8.64 ± 0.66 (I6 sample), and our measurement for the I3 sample is below detection limit (BDL), as shown in Table. 4.4. Our results agree well with the results presented in Refs [59, 79] except for ^{232}Th.

Table 4.4: Specific Activity (Bq/kg) in Indomie samples.

Sample Code	Specific Activity (Bq/kg)		
	^{238}U	^{232}Th	^{40}K
I1	17.48 ± 0.94	20.28 ± 0.9	199.63 ± 2.83
I2	17.53 ± 0.94	15.48 ± 0.78	198.94 ± 2.82
I3	BDL	12.3 ± 0.7	163.74 ± 2.56
I4	11.7 ± 0.77	17.02 ± 0.82	218.03 ± 2.96
I5	18.38 ± 0.96	13.69 ± 0.74	223.6 ± 2.99
I6	8.64 ± 0.66	13.65 ± 0.74	229.58 ± 3.03
I7	14.01 ± 0.84	22.38 ± 0.94	203.67 ± 2.86
I8	13.11 ± 0.81	7.5 ± 0.55	213.3 ± 2.92
I9	9.19 ± 0.68	16.98 ± 0.82	155.32 ± 2.5
I10	10.5 ± 0.73	17.98 ± 0.84	128.14 ± 2.27
Average	12.054 ± 0.733	15.726 ± 0.783	193.395 ± 2.77

The highest value of the ^{40}K is 223.96 ± 3 (Ch9 sample), while the lowest value is 144.01 ± 2.79 (Ch10 sample). For ^{232}Th, the Ch10 sample has the highest value, 20.91 ± 0.91, while the Ch1 sample has the lowest value, 10.08 ± 0.63. The highest value for ^{238}U is 16.98 ± 0.92 (Ch4 sample), while the Ch10 sample has the lowest value, 6.83 ± 0.59. Our measurement for the Ch6 sample is BDL as indicated in the Table. 4.5. The average specific activities for ^{40}K and ^{238}U are in good agreement with the results presented in Ref [62].

Table 4.5: Specific Activity (Bq/kg) in Chips samples

Sample Code	Specific Activity (Bq/kg)		
	^{238}U	^{232}Th	^{40}K
Ch1	11.6 ± 0.76	10.08 ± 0.63	178.34 ± 2.67
Ch2	11 ± 0.74	14.48 ± 0.76	190.64 ± 2.76
Ch3	14.92 ± 0.87	14.5 ± 0.76	167.35 ± 2.59
Ch4	16.98 ± 0.92	5.48 ± 0.47	177.21 ± 2.67
Ch5	11.4 ± 0.76	15.71 ± 0.79	189.6 ± 2.76
Ch6	BDL	14.4 ± 0.76	195.42 ± 2.8
Ch7	6.93 ± 0.59	15.4 ± 0.78	222.36 ± 2.99
Ch8	13.46 ± 0.82	14.8 ± 0.77	215.7 ± 2.94
Ch9	9.19 ± 0.68	12.94 ± 0.72	223.96 ± 3
Ch10	6.83 ± 0.59	20.91 ± 0.91	144.01 ± 2.79
Average	10.231 ± 0.673	13.87 ± 0.735	190.459 ± 2.8

The specific activity for the Cerelac food type is shown in Table. 4.6; the highest value of the ^{40}K is 366.59 ± 5.46 (Ce9 sample), while the lowest value is 240.81 ± 4.4 (Ce4 sample). For ^{232}Th, the Ce2 sample has the highest value, 20.91 ± 0.91, while the Ce3 sample has the lowest value, 5.75 ± 0.4. The highest value for ^{238}U is 19.52 ± 1.21 (Ce5 sample), while the Ce3 sample has the lowest value, 9.35 ± 0.84. We compare our results with those presented in Ref [65], and there is acceptable consistency for the values.

For corn flakes food type, in Table. 4.7, the highest values of the specific activity are also for ^{40}K with the range between the minimum value of $182.99.68 \pm 2.71$ (Co8 sample) and the maximum value of 290.92 ± 3.42 (Co9 sample). It can be noticed that the values vary from 5.4 ± 0.46 (Co2 sample) to 18.65 ± 0.86 (Co7 sample) for ^{232}Th whereas for ^{238}U the variation is between

Table 4.6: Specific Activity (Bq/kg) in Cerelac samples

Sample Code	Specific Activity (Bq/kg)		
	^{238}U	^{232}Th	^{40}K
Ce1	17.13 ± 1.13	8.99 ± 0.5	242.6 ± 4.45
Ce2	14.44 ± 1.04	12.55 ± 0.59	304.76 ± 4.98
Ce3	9.35 ± 0.84	5.75 ± 0.4	314.37 ± 5.06
Ce4	11.45 ± 0.93	6.03 ± 0.41	240.81 ± 4.43
Ce5	19.52 ± 1.21	8.85 ± 0.49	263.21 ± 4.63
Ce6	16.01 ± 1.09	7.96 ± 0.47	266.88 ± 4.66
Ce7	15.04 ± 1.06	9.84 ± 0.52	286.75 ± 4.83
Ce8	15.71 ± 1.08	7.96 ± 0.47	247.73 ± 4.49
Ce9	12.19 ± 0.96	6.47 ± 0.42	366.59 ± 5.46
Ce10	13.24 ± 1	7.25 ± 0.45	299.46 ± 4.94
Average	14.41 ± 1.03	8.165 ± 0.472	283.316 ± 4.793

3.06 ± 0.39 (Co6 sample) and 19.44 ± 0.99 (Co1 sample). However, the average value for ^{40}K is higher than others, but the low average value is for ^{238}U. Comparing our results with other work presented by Ref [111] , we have only good agreement with those results for ^{238}U. In contrast, those results for ^{40}K are approximately four times our results for the average specific activity.

Table 4.7: Specific Activity (Bq/kg) in Corn Flakes samples

Sample Code	Specific Activity (Bq/kg)		
	^{238}U	^{232}Th	^{40}K
Co1	19.44 ± 0.99	17.42 ± 0.83	190.68 ± 2.76
Co2	9.95 ± 0.71	5.4 ± 0.46	203.11 ± 2.85
Co3	15.77 ± 0.89	11.98 ± 0.69	270.99 ± 3.3
Co4	16.83 ± 0.92	14.52 ± 0.76	225.12 ± 3
Co5	15.82 ± 0.89	12.1 ± 0.69	214.34 ± 2.93
Co6	3.06 ± 0.39	13.37 ± 0.73	226.33 ± 3.01
Co7	14.06 ± 0.84	18.65 ± 0.86	194.37 ± 2.79
Co8	11.3 ± 0.75	14.29 ± 0.75	182.99 ± 2.71
Co9	15.22 ± 0.87	11.27 ± 0.67	290.92 ± 3.42
Co10	2.76 ± 0.37	17.26 ± 0.83	243.49 ± 3.12
Average	12.421 ± 0.762	13.622 ± 0.727	224.234 ± 3.089

However, the specific activities for all kinds of foods samples are presented in Figs. 4.1 to 4.6. In general, we notice that the specific activity for all the samples has the highest value for ^{40}K with a rough difference of more than 180 Bq/kg compared with other radioactive isotopes (see Fig. 4.7). Nevertheless, the approximate difference between the average values of ^{238}U and ^{232}Th does not exceed 9 Bg/kg. Also, the minimum average value for milk and cerelac foods is for ^{232}Th, while ^{238}U has the lowest average value for other foods as indicated in Figs. 4.8. Our results do not remarkably exceed the worldwide median values of 35, 30, and 400 (Bq/kg) for ^{238}U, ^{232}Th, ^{40}K, respectively [11].

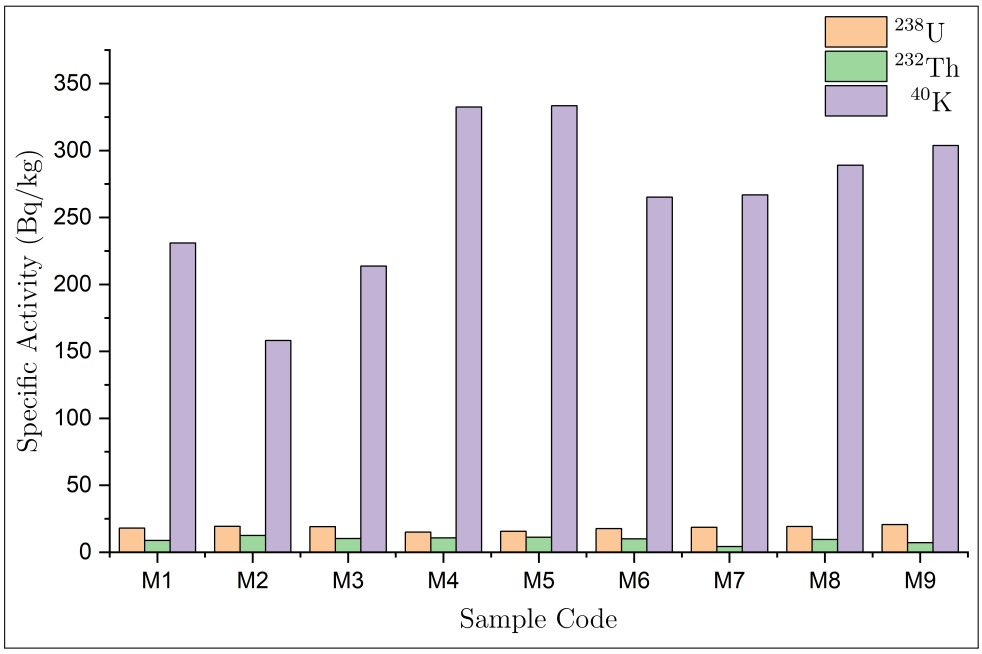

Figure 4.1: The specific activity (Bq/kg) measured in different powdered milk samples for natural radioactive isotopes ^{238}U, ^{232}Th and ^{40}K indicated by orange, green, and violet colors respectively.

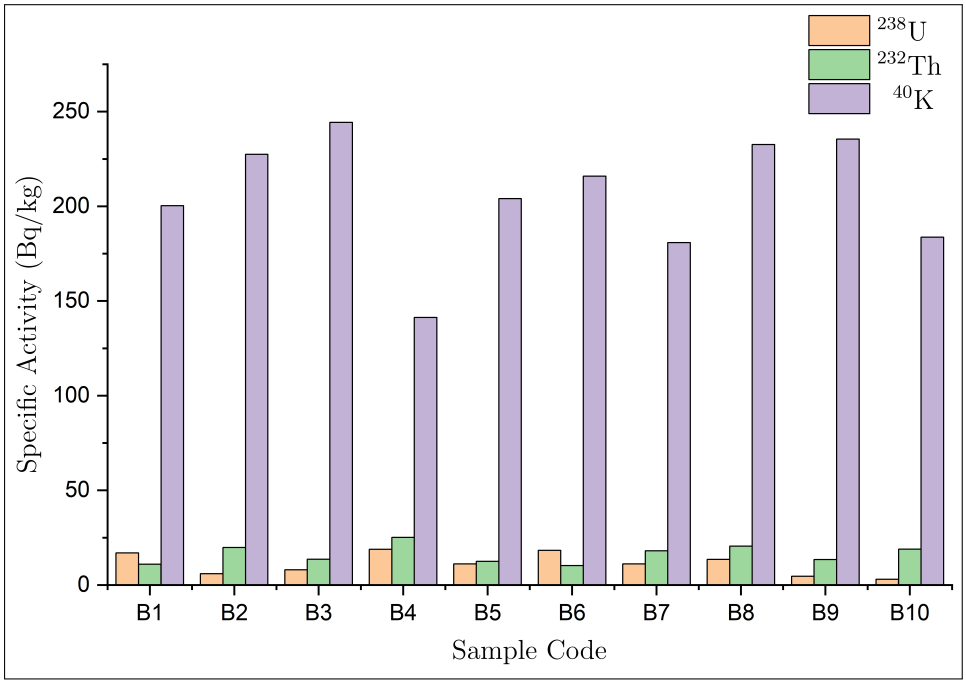

Figure 4.2: The specific activity (Bq/kg) measured in different Biscuit samples for natural radioactive isotopes ^{238}U, ^{232}Th and ^{40}K indicated by orange, green, and violet colors respectively.

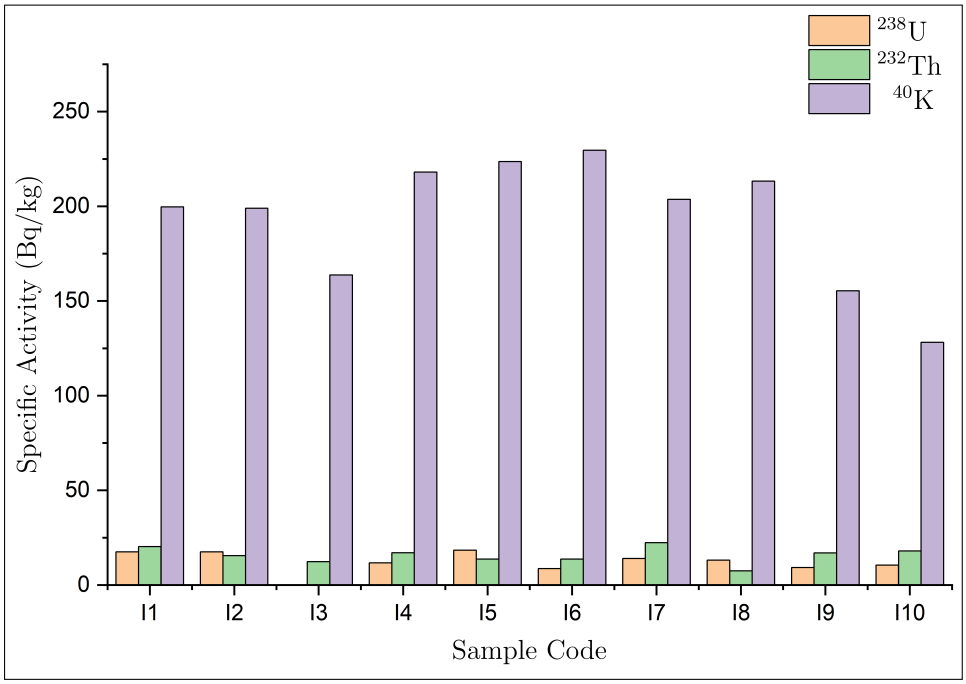

Figure 4.3: The specific activity (Bq/kg) measured in different Indomie samples for natural radioactive isotopes ^{238}U, ^{232}Th and ^{40}K indicated by orange, green, and violet colors respectively.

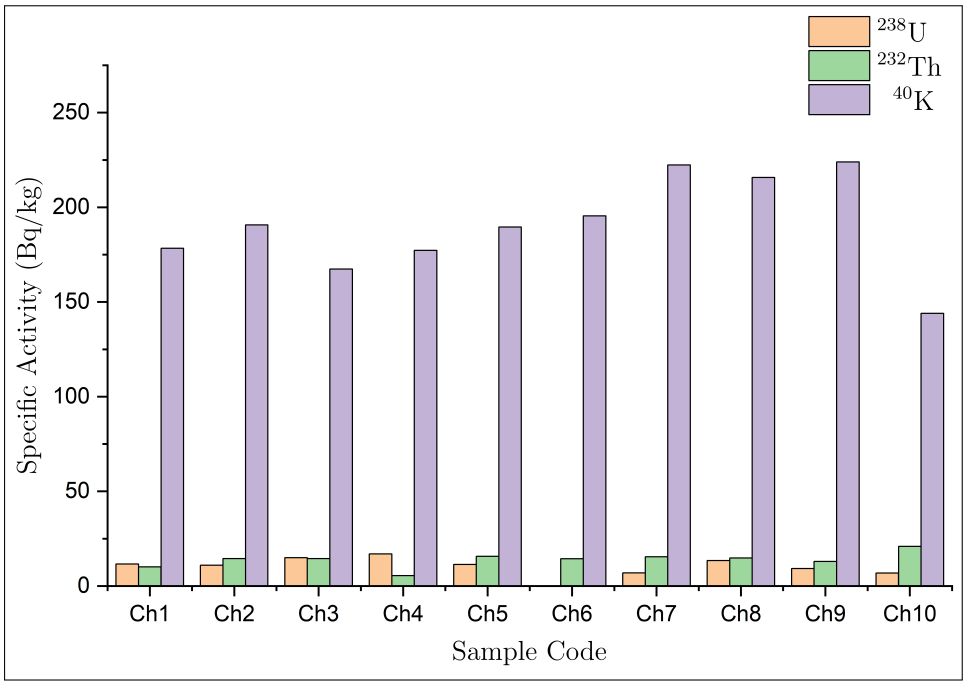

Figure 4.4: The specific activity (Bq/kg) measured in different Chips samples for natural radioactive isotopes ^{238}U, ^{232}Th and ^{40}K indicated by orange, green, and violet colors respectively.

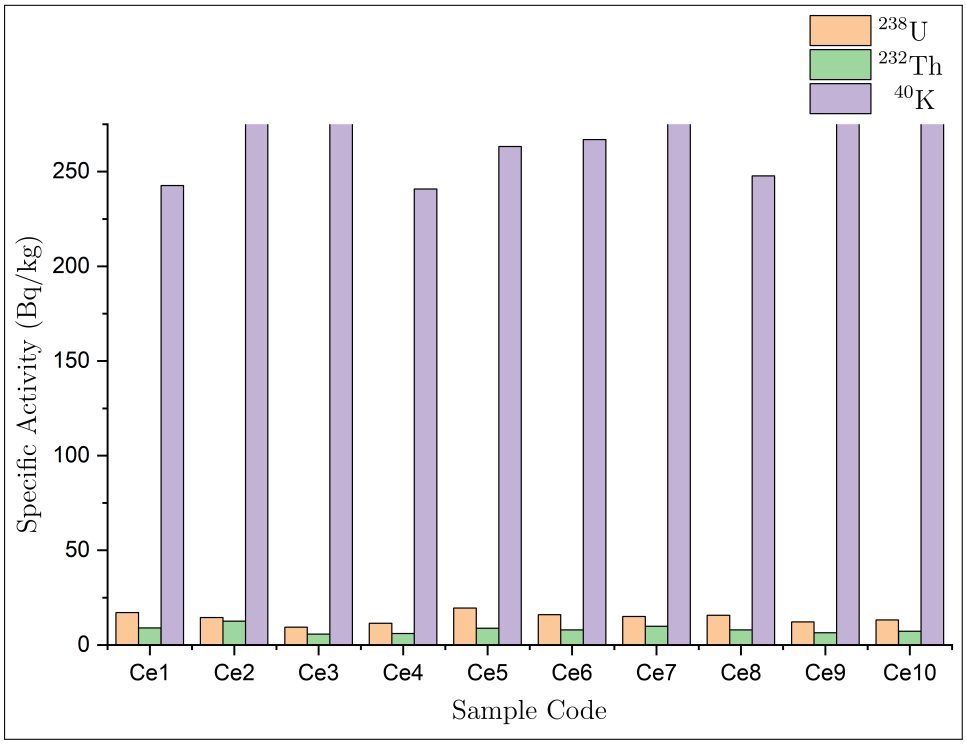

Figure 4.5: The specific activity (Bq/kg) measured in different Cerelac samples for natural radioactive isotopes ^{238}U, ^{232}Th and ^{40}K indicated by orange, green, and violet colors respectively.

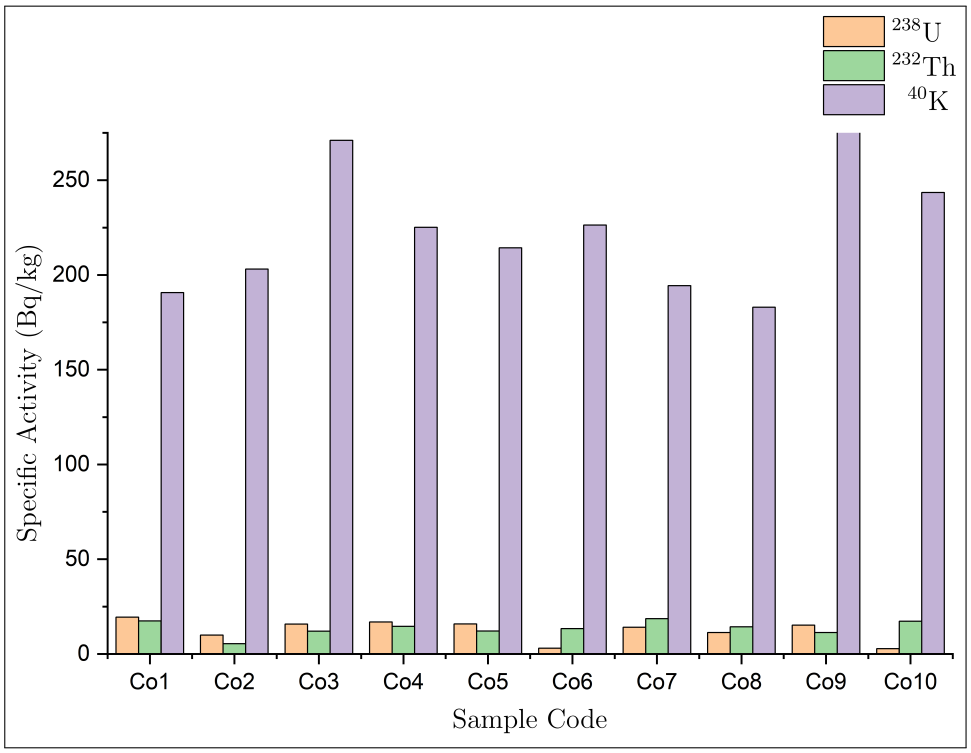

Figure 4.6: The specific activity (Bq/kg) measured in different Corn Flakes samples for natural radioactive isotopes ^{238}U, ^{232}Th and ^{40}K indicated by orange, green, and violet colors respectively.

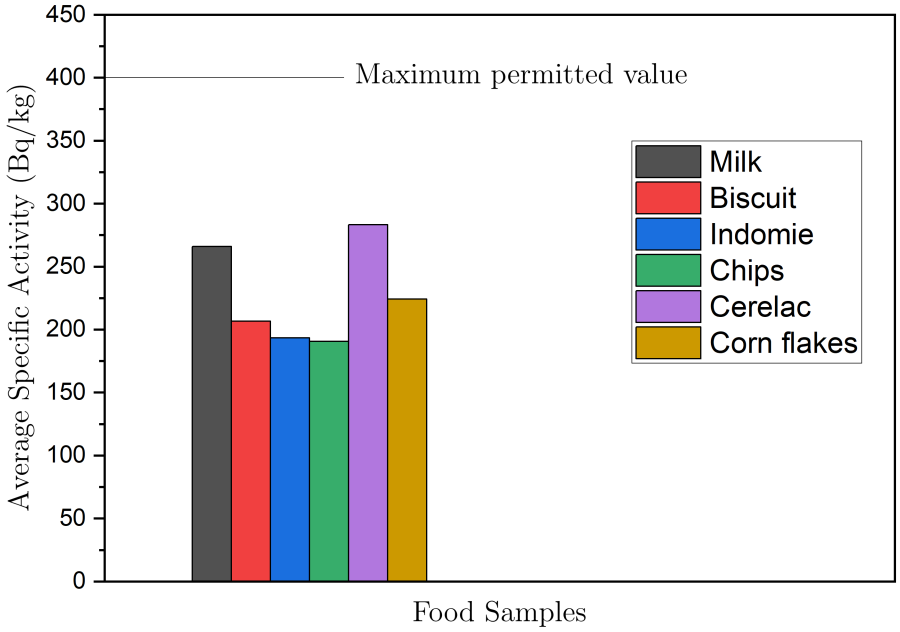

Figure 4.7: The average specific activity (Bq/kg) measured in different food samples for natural radioactive isotope ^{40}K with the worldwide permitted value [11].

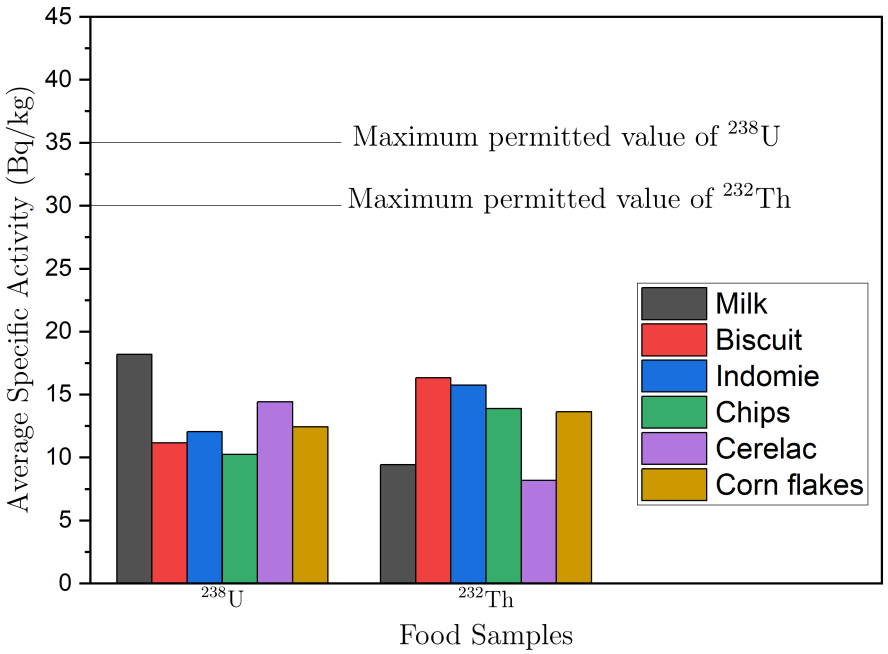

Figure 4.8: The average specific activity (Bq/kg) measured in different food samples for natural radioactive isotopes ^{238}U and ^{232}Th with the worldwide permitted value [11].

4.3 Annual Effective Dose (AED)

The annual effective dose is calculated from Eq. (2.20). The values of E (see Table. 4.8) are under International Commission on Radiological Protection classifications [11], namely, adult, child (10 ys old), and infant (1-y-old). Based on the low values for ^{40}K and high values for ^{238}U and ^{232}Th of the conversion factors, these factors have balanced our calculation of the annual effective dose due to reducing the significantly increased values of the specific activity. Hence, we can see that AED < 1 for all these radioactive isotopes.

Table 4.8: Dose conversion factors (E) given in the unit of (nSv/Bq) [11].

Age Group	^{238}U	^{232}Th	^{40}K
Adults (over 17 y)	280	230	6.2
Children (10) y	800	290	13
Infant (1) y	980	450	42

The annual intake of the food samples I (kg/y) is different from one food type to another depending on the daily habits of people consuming varity of food in different quantities. The infant is taking about 22.4 (kg/y), according to ICRP72 report [112]. Following the United Nations Scientific Committee on the Effects of Atomic Radiation [11], the I values for biscuit samples are 90 and 45 (kg/y) for the child and infant age groups, respectively. The estimated values of consumption rate I for Indomie [59, 113], Chips [114, 115], Cerelac [65, 116], and Corn flakes [55] are 36 , 10, 36, and 45 (kg/y), respectively.

The results for powdered milk samples are indicated in Table. 4.9, we notice the average annual effective dose (AED) of ^{238}U $>$ ^{40}K $>$ ^{232}Th, with the values of 0.391, 0.250, and 0.095 (mSv/y), respectively. The total AED has the highest and lowest values of 0.804 (M9 sample) and 0.694 for both M1 and M2 samples.

The excess life time cancer risk factor (ELCR) can be calculated from Eq. (2.21), and it has been established that its value is directly proportional to the AED value. Therefore, ELCR has maximum and minimum values of 2.813×10^{-3} and 2.429×10^{-3}, respectively as shown in Fig. 4.9.

Table 4.9: Annual effective dose, and the excess lifetime cancer risk factor (ELCR) $\times 10^{-3}$ due to the intake of ^{238}U, ^{232}Th and ^{40}K for infants milk samples.

Sample Code	AED (mSv/y)			Total AED (mSv/y)	ELCR $\times 10^{-3}$
	^{238}U	^{232}Th	^{40}K		
M1	0.388	0.089	0.217	0.694	2.429
M2	0.418	0.127	0.149	0.694	2.429
M3	0.412	0.103	0.201	0.716	2.507
M4	0.325	0.108	0.313	0.746	2.612
M5	0.336	0.113	0.314	0.763	2.671
M6	0.381	0.101	0.250	0.732	2.561
M7	0.402	0.043	0.251	0.696	2.437
M8	0.415	0.097	0.272	0.784	2.744
M9	0.446	0.072	0.286	0.804	2.813
Average	0.391	0.095	0.250	0.737	2.578

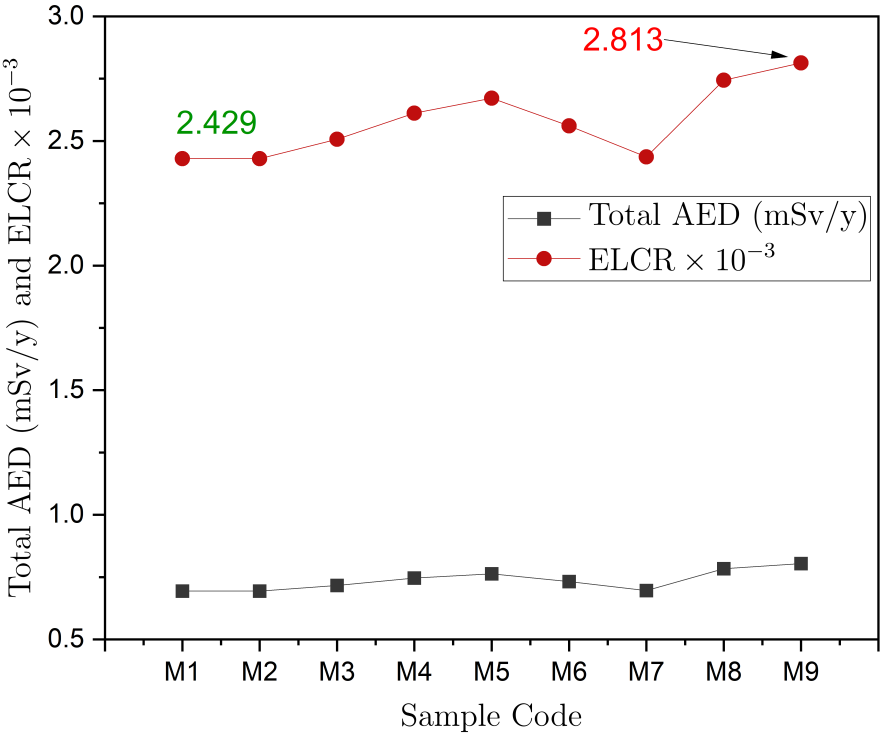

Figure 4.9: The excess lifetime cancer risk factor (ELCR) $\times 10^{-3}$ and the total annual effective dose (mSv/y) due to the intake of ^{238}U, ^{232}Th and ^{40}K for powdered milk samples.

The AED and ELCR for biscuit samples have been discussed for infants and children age groups as shown in Tables. 4.10 and 4.11. Similarly to the milk cases, the average AED for infants has the order of $^{238}\text{U} > {}^{40}\text{K} > {}^{232}\text{Th}$, with the values of 0.482, 0.391, and 0.330 (mSv/y). Regarding the total AED, sample B4 has a maximum value of 1.590 (mSv/y), giving the highest ELCR value of 5.566. The minimum value is for the B10 sample with a magnitude of 0.861, providing the lowest value of 3.012 for ELCR, as shown in Fig. 4.10. On the other hand, for the same samples with the children's case, we have the maximum and minimum values of the total AED such that 2.178 and 0.92 (mSv/y), respectively. In contrast to the infant case, the average AED for the children has the order of $^{238}\text{U} > {}^{232}\text{Th} > {}^{40}\text{K}$, with the values 0.803, 0.426, 0.242 (mSv/y), respectively.

Table 4.10: Annual effective ingestion dose, total annual effective dose (mSv/y) and the excess lifetime cancer risk factor (ELCR) $\times 10^{-3}$ due to the intake of ^{238}U, ^{232}Th and ^{40}K for infant biscuit samples.

Sample Code	AED (mSv/y)			Total AED (mSv/y)	ELCR $\times 10^{-3}$
	^{238}U	^{232}Th	^{40}K		
B1	0.731	0.222	0.379	1.332	4.661
B2	0.258	0.401	0.430	1.089	3.812
B3	0.347	0.275	0.462	1.084	3.793
B4	0.814	0.509	0.267	1.590	5.566
B5	0.480	0.252	0.386	1.117	3.911
B6	0.790	0.207	0.408	1.405	4.918
B7	0.480	0.366	0.342	1.187	4.156
B8	0.586	0.416	0.440	1.442	5.046
B9	0.200	0.272	0.445	0.916	3.206
B10	0.130	0.383	0.347	0.861	3.012
Average	0.482	0.330	0.391	1.202	4.208

The difference in the values of AED and ELCR between the infants and children age group is due to the high consumption rate from the children compared with the infants. In the calculation of the AED for other types of foods, we consider the children's case because the consumption rate for these kinds is higher compared with the infants.

Table 4.11: Annual effective ingestion dose, total annual effective dose (mSv/y) and the excess lifetime cancer risk factor (ELCR) $\times 10^{-3}$ due to the intake of ^{238}U, ^{232}Th and ^{40}K for Children biscuit samples.

Sample Code	AED (mSv/y)			Total AED (mSv/y)	ELCR $\times 10^{-3}$
	^{238}U	^{232}Th	^{40}K		
B1	1.219	0.286	0.234	1.739	6.087
B2	0.431	0.517	0.266	1.213	4.247
B3	0.579	0.354	0.286	1.219	4.266
B4	1.356	0.657	0.165	2.178	7.624
B5	0.799	0.325	0.239	1.363	4.771
B6	1.316	0.267	0.253	1.836	6.426
B7	0.800	0.471	0.212	1.483	5.190
B8	0.976	0.537	0.272	1.785	6.248
B9	0.333	0.350	0.275	0.958	3.353
B10	0.217	0.494	0.215	0.926	3.240
Average	0.803	0.426	0.242	1.470	5.145

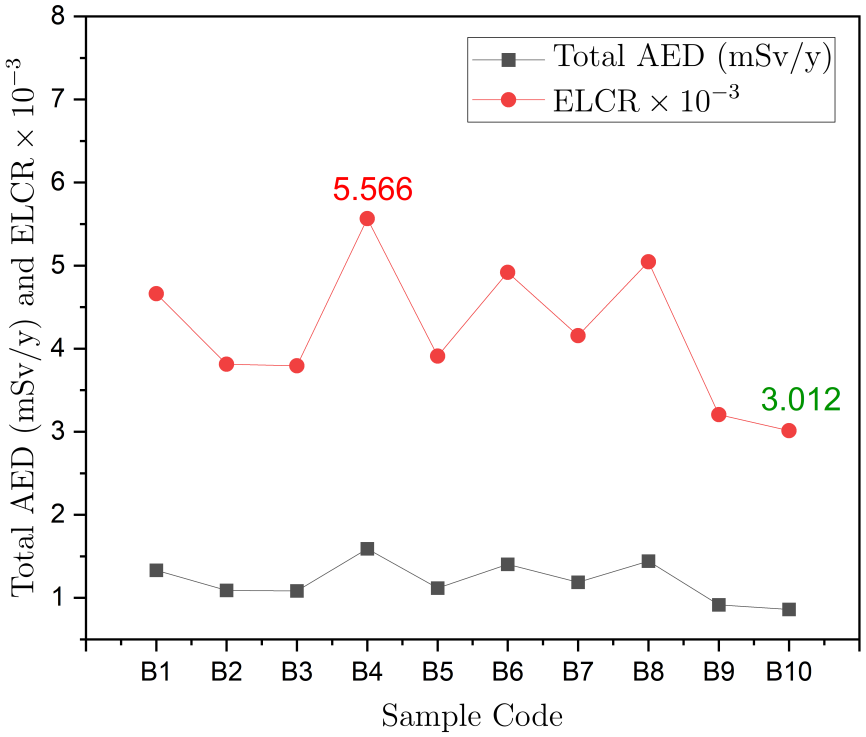

Figure 4.10: The excess lifetime cancer risk factor (ELCR) $\times 10^{-3}$ and the total annual effective dose (mSv/y) due to the intake of ^{238}U, ^{232}Th and ^{40}K for biscuit samples.

The findings for the analyzed samples of indomie are presented in the Table. 4.12. In contrast to the powdered milk and biscuit case for infant, We find that the AED of ^{238}U is higher than that of ^{232}Th, but then for ^{40}K is the lowest estimated magnitude, with values of 0.347, 0.164, and 0.091 (mSv/y), respectively. Nevertheless, the calculated AED is in agreement with those obtained from biscuit samples for children. The total AED has a maximum value of 0.809 (I1 sample) and a minimum value of 0.205 (I3 sample), with the corresponding ELCR highest and lowest values of 2.830 and 0.718, respectively. These results are shown in Fig. 4.11.

Table 4.12: Annual effective dose, and the excess lifetime cancer risk factor (ELCR)$\times 10^{-3}$ due to the intake of ^{238}U, ^{232}Th and ^{40}K for children Indomie samples.

Sample Code	AED (mSv/y)			Total AED (mSv/y)	ELCR $\times 10^{-3}$
	^{238}U	^{232}Th	^{40}K		
I1	0.503	0.212	0.093	0.809	2.830
I2	0.505	0.162	0.093	0.760	2.659
I3	0.000	0.128	0.077	0.205	0.718
I4	0.337	0.178	0.102	0.617	2.158
I5	0.529	0.143	0.105	0.777	2.719
I6	0.249	0.143	0.107	0.499	1.746
I7	0.403	0.234	0.095	0.732	2.564
I8	0.378	0.078	0.100	0.556	1.945
I9	0.265	0.177	0.073	0.515	1.801
I10	0.302	0.188	0.060	0.550	1.925
Average	0.347	0.164	0.091	0.602	2.107

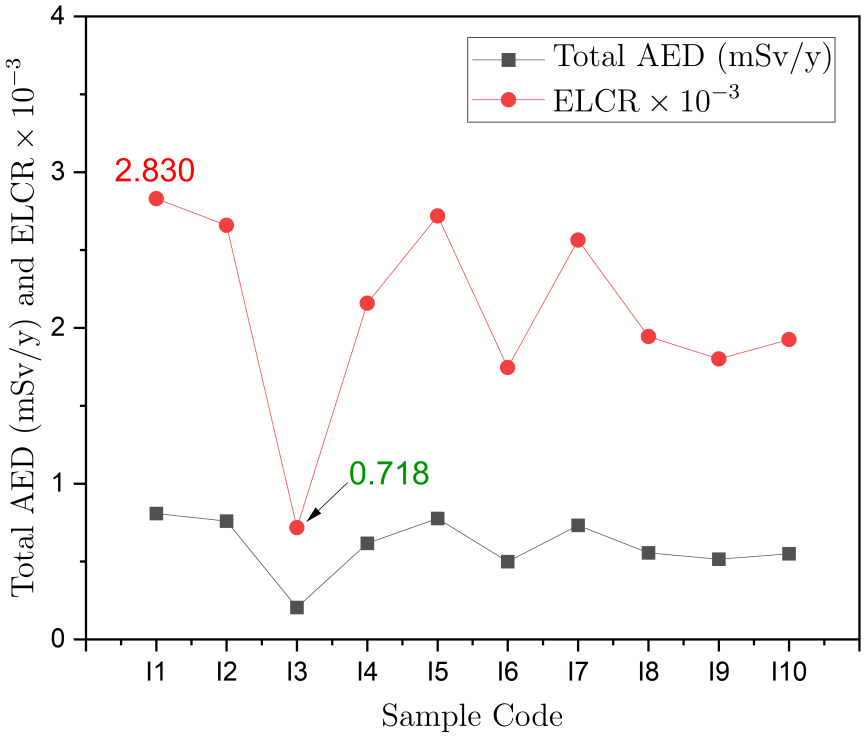

Figure 4.11: The excess lifetime cancer risk factor (ELCR) $\times 10^{-3}$ and the total annual effective dose (mSv/y) due to the intake of ^{238}U, ^{232}Th and ^{40}K for Indomie samples.

Similar to the biscuit and indomie samples for children, the AED for chips samples has to be $^{238}\text{U} > {}^{232}\text{Th} > {}^{40}\text{K}$ with the values given as 0.082, 0.040, and 0.025 (mSv/y) and as presented in Tabel. 4.13. The maximum and minimum values for the total AED are 0.183 (Ch3 sample) and 0.067 (Ch6 sample) (mSv/y), respectively. The related values of ELCR for these samples are 0.641 and 0.235, respectively, as shown in Fig. 4.12.

Table 4.13: Annual effective dose, and the excess lifetime cancer risk factor (ELCR) $\times 10^{-3}$ due to the intake of ^{238}U, ^{232}Th and ^{40}K for children Chips samples.

Sample Code	AED (mSv/y)			Total AED (mSv/y)	ELCR $\times 10^{-3}$
	^{238}U	^{232}Th	^{40}K		
Ch1	0.093	0.029	0.023	0.145	0.508
Ch2	0.088	0.042	0.025	0.155	0.542
Ch3	0.119	0.042	0.022	0.183	0.641
Ch4	0.136	0.016	0.023	0.175	0.612
Ch5	0.091	0.046	0.025	0.161	0.565
Ch6	0.000	0.042	0.025	0.067	0.235
Ch7	0.055	0.045	0.029	0.129	0.452
Ch8	0.108	0.043	0.028	0.179	0.625
Ch9	0.074	0.038	0.029	0.140	0.491
Ch10	0.055	0.061	0.019	0.134	0.469
Average	0.082	0.040	0.025	0.147	0.514

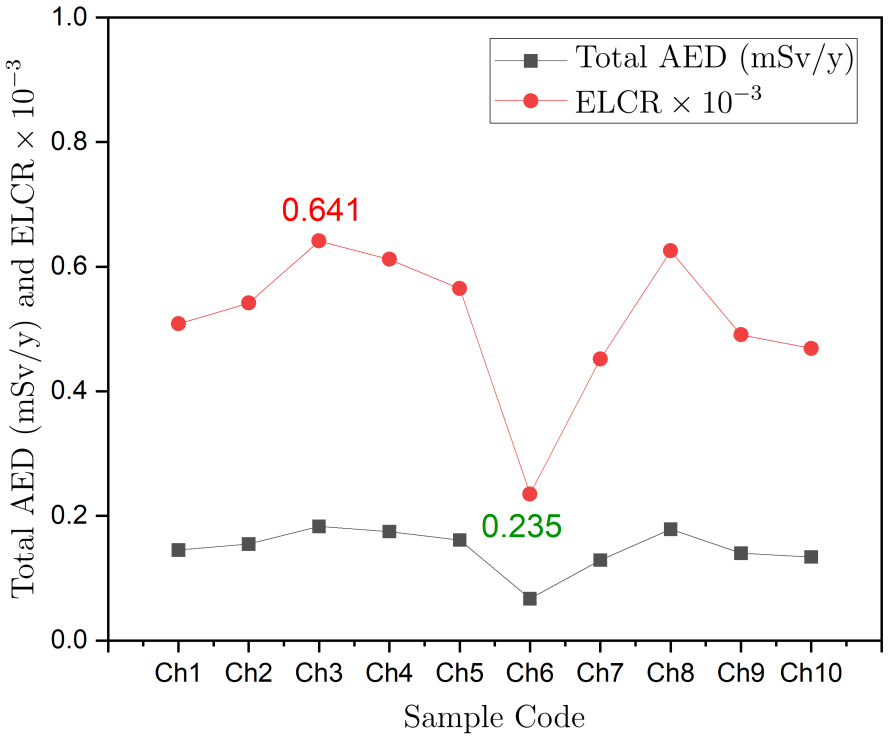

Figure 4.12: The excess lifetime cancer risk factor (ELCR) $\times 10^{-3}$ and the total annual effective dose (mSv/y) due to the intake of ^{238}U, ^{232}Th and ^{40}K for Chips samples.

In contrast to the biscuit indomie and chips samples for children cases and similar to powdered milk and biscuit samples for infants, the AED for cerelac samples has to be $^{238}U > {}^{40}K > {}^{232}Th$ with the values given as 0.498, 0.429, 0.132 (mSv/y) and as presented in Tabel. 4.14. The maximum and minimum values for the total AED are 1.216 (Ce5 sample) and 0.858 (Ce4 sample) (mSv/y), respectively. The related values of ELCR for these samples are 4.256 and 3.001, respectively, as shown in Fig. 4.13.

Table 4.14: Annual effective dose, and the excess lifetime cancer risk factor (ELCR) $\times 10^{-3}$ due to the intake of ^{238}U, ^{232}Th and ^{40}K for children Cerelac samples.

Sample Code	AED (mSv/y)			Total AED (mSv/y)	ELCR $\times 10^{-3}$
	^{238}U	^{232}Th	^{40}K		
Ce1	0.592	0.146	0.367	1.104	3.866
Ce2	0.499	0.203	0.461	1.163	4.071
Ce3	0.323	0.093	0.475	0.892	3.121
Ce4	0.396	0.098	0.364	0.858	3.001
Ce5	0.675	0.143	0.398	1.216	4.256
Ce6	0.553	0.129	0.404	1.086	3.800
Ce7	0.52	0.159	0.434	1.113	3.895
Ce8	0.543	0.129	0.375	1.046	3.663
Ce9	0.421	0.105	0.554	1.08	3.781
Ce10	0.458	0.117	0.453	1.028	3.597
Average	0.498	0.132	0.429	1.059	3.705

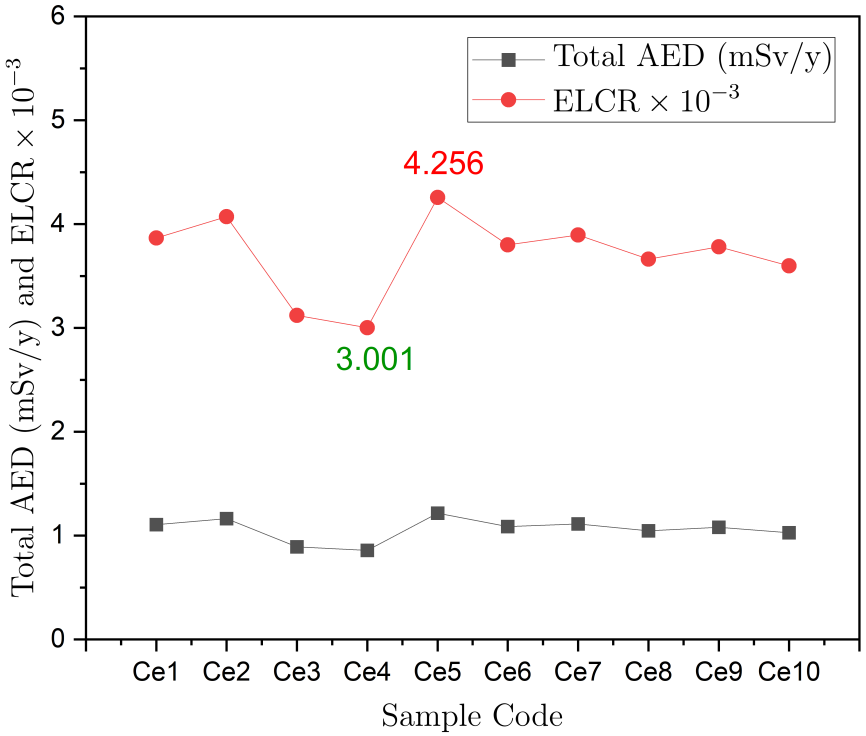

Figure 4.13: The excess lifetime cancer risk factor (ELCR) $\times 10^{-3}$ and the total annual effective dose (mSv/y) due to the intake of ^{238}U, ^{232}Th and ^{40}K for Cerelac samples.

It can be seen clearly from Tabel. 4.15, the AED values for the Corn flakes have the order of ^{238}U $>$ ^{232}Th $>^{40}$K with the values given as 0.447, 0.178, 0.131 (mSv/y) respectively. This is consistence with all food samples in our study except powdered milk and biscuit for infants. The maximum and minimum values for the total AED are 1.039 (Co1 sample) and 0.417 (Co6 sample) (mSv/y), respectively. The related values of ELCR for these samples are 3.636 and 1.46, respectively, as shown in Fig. 4.14.

Table 4.15: Annual effective dose, and the excess lifetime cancer risk factor (ELCR) $\times 10^{-3}$ due to the intake of ^{238}U, ^{232}Th and ^{40}K for children Corn Flakes samples.

Sample Code	AED (mSv/y)			Total AED (mSv/y)	ELCR $\times 10^{-3}$
	^{238}U	^{232}Th	^{40}K		
Co1	0.7	0.227	0.112	1.039	3.636
Co2	0.358	0.07	0.119	0.547	1.916
Co3	0.568	0.156	0.159	0.883	3.089
Co4	0.606	0.189	0.132	0.927	3.245
Co5	0.57	0.158	0.125	0.853	2.985
Co6	0.11	0.174	0.132	0.417	1.46
Co7	0.506	0.243	0.114	0.863	3.021
Co8	0.407	0.186	0.107	0.7	2.451
Co9	0.548	0.147	0.17	0.865	3.028
Co10	0.099	0.225	0.142	0.467	1.635
Average	0.447	0.178	0.131	0.756	2.647

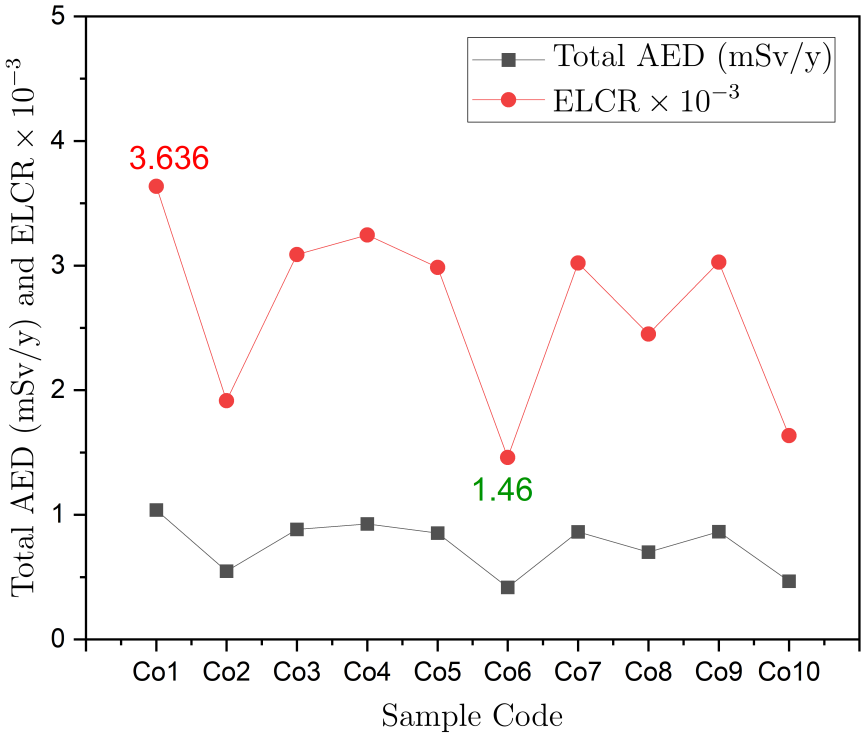

Figure 4.14: The excess lifetime cancer risk factor (ELCR) $\times 10^{-3}$ and the total annual effective dose (mSv/y) due to the intake of ^{238}U, ^{232}Th and ^{40}K for Corn Flakes samples.

Fortunately, with all the results for the evaluated AED, these outcomes are within the typical worldwide range of annual dose 1 (mSV/y) due to the ingestion of all-natural radiation sources reported by Ref [11]. It has been clear that the average of the total AED for children's biscuit samples has the maximum value and higher than the worldwide limits. The values of other samples come in sequence: cerelac, Corn flakes, powdered milk, Indomie, and Chips which has the lowest value. In the pie chart Fig. 4.15, we show the percentage of the average ELCR for all food types. Clearly, we have the highest value for biscuit of children due to the high AED value and vice versa for the chips samples. The results are 30.8%, 22.2%, 15.9%, 15.4%, 12.6%, and 3.1% for biscuit, cerelac, corn flakes, powdered milk, indomie, and chips, respectively, with all the values below the worldwide limits [11, 112].

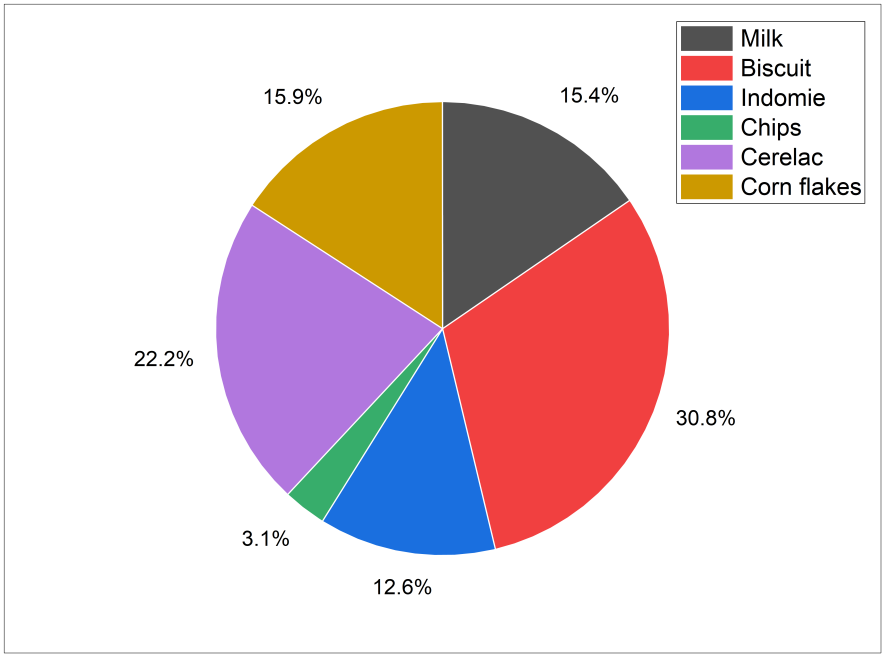

Figure 4.15: The percentage of average excess lifetime cancer risk factor (ELCR) due to the intake of ^{238}U, ^{232}Th and ^{40}K in various food samples.

4.4 Radium Equivalent and Hazard index

The Radium equivalent activity index Ra_{eq} and the radiation internal hazard index H_{in} are related to the specific activities of the natural radioactivity as given by Eqs. (2.18) and (2.19), respectively. The average values of Ra_{eq} (Bq/kg)for powdered milk, biscuit, indomie, chips, cerelac, and corn flakes are 52.151, 50.382, 49.434, 44.731, 470.899, and 49.172, respectively as shown in Tables. 4.16 to 4.21. Also, the calculated values of H_{in} are presented in the tables for these food samples with the values of 0.190, 0.166, 0.166, 0.149, 0.168, and 0.166, respectively.

Table 4.16: Radium equivalent activity $Ra_{eq}(Bq/kg)$ and internal hazard index H_{in} in powdered milk samples

Sample code	$Ra_{eq}(Bq/kg)$	H_{in}
M1	48.432	0.180
M2	49.627	0.187
M3	50.281	0.188
M4	56.102	0.192
M5	57.398	0.197
M6	52.469	0.190
M7	45.342	0.173
M8	55.312	0.202
M9	54.393	0.203
Average	52.151	0.190

Table 4.17: Radium equivalent activity $Ra_{eq}(Bq/kg)$ and internal hazard index H_{in} in biscuit samples

Sample code	$Ra_{eq}(Bq/kg)$	H_{in}
B1	48.012	0.175
B2	51.805	0.156
B3	46.255	0.147
B4	65.695	0.228
B5	44.629	0.151
B6	49.544	0.183
B7	50.856	0.167
B8	60.873	0.201
B9	41.924	0.126
B10	44.226	0.128
Average	50.382	0.166

Table 4.18: Radium equivalent activity $Ra_{eq}(Bq/kg)$ and internal hazard index H_{in} in Indomie samples

Sample code	$Ra_{eq}(Bq/kg)$	H_{in}
I1	61.852	0.214
I2	54.985	0.196
I3	30.197	0.082
I4	52.827	0.174
I5	55.174	0.199
I6	45.837	0.147
I7	61.696	0.204
I8	40.259	0.144
I9	45.431	0.148
I10	46.078	0.153
Average	49.434	0.166

Table 4.19: Radium equivalent activity $Ra_{eq}(Bq/kg)$ and internal hazard index H_{in} in Chips samples

Sample code	$Ra_{eq}(Bq/kg)$	H_{in}
Ch1	39.747	0.139
Ch2	46.386	0.155
Ch3	48.541	0.171
Ch4	38.462	0.15
Ch5	48.465	0.162
Ch6	35.639	0.096
Ch7	46.074	0.143
Ch8	51.233	0.175
Ch9	44.939	0.146
Ch10	47.82	0.148
Average	44.731	0.149

Table 4.20: Radium equivalent activity $Ra_{eq}(Bq/kg)$ and internal hazard index H_{in} in Cerelac samples

Sample code	$Ra_{eq}(Bq/kg)$	H_{in}
Ce1	48.666	0.178
Ce2	55.853	0.19
Ce3	41.779	0.138
Ce4	38.615	0.135
Ce5	52.443	0.194
Ce6	47.943	0.173
Ce7	51.191	0.179
Ce8	46.168	0.167
Ce9	49.67	0.167
Ce10	46.666	0.162
Average	47.899	0.168

Table 4.21: Radium equivalent activity $Ra_{eq}(Bq/kg)$ and internal hazard index H_{in} in Corn Flakes samples

Sample code	$Ra_{eq}(Bq/kg)$	H_{in}
Co1	59.033	0.212
Co2	33.311	0.117
Co3	53.768	0.188
Co4	54.928	0.194
Co5	49.627	0.177
Co6	39.607	0.115
Co7	55.696	0.188
Co8	45.825	0.154
Co9	53.737	0.186
Co10	46.191	0.132
Average	49.172	0.166

The average Radium equivalent activity index Ra_{eq} for milk samples is the highest in our results, with a percentage of 17.8 %. In contrast, the lowest value is for Chips samples with a percentage of 15.2 % as shown in Fig. 4.16. The percentages of the other samples are 17.2 %, 16.8 %, 16.7 %, and 16.3 % for the food samples of biscuit, indomie, corn flakes, and cerelac, respectively. It is worth mentioning that our estimations of the Radium equivalent activity are lower than the worldwide average value of (370 Bq/kg) [11].

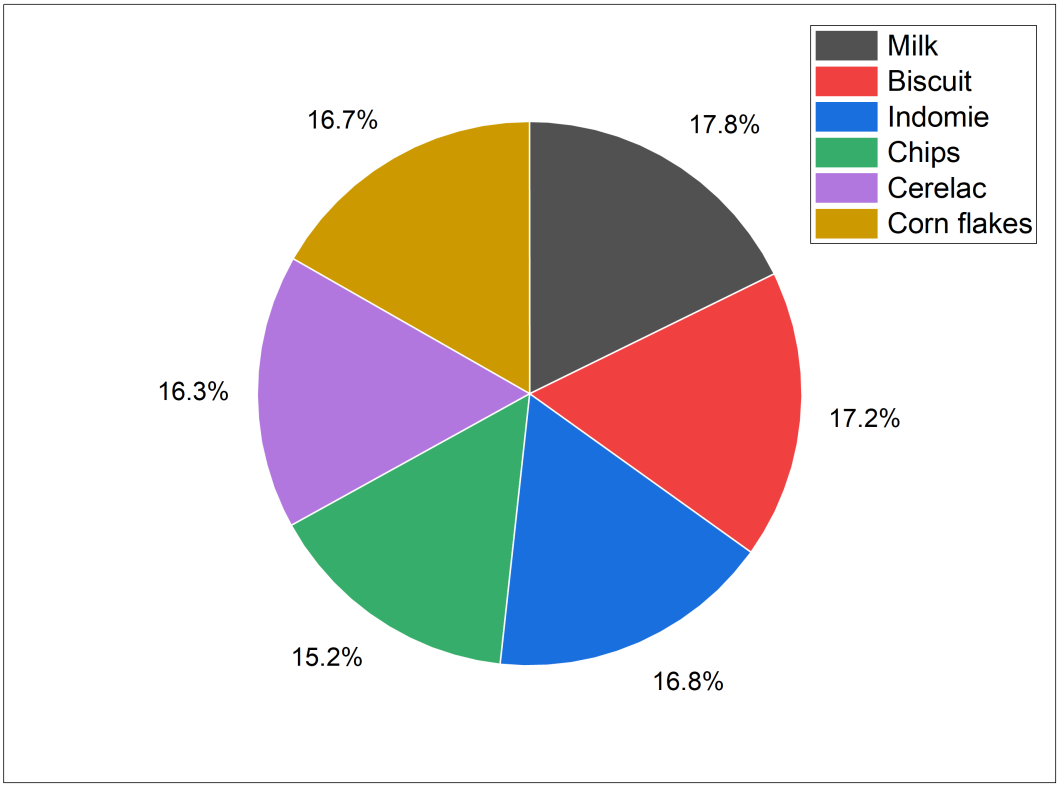

Figure 4.16: The percentage of average Radium equivalent activity $Ra_{eq}(Bq/kg)$ due to the intake of ^{238}U, ^{232}Th and ^{40}K in various food samples.

Regarding the radiation internal hazard index H_{in}, the powdered milk has also the highest percentage of 18.9 % and the lowest percentage of 14.8 % for Chips as shown in Fig. 4.17. Notably, the biscuit, indomie, and corn flakes have the same estimation for H_{in} with a percentage of 16.5 %, where its value is 0.166. However, the estimations of the radiation internal hazard index are lower than the worldwide average value of (≤ 1) [11]. On the other hand, we notice that the maximum or minimum values of Ra_{eq} and H_{in} are almost not calculated at the same food sample which contrast the case between AED and ELCR values. For example, Ra_{eq} for the powdered milk has the maximum value of 57.398 (Bq/kg) by M5 sample, but the evaluated maximum value of H_{in} is 0.203 Bq/kg by M9 sample. Also, the minimum value of Ra_{eq} is 48.432 (Bq/kg) obtained from M1 sample, whereas the minimum value of Ra_{eq} is obtained from M7 sample with a value of 0.173.

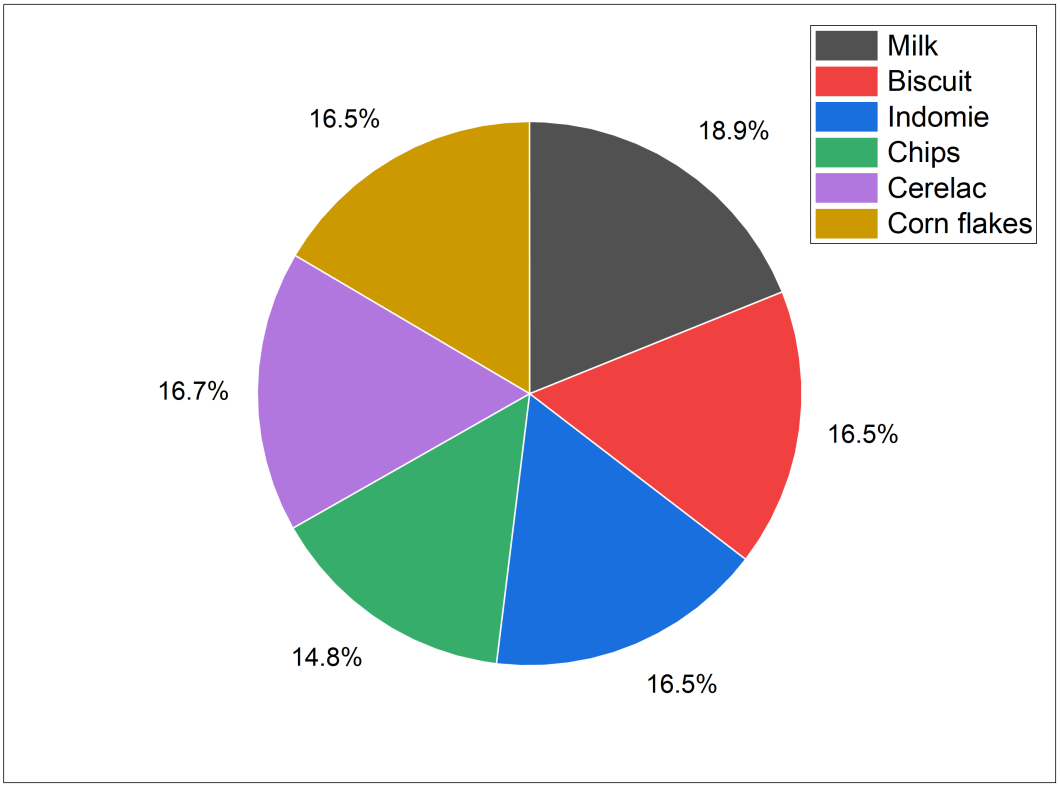

Figure 4.17: The percentage of average internal hazard index H_{in} due to the intake of ^{238}U, ^{232}Th and ^{40}K in various food samples.

This inconsistency between the highest and lowest values with their distinct samples can be explained using Eqs. (2.18) and (2.19). We can rewrite Ra_{eq} as follow [117]:

$$Ra_{eq} = \left(\frac{A_{Ra}}{370} + \frac{A_{Th}}{259} + \frac{A_K}{4810}\right) \times 370, \tag{4.1}$$

note that $A_{Ra} \equiv A_U$, with this expression, we can write Ra_{eq} in terms of H_{in} as

$$Ra_{eq} = 370 \times H_{in} - A_{Ra}, \tag{4.2}$$

or

$$H_{in} = (Ra_{eq} + A_{Ra}) \times \frac{1}{370}. \tag{4.3}$$

Thus, from the above equation, these indices are more sensitive to the specific activity values of ^{232}Th and ^{238}U compared to that of ^{40}K. For example, for any given values of the three specific activities, the increase of A_{Ra} by two with fixing the values of others can produce an increment in Ra_{eq} equal to 2, and increment in H_{in} equal to 0.0108. When we increase A_{Th} by two and fix the

others to the first configuration, the increment in Ra_{eq} becomes 2.8571 and the increment in H_{in} is 0.0077. For changing A_K by two and preserving others to the first case, this will produce a small increment in Ra_{eq} of 0.1538 and very small increment in H_{in} of 4.16×10^{-4}. Hence we conclude that, the magnitude of A_{Th} has more effect on the value of Ra_{eq}, whereas the magnitude of A_{Ra} impact more the value of H_{in}, but a low effect we have from the value of A_K particularly on H_{in}. Thus, the fluctuation of the specific activity values from different food samples can produce distinct maximum and minimum values for Ra_{eq} and H_{in} from various samples numbers.

4.5 Statistical Analysis of Complete Blood Count (CBC)

In this section, we present the second part of our work. Thirty children were chosen in our study and infected with different types of cancer and treated using high doses of radiation to kill cancer cells and shrink tumors at the Warith International Cancer Institute. They aged between one and thirteen years old. The selected number of children per age is shown in Table. 4.22. These children have been treated using high doses of radiation using Truebeam linear accelerator for three months. Each child has taken four treatment sessions per month, and hence the number of total sessions was 12.

We have investigated the effect of high radiation on hemoglobin (Hb g/dl), white blood count (WBC $\times 10^3/\mu$L), and platelet count (PLT $\times 10^3/\mu$L). A P-value of less than 0.05 ($P \leq 0.05$) is considered statistically significant in this study based on a T-test using Graph-pad Prism version 10 software. We describe the data in statistical figures for patients and healthy control by using mean and standard deviation (SD) values.

Table 4.22: Age group of chosen children at Warith International Cancer Institute to investigate the effect of radiation on their CBC test using Truebeam radiotherapy.

Child Age (y)	Numbers of Children
1	1
2	2
3	2
4	5
5	1
6	3
7	3
8	4
9	3
10	1
11	3
12	0
13	2
Total	30

Fig. 4.18 shows the statistical analysis for Hb (g/dl) level for the age group with three months of treatment sessions and control. Regarding the Hb level, the statistical results were compared with the control (12.23 ± 0.46). A significant decrease has been obtained for the three months and follows: for the first (P-Value = 0.0290) month with the mean level of (10.23 ± 0.16 g/dl); second month (P-Value = 0.00028) with the level of (9.922 ± 0.14 g/dl); third month (P-Value = 0.0053) with the mean level of (9.916 ± 0.16 g/dl). Moreover, we notice a significant decrease (P-Value = 0.0081) between the first and second months, but there is no statistical increase or decrease between the second and third month (P-Value = 0.4894, P-Value must be ≤ 0.05).

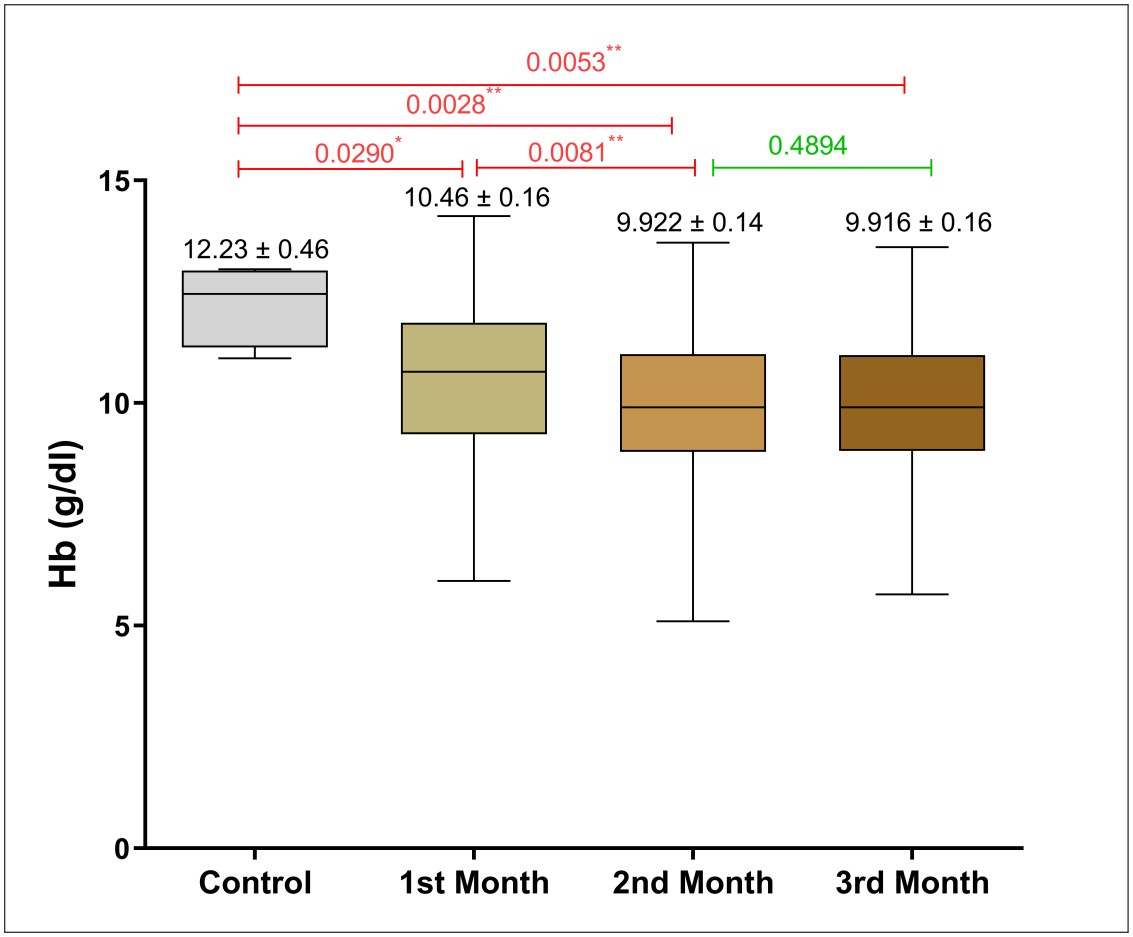

Figure 4.18: Statistical analysis for Hb g/dl level for the age group with three months of treatment sessions and control.

Regarding the white blood count (WBC) level, there is a significant decrease (P-Value ≤ 0.05) in its mean values over the three months compared with the control (12.15 ± 0.60) as shown in Fig. 4.19. For the first month (P-Value = 0.0122) with the mean level of (8.121 ± 0.67 g/dl); the second month (P-Value = 0.0015) with the level of (5.672 ± 0.38 g/dl); the third month (P-Value = 0.0007) with the mean level of (6.523 ± 0.81 g/dl). There was also a significant decrease for the second month (P-Value = 0.0299) compared with the first month. The third month has no significant decrease (P-Value = 0.0653) compared with the first month and no significant increase (P-Value = 0.1723) compared with the second month.

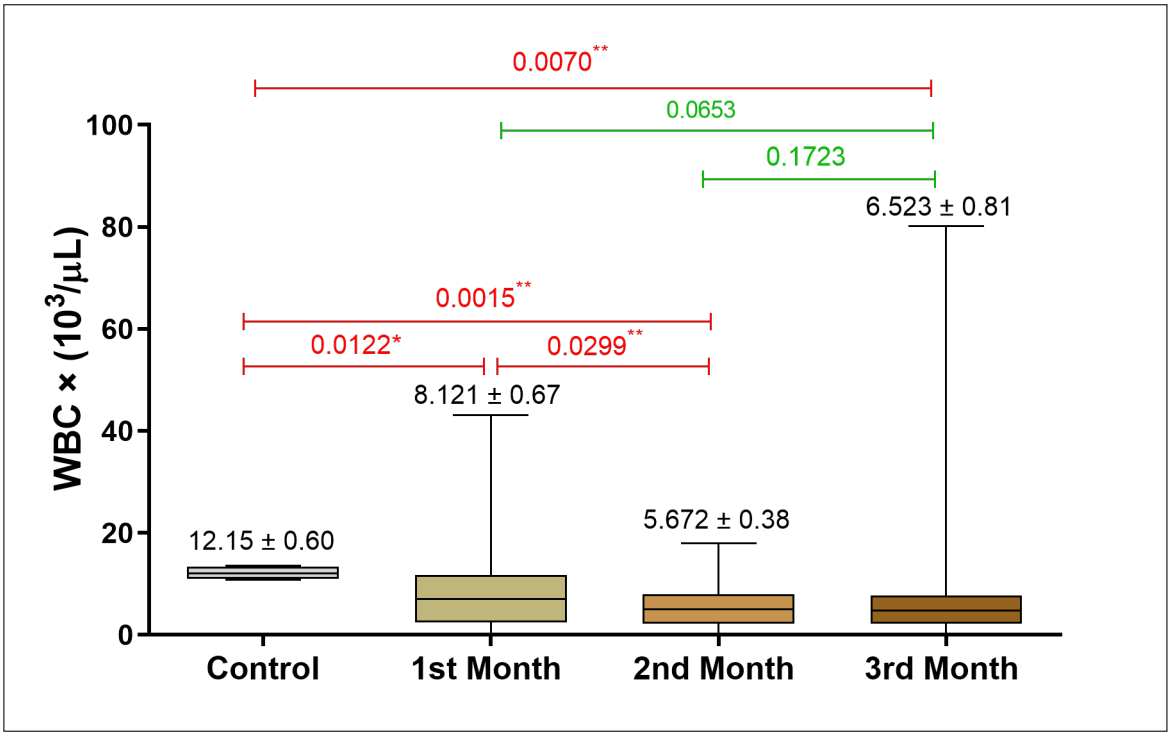

Figure 4.19: Statistical analysis for WBC $\times 10^3/\mu$L level for the age group with three months of treatment sessions and control.

Concerning the plates count (PLT), the statistical analysis for WBC $\times 10^3/\mu$L level for the age group with three months of treatment sessions and control of (347.5 $\pm$34.25) is presented in Fig. 4.20. For the first month, we have no significant increase (P-Value = 0.4457) with a mean value of (328.8$\pm$24.82) compared with the control. For the second month, there was a significant decrease (P-Value = 0.0234) with a mean value of (278.4$\pm$17.28) compared with the control, and a significant decrease (P-Value = 0.0483) compared with the first month. For the third month and compared with the control, we have no significant decrease (P-Value = 0.2070) with a mean value of (268.0 $\pm$ 17.61). A significant decrease for the second month compared with the first month (P-Value = 0.0483). Also, a significant decrease for the third month compared with the first month (P-Value = 0.0483), but no significant decrease compared with the third month (P-Value = 0.3374). It has been clear that a high standard deviation for the Hb mean values compared with those of WBC and PLT. Thus, these results indicate much variance in the observed data around the mean for

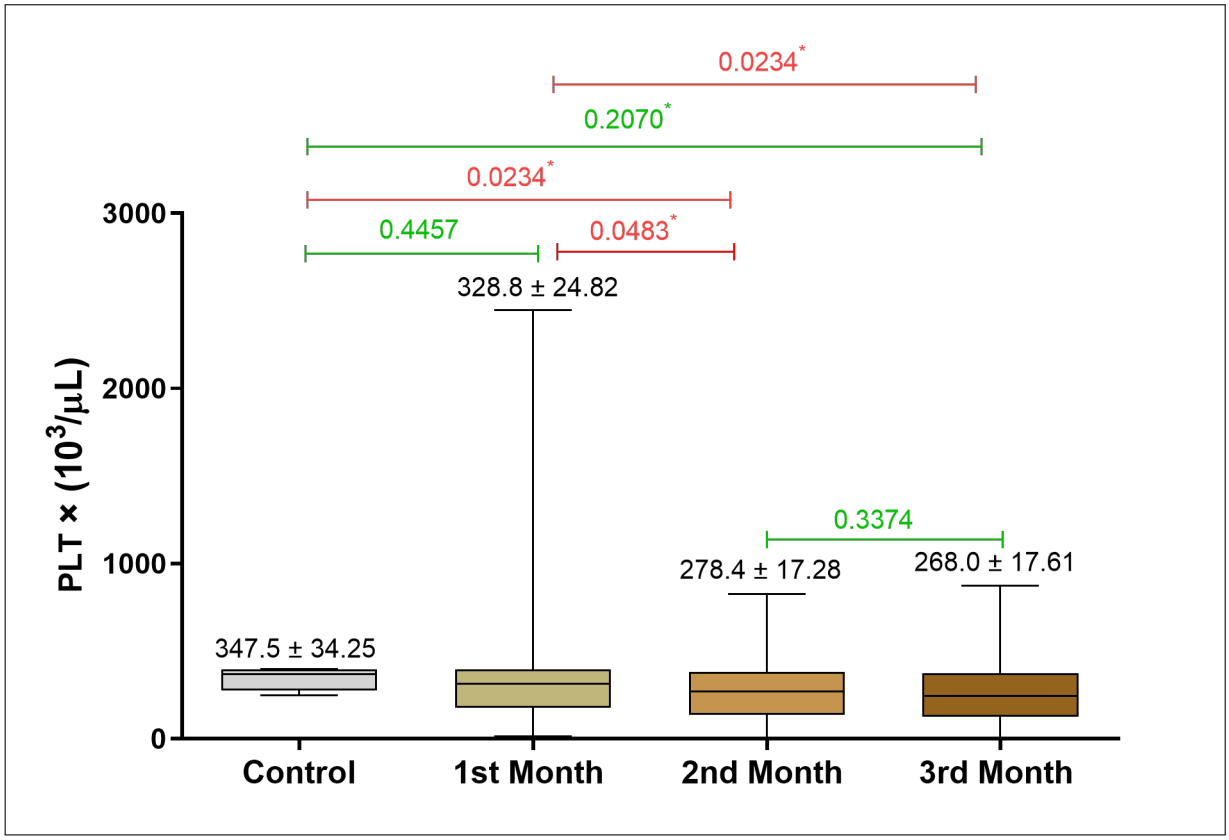

Figure 4.20: Statistical analysis for PLT $\times 10^3/\mu$L level for the age group with three months of treatment sessions and control.

Hb, and the data observed is entirely spread out. The slight standard deviation of WBC and PLT indicates that much of the data observed is clustered tightly around the mean.

4.6 The Annual Effective Dose (AED) and CBC Test

In this section, we have performed a statistical correlation analysis between the evaluated annual effective dose for the food samples presented their results in Chp. 3, with hemoglobin (Hb g/dl) for the children patients infected with cancer and tumor and who were treated at the Warith International Cancer Institute. The focus was on Hb because it can be highly affected by the food types and might be by also the natural radionuclide in these foods. As mentioned, we have 30 infected children with the age group shown in Table. 4.22.

In Fig. 4.21, the correlation between AED (Bq/kg) of powdered milk and Hb is a too Weak partial positive correlation, with a correlation coefficient equal to ($R^2 = 0.025$) as shown in Fig. 4.22. The AED for biscuit samples has a tiny negative correlation coefficient of ($R^2 = 0.0003$) from a partial negative correlation. This value of R^2, which is approximately zero, indicates zero correlation between the biscuit's AED and Hb.

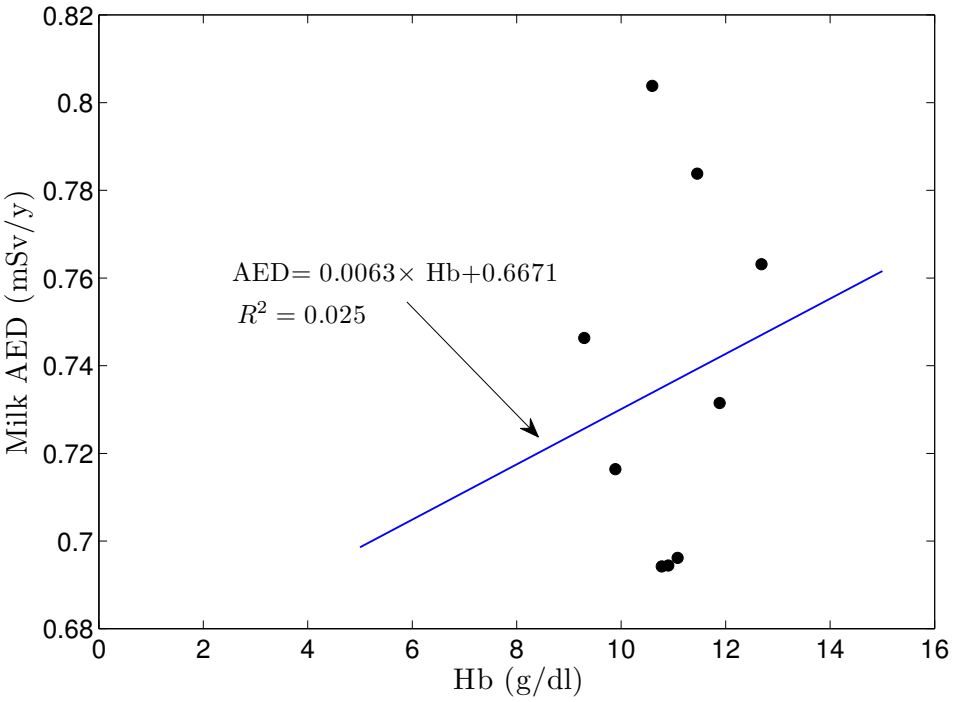

Figure 4.21: Partial positive correlation between annual effective does (AED) (Bq/kg) for powdered milk and hemoglobin (Hb g/dl) level.

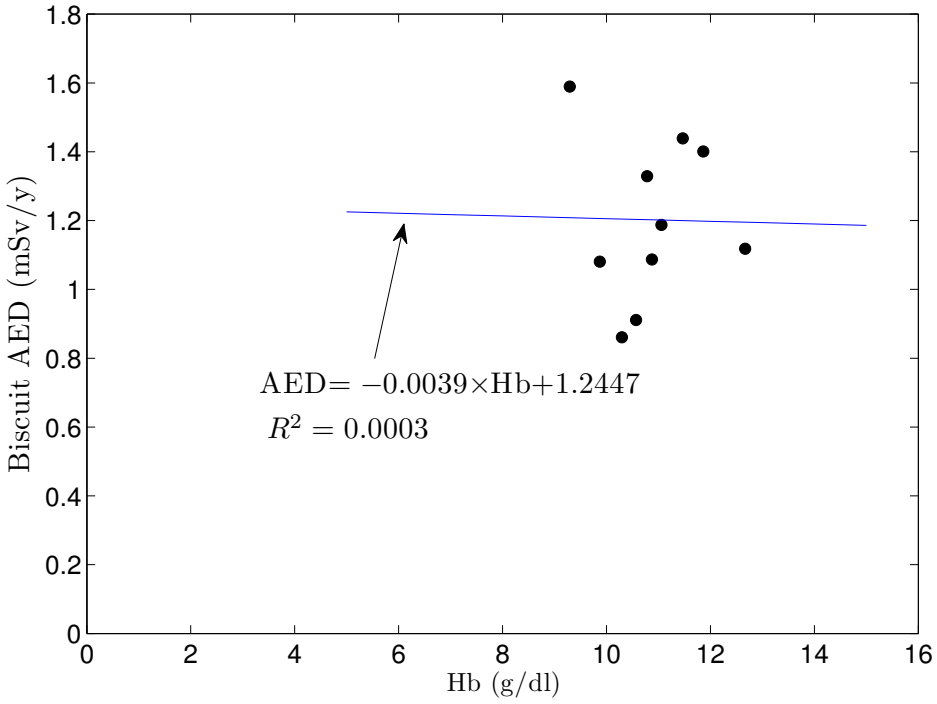

Figure 4.22: Zero correlation between annual effective does (AED) (Bq/kg) for biscuit and hemoglobin (Hb g/dl) level.

In Fig. 4.23, we found a Weak partial positive correlation between AED (Bq/kg) of indomie and Hb with $R^2 = 0.15$. For chips, a weak negative correlation has been obtained with AED and Hb with $R^2 = 0.1339$ as shown in Fig. 4.24. In contrast, we found a good partial positive correlation between AED and Hb for cerelac with $R^2 = 0.6804$ as shown in Fig. 4.25. Finally, we found a too weak negative correlation between AED and Hb for Corn flakes with $R^2 = 0.0618$ as shown in Fig. 4.26.

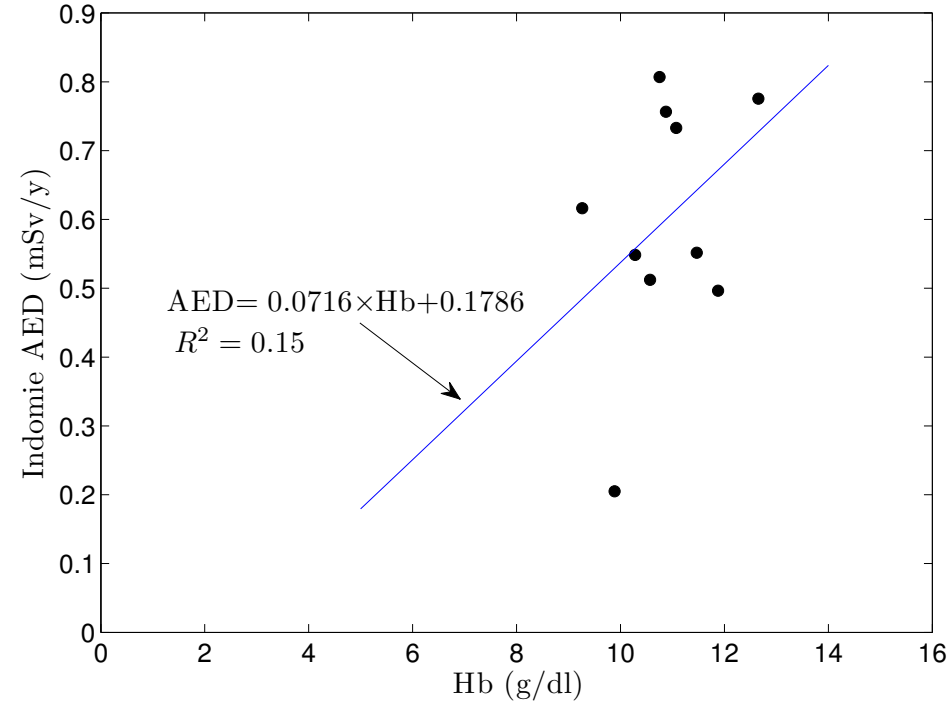

Figure 4.23: Partial positive correlation between annual effective does (AED) (Bq/kg) for Indomie and hemoglobin (Hb g/dl) level.

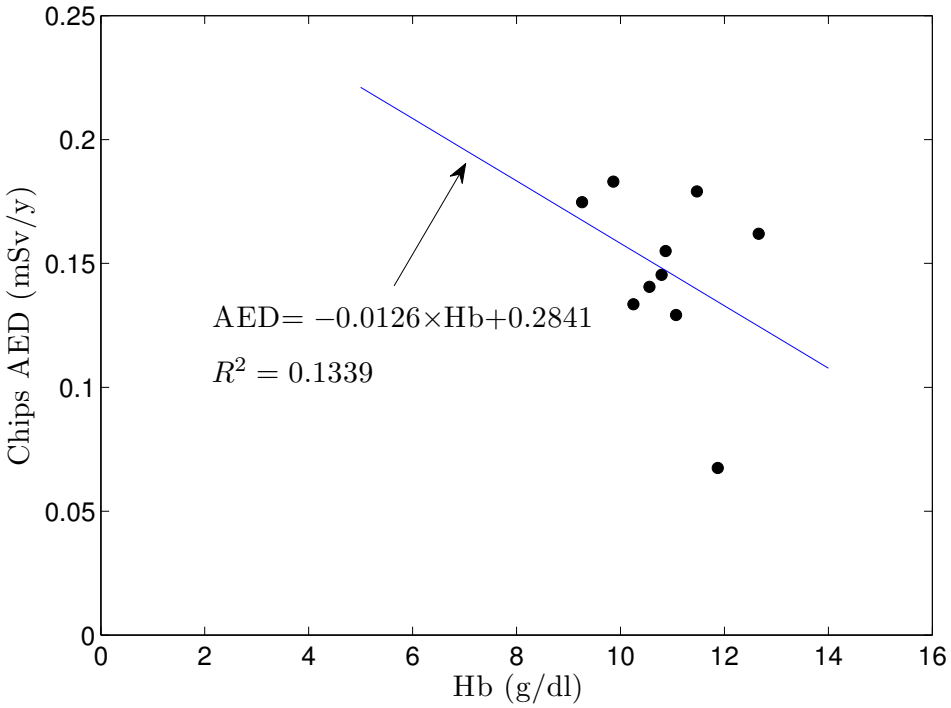

Figure 4.24: Partial negative correlation between annual effective does (AED) (Bq/kg) for Chips and hemoglobin (Hb g/dl) level.

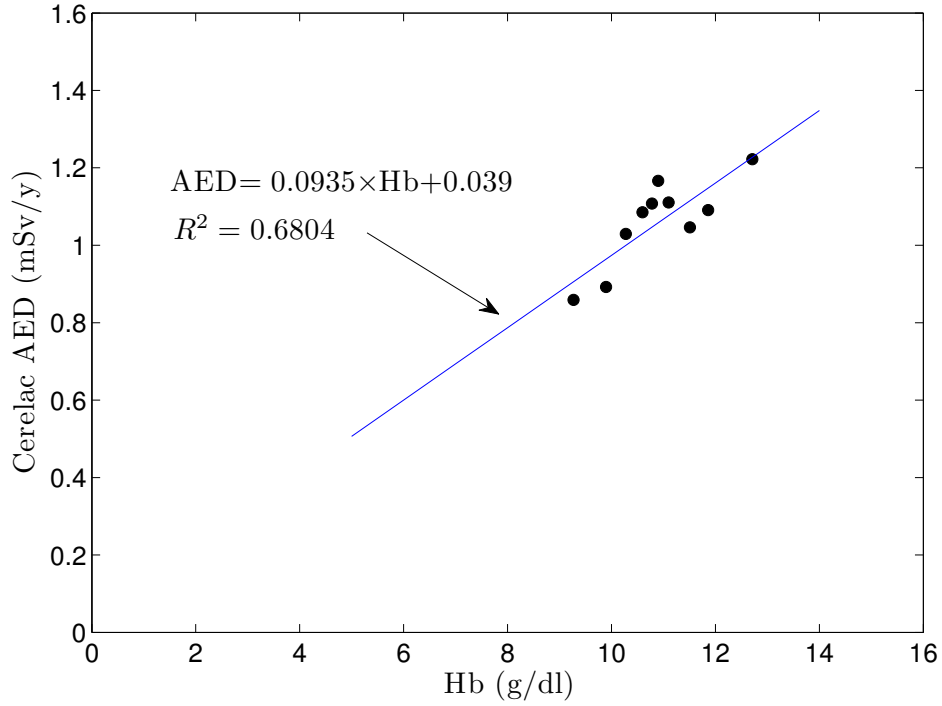

Figure 4.25: Partial positive correlation between annual effective does (AED) (Bq/kg) for Cerelac and hemoglobin (Hb g/dl) level.

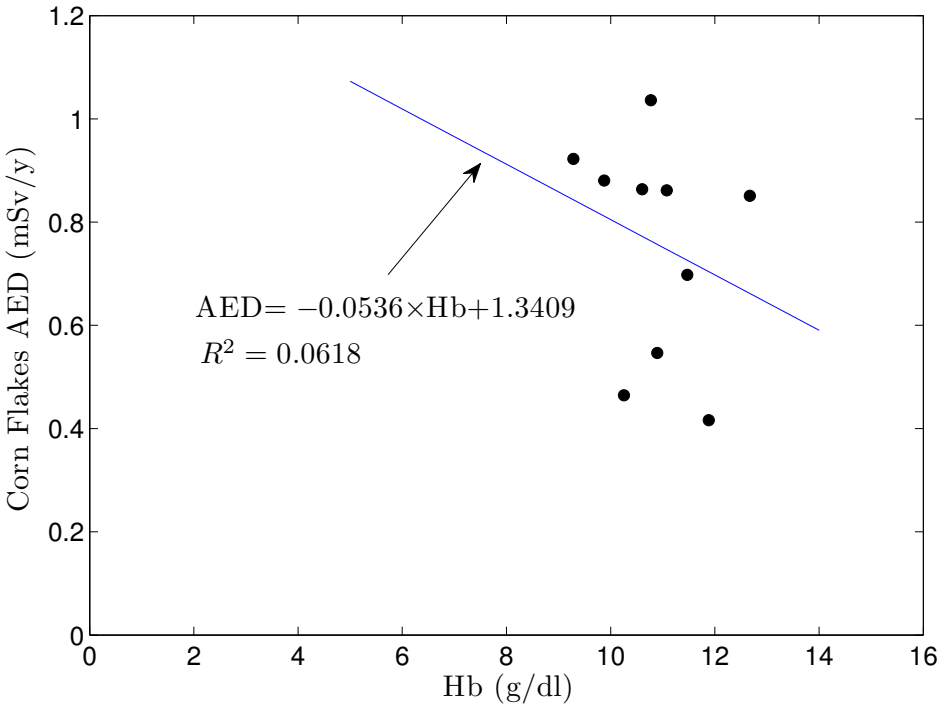

Figure 4.26: Partial negative correlation between annual effective does (AED) (Bq/kg) for Corn flakes and hemoglobin (Hb g/dl) level.

4.7 Conclusions

Our work consisted of two main parts. The first part focused on studying the natural radioactivity in various types of food consumed regularly by children. The second part investigated the effect of radiation radiotherapy treatment on children infected with cancer and its potential relationship to the first part of our study. In summary, our conclusions can be summarized in the following points:

1. The specific activity of ^{40}K was found to be generally higher than ^{238}U and ^{232}Th in all food samples. However, the measured values were within the worldwide average limits and do not pose a significant radiation hazard.

2. Among the food samples, biscuits for children had the highest annual effective dose (AED) (mSv/y) while chips had the lowest. However, all were within safe limits. The estimated annual effective doses from ingestion of the radionuclides in all food samples were below the worldwide limit of 1 mSv/y, indicating minimal radiation risk.

3. Also, biscuits for children had the highest excess lifetime cancer risk factor (ELCR) while chips had the lowest. Nevertheless, all were within safe limits.

4. The highest average radium equivalent activity $Ra_{eq}(Bq/kg)$ was observed for powdered milk samples while the lowest was for chips samples. However, all values were below the worldwide average limit of 370 Bq/kg.

5. Regarding the internal hazard index H_{in}, the highest value was found for powdered milk samples and the lowest value was for chips samples. All values were below the acceptable limit of 1.

6. Hematological parameters were analyzed statistically for pediatric cancer patients of 30 children aged 1-13 years undergoing radiation therapy over three months. Significant declines in hemoglobin, white blood cells, and platelets were observed during treatment. These results agree with some previous studies presented in the literature.

7. A correlation analysis between the annual effective doses of different food types and hemoglobin levels for the patients showed: Too weak positive and negative correlations for powdered milk and corn flakes samples, respectively, Zero correlation for biscuit samples, low positive and negative correlations for indomie and chips samples, and a good positive correlation for cerelac samples.

8. Natural radioactivity levels in the analyzed food samples pose a minimal risk to children in Iraq. However, high radiation doses during cancer treatment can significantly affect blood parameters, necessitating close monitoring of blood tests for such patients.

4.8 Future Research Proposals

1. Expanding the food samples analyzed to cover a wider range of children's foods in Iraq and also imported foods. Assess impact of food processing.
2. Using more sensitive detection techniques like alpha spectrometry to quantify plutonium, uranium isotopes in foods. Compare to gamma results.
3. Investigating if certain food types correlate with specific cancer types in pediatric patients using retrospective data. Also, Measure radon levels in homes/schools of pediatric patients and correlate with blood counts and dietary radioactivity.
4. Conducting in-vitro study exposing blood samples to food radioactivity levels to directly assess effects on blood cells.
5. Conducting a risk assessment study evaluating the combined effects of natural radioactivity in food and environmental radiation exposure for children. Measure outdoor/indoor radiation levels in homes, schools, play areas and correlate with food radioactivity intake and blood test results.
6. Evaluating the radiosensitivity of blood cells from pediatric cancer patients compared to healthy children by exposing samples in-vitro to radiation. Assess DNA damage, chromosomal aberrations, apoptosis.
7. Using CRISPR-Cas9 gene editing technology to introduce mutations that modulate radiosensitivity in blood cell lines, then assess response to radiation exposure in-vitro after feeding with radioactve foods.
8. Investigating approaches to reduce gastrointestinal absorption of radionuclides from food, such as using dietary binders like alginate or animal studies with radioactively-labeled foods. Analyze blood, urine, feces.

References

[1] P. Manning, *Atoms, Molecules, and Compounds*, Infobase Publishing (2008).

[2] W. Demtröder. *Atoms, Molecules and Photons: An Introduction to Atomic-, Molecular- and Quantum Physics*, Springer, Second Edition (2010).

[3] A. Das, T. Ferbel, and N. Gauthier, Introduction to Nuclear and Particle Physics, Physics Today, Vol. 47, pp. 73–76 (1994).

[4] E. B. Podgoršak, *Radiation Physics for Medical Physicists*, Springer (2016).

[5] F. H. Al Marzooqi, Determination of Natural Radioactivity Levels Using High Resolution Gamma-Ray Spectrometry, M. Sc. Thesis, University of Surrey, United Kingdom (2009).

[6] IAEA Safety Glossary, *Terminology Used in Nuclear Safety and Radiation Protection*, Vienna: IAEA (2007).

[7] M. Pöschl and L.M.L. Nollet, *Radionuclide Concentrations in Food and the Environment*, CRC Press (2007).

[8] J. E. Martin, *Physics for Radiation Protection: A Handbook*, Wiley-VCH (2006).

[9] M. F. Attallah, N. S. Awwad, and H. F. Aly, Environmental Radioactivity of Te-Norm Waste Produced From Petroleum Industry in Egypt: Review on Characterization and Treatment, Natural Gas-Extraction to End Use, pp. 548–603 (2012).

[10] T. J. Ahrens, *Global Earth Physics: A Handbook of Physical Constants*, American Geophysical Union (1995).

[11] UNSCEAR, *Sources and Effects of Ionizing Radiation*, United Nations Scientific Committee on the Effects of Atomic Radiation, Report to the General Assembly, with Scientific Annexes-Sources, United Nation (2000).

[12] P. Rullhusen, X. Artru, and P. Dhez, *Novel Radiation Sources Using Relativistic Electrons: From Infrared to X-Rays*, World Scientific (1998).

[13] H. D. Barth, E. A. Zimmermann, E. Schaible, S. Y. Tang, T. Alliston, and R. O. Ritchie, Characterization of the Effects of X-Ray Irradiation on the Hierarchical Structure and Mechanical Properties of Human Cortical Bone, Biomaterials, Vol. 32, pp. 8892–8904 (2011).

[14] UNEP, *Radiation Effects and Sources*, United Nations Environment Programme (2016).

[15] R. A. Powsner and E. R. Powsner, *Essential nuclear medicine physics*, John Wiley & Sons (2008).

[16] J.-L. Basdevant and J. Rich, *Fundamentals in Nuclear Physics: From Nuclear Structure to Cosmology*, Springer Science & Business Media (2005).

[17] J. K. Shultis and R. E. Faw, *Fundamentals of Nuclear Science and Engineering, Third Edition*, CRC press (2016).

[18] B. R. Martin and G. Shaw, *Nuclear and Particle Physics: An Introduction*, John Wiley & Sons (2019).

[19] R. Wakeford, G. M. Kendall, and M. P. Little, The Proportion of Childhood Leukaemia Incidence in Great Britain That May Be Caused by

Natural Background Ionizing Radiation, Leukemia, Vol. 23, pp. 770–776 (2009).

[20] S. Borzoueisileh and A. Shabestani Monfared, Natural Background Radiations, Radioadaptive Response and Radiation Hormesis, Journal of Babol University of Medical Sciences, Vol. 17, pp. 15–21 (2015).

[21] J. D. Carrillo-Sánchez, D. Nesvornỳ, P. Pokornỳ, D. Janches, and J. M. C. Plane, Sources of Cosmic Dust in the Earth's Atmosphere, Geophysical Research Letters, Vol. 43, pp. 11,979–11,986 (2016).

[22] J. Magill and J. Galy, *Radioactivity-Radionuclides-Radiation: Including the Universal Nuclide Chart on CD-ROM*, Springer (2005).

[23] I. Obodovskiy, *Fundamentals of Radiation and Chemical Safety*, Elsevier (2015).

[24] K. Coulson, *Solar and Terrestrial Radiation: Methods and Measurements*, Elsevier (2012).

[25] E. I. Hamilton, Terrestrial Radiationan Overview, International Journal of Radiation Applications and Instrumentation. Part C. Radiation Physics and Chemistry, Vol. 34, pp. 195–212 (1989).

[26] M. Tufail, N. Akhtar, and M. Waqas, Measurement of Terrestrial Radiation for Assessment of Gamma Dose From Cultivated and Barren Saline Soils of Faisalabad in Pakistan, Radiation measurements, Vol. 41, pp. 443-451 (2006).

[27] G. P. Jacobs, *A Review on the Effects of Ionizing Radiation on Blood and Blood Components*, Radiation Physics and Chemistry, Vol. 53, pp. 511–523 (1998).

[28] H. A. Ziessman, J. P. O'Malley, and J. H. Thrall, *Nuclear Medicine: The Requisites E-book*, Elsevier Health Sciences (2013).

[29] J. A. Sorenson, M. E. Phelps, *Physics in Nuclear Medicine*, Grune & Stratton, New York (1987).

[30] V. Carter, *Advanced Nuclear Physics*, Global Media (2009).

[31] W. D. Loveland, D. J. Morrissey, and G. T. Seaborg, *Modern Nuclear Chemistry*, John Wiley & Sons (2017).

[32] D. Bodansky, *Nuclear Energy: Principles, Practices, and Prospects*, Springer Science & Business Media (2007).

[33] J. P. Schiffer, *Nuclear Physics: The Core of Matter, the Fuel of Stars*, National Academies Press (1999).

[34] T. Jevremovic, *Nuclear Principles in Engineering*, Springer (2009).

[35] P. P. Dendy and B. Heaton, *Physics for Diagnostic Radiology*, CRC press (2011).

[36] R. F. Dondelinger, P. Rossi, J. C. Kurdziel, and S. Wallace, *Interventional Radiology*, Germany: Thieme (1990).

[37] P. Mayles, A. Nahum, and J.-C. Rosenwald, *Handbook of Radiotherapy Physics: Theory and Practice*. CRC Press, (2007).

[38] F. M. Khan and J. P. Gibbons, *Khan's the Physics of Radiation Therapy*, Lippincott Williams & Wilkins (2014).

[39] M. Mahesh, A. J. Ansari, and F. A. Mettler Jr, Patient Exposure from Radiologic and Nuclear Medicine Procedures in the United States and Worldwide: 2009–2018, Radiology, Vol. 307, pp. e221263:1–10 (2022).

[40] M. C. Korpics, A. M. Block, B. Martin, C. Hentz, E. R. Gaynor, E. Henry, M. M. Harkenrider, and A. A. Solanki, Concurrent Chemotherapy is Associated With Improved Survival in Elderly Patients With Bladder Cancer Undergoing Radiotherapy, Cancer, Vol. 123, pp. 3524–3531 (2017).

[41] M. Hejmadi, *Introduction to Cancer Biology*, Bookboon (2014).

[42] R. W. Ruddon, *Cancer Biology*, Oxford University Press (2007).

[43] R. L. Siegel, A. Jemal, R. C. Wender, T. Gansler, J. Ma, and O. W. Brawley, An Assessment of Progress in Cancer Control, Ca: A Cancer Journal for Clinicians, Vol. 68, pp. 329–339 (2018).

[44] M. J. Gonzalez, *Complete Blood Count (CBC): The Complete Guide*, Amazon Digital Services LLC - Kdp (2022).

[45] M. S. Blumenreich, *The White Blood Cell and Differential Count, Clinical Methods: The History, Physical, and Laboratory Examinations*, Third Edition, Butterworth Publishers (1990).

[46] K. Tamakoshi, H. Toyoshima, H. Yatsuya, K. Matsushita, T. Okamura, T. Hayakawa, A. Okayama, H. Ueshima, N. D. R. Group, White Blood Cell Count and Risk of All-Cause and Cardiovascular Mortality in Nationwide Sample of Japanese Results From the Nippon Data90, Circulation Journal, Vol. 71, pp. 479–485 (2007).

[47] J. P. Gligoroska, S. Gontarev, B. Dejanova, L. Todorovska, D. S. Stojmanova, and S. Manchevska, Red Blood Cell Variables in Children and Adolescents Regarding the Age and Sex, Iranian Journal of Public Health, Vol. 48, pp. 704-712 (2019).

[48] A. Alrubaie, S. Majid, R. Alrubaie, and F. A.-Z. B. Kadhim, Effects of Body Mass Index (BMI) on Complete Blood Count Parameters, Inflammation, Vol. 105, pp. 164–171 (2019).

[49] D. P. Lokwani, *The Abc of Cbc: Interpretation of Complete Blood Count and Histograms*, JP Medical Ltd (2013).

[50] J. W. Hopewell, Radiation-Therapy Effects on Bone Density, Medical and Pediatric Oncology, Vol. 41, pp. 208–211 (2003).

[51] F. E. Yang, F. Vaida, L. Ignacio, A. Houghton, J. Nautiyal, H. Halpern, H. Sutton, and S. Vijayakumar, Analysis of Weekly Complete Blood Counts in Patients Receiving Standard Fractionated Partial Body Radiation Therapy, International Journal of Radiation Oncology, Biology, Physics, Vol. 33, pp. 607–617 (1995).

[52] F. L. Melquiades and C. R. Appoloni, Natural radiation levels in powdered milk samples, Food Science and Technology, Vol. 24, pp. 501–504 (2004).

[53] Z. Q. Ababneh, A. M. Alyassin, K. M. Aljarrah, and A. M. Ababneh, Measurement of Natural and Artificial Radioactivity in Powdered Milk Consumed in Jordan and Estimates of the Corresponding Annual Effective Dose, Radiation Protection Dosimetry, Vol. 138, pp. 278–283 (2009).

[54] N. S. Afshari, F. Abbasisiar, P. Abdolmaleki, and M. G. Nejad, Determination of ^{40}K Concentration in Milk Samples Consumed in Tehran-Iran and Estimation of Its Annual Effective Dose, Iranian Journal of Radiation Research, Vol. 7, pp. 159–164 (2009).

[55] T. Alrefae, T. N. Nageswaran, and T. Al-Shemali, Radioactivity of

Long Lived Gamma Emitters in Breakfast Cereal Consumed in Kuwait and Estimates of Annual Effective Doses, Iranian Journal of Radiation Research, Vol. 10, pp. 117–122 (2012).

[56] J. H. Al-Zahrani, Natural Radioactivity and Heavy Metals in Milk Consumed in Saudi Arabia and Population Dose Rate Estimates, Life Science Journal, Vol. 9, pp. 651–656 (2012).

[57] A. A. Abojassim, H. H. Al-Gazaly, and S. H. Kadhim, Estimated the Radiation Hazard Indices and Ingestion Effective Dose in Wheat Flour Samples of Iraq Markets, International Journal of Food Contamination, Vol. 1, pp. 1–5 (2014).

[58] S. Shahid, N. Mahmood, M. N. Chaudhry, S. Sheikh, and N. Ahmad, Assessment of Impacts of Hematological Parameters of Chronic Ionizing Radiation Exposed Workers in Hospitals, FUUAST Journal of Biology, Vol. 4, pp. 135–146 (2014).

[59] A. A. Abojassim, NORM in Instant Noodles (Indomie) Sold in Iraq, Journal of Environmental Analytical Chemistry, Vol. 2, pp. 2380–2391 (2015).

[60] A. A. Abojassim, L. A. Al-Alasadi, A. R. Shitake, F. A. Al-Tememie, and A. A. Husain, Assessment of Annual Effective Dose for Natural Radioactivity of Gamma Emitters in Biscuit Samples in Iraq, Journal of Food Protection, Vol. 78, pp. 1766–1769 (2015).

[61] S. Shahid, M. N. Chauhdry, N. Mahmood, and S. Sheikh, Impacts of Terrestrial Ionizing Radiation on the Hematopoietic System, Polish Journal of Environmental studies, Vol. 24, pp. 1783–1794 (2015).

[62] D. M. Daher, Natural Radioactivity in Chips Samples in Locally of Iraq, Journal of Kufa-Physics, Vol. 9, pp. 29–33 (2017).

[63] T. A. Hafiz, A. A. Alghamdi, N. M. Aljameel, E. F. Alsaeed, and A. A. Hassan, Efficiency of Granulocytes and Monocytes in Breast Cancer Patients Following Radiotherapy in Ksa, Biomedical Research, Vol. 29, pp. 3880–3887 (2018).

[64] A. A. Abojassim, S. H. Kadhim, M. Guida, A. A. Abojassim, H. H. Al-Gazaly, and S. H. Kadhim, Natural Radioactivity and Radon Activity Concentrations in Canned Milk Samples in Iraq, Mastorakis NE (ed) pp. 354–362 (2019).

[65] A. Q. Ahmed, A. A. H. Mohsen, A. N. Al-Khayyat, A. A. Abojassim, and R. R. Munim, Natural Radioactivity in Cerelac Baby Food Samples Commonly Used in Iraq, Plant Archives, Vol. 19, pp. 1057–1061 (2019).

[66] H. N. Surniyantoro, T. Rahardjo, Y. Lusiyanti, N. Rahajeng, A. H. Sadewa, P. Hastuti, and H. Date, Assessment of Ionizing Radiation Effects on the Hematological Parameters of Radiation-Exposed Workers, Atom Indonesia, Vol. 45, pp. 123–129 (2019).

[67] V. H. Duong, T. D. Nguyen, M. Hegeds, E. Tóth-Bodrogi, and T. Kovács, Assessment of ^{232}Th, ^{226}Ra, ^{137}Cs, and ^{40}K concentrations And Annual Effective Dose Due to the Consumption of Vietnamese Fresh Milk, Journal of Radioanalytical and Nuclear Chemistry, Vol. 328, pp. 1399–1404 (2021).

[68] N. Liu, Y. Peng, X. Zhong, Z. Ma, S. He, Y. Li, W. Zhang, Z. Gong, and Z. Yao, Effects of Exposure to Low-Dose Ionizing Radiation on Changing Platelets: A Prospective Cohort Study, Environmental Health and Preventive Medicine, Vol. 26, pp. 1–10 (2021).

[69] J. J. Guo, N. Liu, Z. Ma, Z. J. Gong, Y. L. Liang, Q. Cheng, X. G. Zhong, and Z. J. Yao, Dose-Response Effects of Low-Dose Ionizing Radiation on Blood Parameters in Industrial Irradiation Workers, Dose-Response, Vol. 20, pp. 1–13 (2022).

[70] B. Kahn and J. Lahr, Measuring Environmental Radioactivity: A Brief History, Technology, Vol. 7, pp. 363–379 (2000).

[71] US. Department of Energy, *DOE Fundamentals Handbook: Nuclear Physics and Reactor Theory*, Technical Report (1993).

[72] M. P. Little, C. R. Muirhead, L. H. J. Goossens, B. C. P. Kraan, R. M. Cooke, F. T. Harper, Probabilistic Accident Consequence Uncertainty Analysis, Late Health Effects Uncertainty Assessment. Main Report pp. 1–62 (1997).

[73] C. J. Foot, *Atomic Physics*, Vol. 7, OUP Oxford, (2004).

[74] A. D. McNaught, and A. Wilkinson, *Compendium of Chemical Terminology*, Blackwell Science (1997).

[75] T. E. Johnson and B. K. Birky, *Health Physics and Radiological Health*, Lippincott Williams & Wilkins (2012).

[76] E. F. Elstner, R. Fink, W. Höll, E. Lengfelder, and H. Ziegler, Natural and Chernobyl-Caused Radioactivity in Mushrooms, Mosses and Soil-Samples of Defined Biotops in Sw Bavaria, Oecologia,Vol. 73, pp. 553–558 (1987).

[77] P. Kalač, A Review of Edible Mushroom Radioactivity, Food Chemistry, Vol. 75, pp. 29-35 (2001).

[78] K. KANT, R. Gupta, R. Kumari, N. Gupta, and M. Garg, Natural Radioactivity in Indian Vegetation Samples, International Journal of Radiation Research, Vol. 13, pp. 143–150 (2015).

[79] A. A. Abojassim, Study of Norm and Some Radiological Parameters in Instant Noodles Sold in Iraq, World Applied Sciences Journal, Vol. 33, pp. 974–979 (2015).

[80] C. E. Crouthamel, F. Adams, and R. Dams, *Applied Gamma-Ray Spectrometry*, Elsevier (2013).

[81] M. Beyzadeoglu, G. Ozyigit, and C. Ebruli, *Basic Radiation Oncology*, Springer (2010).

[82] K. Siegbahn, *Alpha-, Beta-and Gamma-Ray Spectroscopy*, Elsevier (2012).

[83] R. S. Peterson, Experimental γ Ray Spectroscopy and Investigations of Environmental Radioactivity, Spectrum Techniques, Vol. 6, pp. 1–83 (1996).

[84] G. F. Knoll, *Radiation Detection and Measurement*, John Wiley & Sons (2010).

[85] A. A. Abojassim, Estimation of Human Radiation Exposure From Natural Radioactivity and Radon Concentrations in Soil Samples at Green Zone in Al-Najaf, Iraq, Iranian (Iranica) Journal of Energy & Environment, Vol. 8, pp. 239–248 (2017).

[86] A. Al-Hamidawi, Assessment of Radiation Hazard Indices and Excess Life Time Cancer Risk Due to Dust Storm for Al-Najaf, Iraq, WSEAS Transactions on Environment and Development, Vol. 10, pp. 312–319 (2014).

[87] G. Viruthagiri and K. Ponnarasi, Measurement of Natural Radio Activity in Brick Samples, Adv Appl Sci Res, Vol. 2, pp. 103–108 (2011).

[88] S. M. Siddeeg, M. A. Suliman, F. Ben Rebah, W. Mnif, A. Y. Ahmed, and I. Salih, Comparative Study of Natural Radioactivity and Radiological Hazard Parameters of Various Imported Tiles Used for Decoration in Sudan, Symmetry, Vol. 10, pp. 746–756 (2018).

[89] Z. M. Alamoudi, Assessment of Natural Radionuclides in Powdered Milk Consumed in Saudi Arabia and Estimates of the Corresponding Annual Effective Dose, J Am Sci, Vol. 9, pp. 267–273 (2013).

[90] S. M. El-Bahi, A. Sroor, G. Y. Mohamed, and N. S. El-Gendy, Radiological Impact of Natural Radioactivity in Egyptian Phosphate Rocks, Phosphogypsum and Phosphate Fertilizers, Applied Radiation and Isotopes, Vol. 123, pp. 121–127 (2017).

[91] R. S. Reneman and J. Strackee, *Data in Medicine: Collection, Processing and Presentation: A Physical-Technical Introduction for Physicians and Biologists*, Instrumentation and Techniques in Clinical Medicine Springer Netherlands (2012).

[92] A. P. Bedmar and L. Araguas, *Detection and the Prevention of Leaks from Dams*, Taylor & Francis (2002).

[93] S. Breur, The Performance of Nai (Tl) Scintillation Detectors, University of Amsterdam, M.Sc Thesis (2013).

[94] H. I. West Jr, W. E. Meyerhof, and R. Hofstadter, Detection of X-Rays by Means of Nai (Tl) Scintillation Counters, Physical Review, Vol. 81, pp. 141–142 (1951).

[95] M. F. Kuluöztürk, Optimization of 3× 3 inch NaI (Tl) Detector Related to Energy, Distance and Bias Voltage, Journal of Radiation Research and Applied Sciences, Vol. 16, pp. 100601–100607 (2023).

[96] M. F. L'Annunziata, *Handbook of Radioactivity Analysis*, Academic press (2012).

[97] B. A. Almayahi, Gamma Spectroscopic of Soil Samples From Kufa in Najaf Governorate, Iraq, World Applied Sciences Journal, Vol. 31, pp. 1582–1588 (2014).

[98] B. Rajamannan, G. Viruthagiri, and K. Suresh Jawahar, Natural Radionuclides in Ceramic Building Materials Available in Cuddalore District, Tamil Nadu, India, Radiation protection dosimetry, Vol. 156, pp. 531–534 (2013).

[99] M. Gröning and K. Rozanski, Uncertainty Assessment of Environmental Tritium Measurements in Water, Accreditation and Quality Assurance, Vol. 8, pp. 359–366 (2003).

[100] G. Lowenthal and P. Airey, *Practical Applications of Radioactivity and Nuclear Radiations*, Cambridge University Press (2001).

[101] Nucaremed. RAD IQ^{TM} FS200/300, http://www.nucaremed.com/products/radiation-measurement/food-monitors/rad-iq-fs200300/, Retrieved Date 20-1-2023.

[102] W. H. Organization, *Technical Specifications of Radiotherapy Equipment for Cancer Treatment*, World Health Organization (2021).

[103] D. Greene and P. C. Williams, *Linear Accelerators for Radiation Therapy*, CRC Press (1997).

[104] C. Glide-Hurst, M. Bellon, R. Foster, C. Altunbas, M. Speiser, M. Altman, D. Westerly, N. Wen, B. Zhao, M. Miften, Commissioning of the Varian TrueBeam linear accelerator: A Multi-Institutional Study, Medical Physics, Vol. 40, pp. 31719–31734 (2013).

[105] P. Mayles, A. E. Nahum, and J. C. Rosenwald, *Handbook of Radiotherapy Physics: Theory and Practice*, CRC Press (2021).

[106] Varian. The Truebeam Radiotherapy System, https://www.varian.com/products/radiotherapy/treatment-delivery/truebeam, Retrieved Date 20-1-2023.

[107] G. Shanthi, J. T. T. Kumaran, G. A. G. Raj, and C. G. Maniyan, Natural radionuclides in the South Indian foods and their annual dose, in Nuclear Instruments and Methods in Physics Research, Section A: Accelerators, Spectrometers, Detectors and Associated Equipment, Vol. 619, pp. 436–440 (2010).

[108] M. S. Al-Masri, H. Mukallati, A. Al-Hamwi, H. Khalili, M. Hassan, H. Assaf, Y. Amin, and A. Nashawati, Natural Radionuclides in Syrian Diet and Their Daily Intake, Journal of Radioanalytical and Nuclear Chemistry, Vol. 260, pp. 405–412 (2004).

[109] T. Hosseini, A. A. Fathivand, H. Barati, and M. Karimi, Assessment of Radionuclides in Imported Foodstuffs in Iran, Iranian Journal of Radiation Research, Vol. 4, pp. 149–153 (2006).

[110] I. H. Saleh, A. F. Hafez, N. H. Elanany, H. A. Motaweh, and M. A. Naim, Radiological Study on Soils, Foodstuff and Fertilizers in the Alexandria Region, Egypt, Turkish Journal of Engineering and Environmental Sciences, Vol. 31, pp. 9–17 (2007).

[111] H. H. Abbas, S. A. Kadhim, S. F. Alhous, H. H. Hussein, F. A. AL-Temimei, and H. A. Mraity, Radiation Risk Among Children due to Natural Radioactivity in Breakfast Cereals, Nature Environment and Pollution Technology, Vol. 22, pp. 527–533 (2023).

[112] ICRP, *ICRP Publication 72: Age-dependent Doses to the Members of the Public from Intake of Radionuclides Part 5, Compilation of Ingestion and Inhalation Coefficients*, Elsevier Health Sciences (1996).

[113] F. Caridi, G. Paladini, V. Venuti, S. E. Spoto, V. Crupi, G. Belmusto, and D. Majolino, Natural and Anthropogenic Radioactivity Content and Radiation Hazard Assessment of Baby Food Consumption in Italy, Applied Sciences, Vol. 12, pp. 5244–5251 (2022).

[114] S. A. A. M. S. Ibrahem, Detection and Measurement of Radon ^{222}Rn in Some of the Local and Imported Chips Are Available in Local Markets Using the Cn-85 Nuclear Impact Detector, Journal of Education and Scientific Studies, Vol. 4, pp. 75–82 (2020).

[115] A. K. Hashim, A. S. Hameed, E. J. Mohammed, and F. K. Fuliful, Measurement of alpha particle concentrations in different chips samples from Iraqi market, in *AIP Conference Proceedings*, AIP Publishing, Vol. 2144, pp. 30017–30026 (2019).

[116] A.-R. Abizari, Z. Ali, C. N. Essah, P. Agyeiwaa, and M. Amaniampong, Use of Commercial Infant Cereals as Complementary Food in Infants and Young Children in Ghana, BMC Nutrition, Vol. 3, pp. 1–8 (2017).

[117] A. A. Qureshi, S. Tariq, K. U. Din, S. Manzoor, C. Calligaris, and A. Waheed, Evaluation of Excessive Lifetime Cancer Risk Due to Natural Radioactivity in the Rivers Sediments of Northern Pakistan, Journal of Radiation Research and Applied Sciences, Vol. 7, pp. 438–447 (2014).

الخلاصة

تم دراسة مستويات الإشعاع الطبيعي في عينات مختلفة من الأطعمة التي يستهلكها الأطفال في العراق وقدرنا مؤشرات مخاطر الإشعاع والجرعات السنوية الفعالة الناتجة عن تناول النظائر النووية الطبيعية. تم جمع 59 عينة من مسحوق الحليب للأطفال والبسكويت والإندومي والشيبس والسيريلاك والكورن فليكس. وتحليلها باستخدام جهاز الكشف عن الكاما باستخدام كاشف يوديد الصوديوم المطعم بالثاليوم NaI(Tl) . تم حساب وتقييم النشاط النووي النوعي والجرعة السنوية الفعالة ومخاطر الإصابة بالسرطان الزائدة والنشاط النووي المكافئ للراديوم ومؤشر الخطر الداخلي. تمت مقارنة جميع النتائج للنظائر الطبيعية في عينات الأغذية مع المديات العالمية المتوسطة التي أعلنتها لجنة الأمم المتحدة العلمية للآثار النووية في تقاريرها. أظهرت نتائج النشاط النوعي أن البوتاسيوم هو الأول، يليه اليورانيوم والثوريوم في الحليب والسيريلاك، في حين يجب أن تكون القيم للبسكويت والإندومي والشيبس والكورن فليكس بالترتيب $^{40}K > ^{232}Th > ^{238}U$. القيم الأدنى والأعلى للنشاط النوعي المتوسط للبوتاسيوم كانت 190.459 ± 2.8 بيكرل/كغم للشيبس و 283.316 ±4.793 بيكرل/كغم للسيريلاك على التوالي. تشير هذه النتائج إلى وجود اختلافات كبيرة بين القيم المقاسة للبوتاسيوم وتلك القيم المقاسة للثوريوم واليورانيوم، والتي كانت تبلغ 16.314 ±0.797 بيكرل/كغم و 18.2 ± 1.16 بيكرل/كغم على التوالي للبسكويت والحليب. أعلى قيمة للجرعة السنوية الفعالة الإجمالية المقاسة كانت 1.470 ملي سيفرت للبسكويت (حالة الأطفال)، في حين لوحظت أقل قيمة في الشيبس (0.147 ملي سيفرت/سنة). يؤدي تأثير هذه النتائج إلى أعلى قيم وأقل قيم لمؤشر الخطر الزائد للإصابة بالسرطان بقيم 5.145×10^{-3} و 0.514×10^{-3} للبسكويت والشيبس على التوالي. أما النتائج المقدرة لعينات الأغذية الأخرى فتقع ضمن هذه النطاقات، وكانت جميع النتائج عدا البسكويت دون الحد العالمي المسموح به للجرعة السنوية الفعالة والبالغة 1 ملي سيفرت/سنة.

اما بالنسبة للنشاط النووي المكافئ للراديوم، تم العثور على أعلى قيمة محسوبة للحليب المجفف بلغت 52.151 بيكرل/كغم، في حين كانت القيمة الأدنى 44.731 بيكرل/كغم للشيبس، ولكن كانت

جميع القيم دون الحد العالمي الأوسط المسموح به والبالغ 370 بيكرل/كغم بالنسبة للنماذج الخاصة بالحليب المجفف، كانت لديها أعلى قيمة لمؤشر الخطر الداخلي Hin بلغت 0.190، في حين كانت لعينات الشيبس القيمة الأدنى والتي بلغت 0.149، وكانت جميع القيم دون الحد المسموح به والبالغ 1. بشكل عام، أظهرت النتائج أن مستويات الإشعاع الطبيعي في عينات الأطعمة التي تم تحليلها للأطفال العراقيين تشكل خطراً ضئيلًا من ناحية الإشعاع. علاوة على ذلك، تمت دراسة تأثير الجرعات العالية من الإشعاعات النووية من العلاج الإشعاعي على المعايير الدموية للأطفال الذين يعانون من السرطان في مستشفى متخصص. أظهر التحليل الإحصائي انخفاضًا ملحوظًا للشهر الأخير كما يلي: الهيموجلوبين 9.916 ± 0.16 جرام/ديسيلتر مقارنة بالسيطرة التي كانت 12.23 ± 0.46 جرام/ديسيلتر، وخلايا الدم البيضاء (6.523 ± 0.81) × 10^3/ مايكرولتر مقارنة بالسيطرة التي كانت (12.15 ± 0.60) × 10^3/ مايكرولتر ، والصفائح الدموية (268.0 ± 17.61) × 10^3/ مايكرولتر مقارنة بالسيطرة التي كانت (347.5 ± 34.25) × 10^3/ مايكرولتر. تحليل الارتباط بين الجرعات السنوية الفعالة لأنواع الأطعمة المختلفة ومستويات الهيموجلوبين للمرضى أظهر درجات متفاوتة من الارتباط. بالنسبة لعينات السيريلاك، وجدنا ارتباطًا إيجابيًا جيداً بين الجرعة السنوية الفعالة ومستويات الهيموجلوبين بقيمة معامل الارتباط R^2=0.68 ومع ذلك، على الرغم من أن مستويات الإشعاع الطبيعي في عينات الأغذية التي تم تحليلها للأطفال العراقيين تشكل خطراً ضئيلًا، فمن المهم ملاحظة أن الجرعات العالية من الإشعاعات النووية التي تلقاها المرضى أثناء العلاج الاشعاعي يمكن أن تؤثر سلبًا على معايير الدم.

جمهورية العراق
وزارة التعليم العـــالي والبحث العلـمي
جامـــعة بابـــل
كليـــة التربية للعلوم الصرفة
قســـم الفيزيـــاء

تحديد النشاط الاشعاعي الطبيعي في أغذية الأطفال وتأثير العلاج الاشعاعي على CBC

اطروحة مقدمة
إلى مجلس كلية التربية للعلوم الصرفة في جامعة بابل
وهي جزء من متطلبات نيل درجة الدكتوراه
فلسفة في التربية / الفيزياء

من قبل الطالب

فاتن احمد مهدي حسين

بكالوريوس تربية فيزياء
جامعة بابل 2016 م

ماجستير تربية فيزياء
جامعة بابل 2019 م

بأشراف

أ.د. فؤاد عطية مجيد
كلية التربية للعلوم الصرفة
قسم الفيزياء

أ.د. نهاد عبد الأمير صالح
كلية العلوم
قسم الفيزياء

1445 هـ

2023 م